

إقرار

أنا الموقع أدناه مقدم الرسالة التي تحمل العنوان:

**BACKPROPAGATION FEEDFORWARD NEURAL NETWORK FOR
FAULT DETECTION OF OVERHEAD BIPOLAR HVDC TRANSMISSION-
LINE**

أقر بأن ما اشتملت عليه هذه الرسالة إنما هي نتاج جهدي الخاص، باستثناء ما تمت الإشارة إليه حيثما ورد، وإن هذه الرسالة ككل، أو أي جزء منها لم يقدم من قبل لنيل درجة أو لقب علمي أو بحثي لدى أية مؤسسة تعليمية أو بحثية أخرى.

DECLARATION

The work provided in this thesis, unless otherwise referenced, is the researcher's own work, and has not been submitted elsewhere for any other degree or qualification

Student's name:

اسم الطالب: م. محمد يوسف محمور عاشور

Signature

التوقيع: 215

Date:

التاريخ: 2015 / 13 / 15



The Islamic University of Gaza
Faculty of Engineering
Electrical Engineering Department

Master Thesis

BACKPROPAGATION FEEDFORWARD NEURAL NETWORK FOR FAULT DETECTION OF OVERHEAD BIPOLAR HVDC TRANSMISSION-LINE

*A Thesis Submitted in Partial Fulfillment of the Requirements for the Degree of Master in
Electrical Engineering*



By
Eng. Mahmoud Y. Ashour

Advisor
Dr. Assad Abu-Jasser

2015/1436



مكتب نائب الرئيس للبحث العلمي والدراسات العليا هاتف داخلي 1150

الرقم...ج.س.ع/35/..... Ref

التاريخ: 2015/02/24 Date


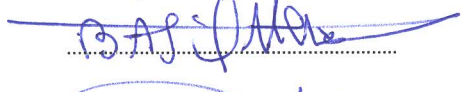

نتيجة الحكم على أطروحة ماجستير

بناءً على موافقة شئون البحث العلمي والدراسات العليا بالجامعة الإسلامية بغزة على تشكيل لجنة الحكم على أطروحة الباحث/ محمود يوسف محمود عاشور لنيل درجة الماجستير في كلية الهندسة قسم الهندسة الكهربائية - أنظمة الاتصالات وموضوعها:

الخلايا العصبية الاصطناعية التي تعمل بنظام الانتشار الخلفي والتغذية الأمامية لاكتشاف الأعطال في خطوط النقل الكهربائي ذات التيار المستمر والفولتية العالية

BACKPROPAGATION FEEDFORWARD NEURAL NETWORK FOR FAULT DETECTION OF OVERHEAD BIPOLAR HVDC TRANSMISSION-LINE

وبعد المناقشة العلنية التي تمت اليوم الثلاثاء 05 جمادى الأولى 1436هـ، الموافق 2015/02/24م الساعة الثانية عشرة ظهراً بمبنى القدس، اجتمعت لجنة الحكم على الأطروحة والمكونة من:

	مشرفاً ورئيساً	د. أسعد نمر أبو جاسر
	مناقشاً داخلياً	د. باسل محمود حمد
	مناقشاً خارجياً	د. محمد حاتم مشتهى

وبعد المداولة أوصت اللجنة بمنح الباحث درجة الماجستير في كلية الهندسة / قسم الهندسة الكهربائية - أنظمة الاتصالات.

واللجنة إذ تمنحه هذه الدرجة فإنها توصيه بتقوى الله ولزوم طاعته وأن يسخر علمه في خدمة دينه ووطنه.

والله ولي التوفيق ،،،

مساعد نائب الرئيس للبحث العلمي والدراسات العليا


أ.د. فؤاد علي العاجز



Abstract

This research handles detecting, classifying and locating of faults on high voltage direct current (HVDC) transmission line (TL) using backpropagation feedforward artificial neural network (ANN).

An overhead bipolar HVDC TL model of 940-km long and ± 500 -kV is chosen to be studied. The HVDC TL post-fault measurements of ac and dc voltages and currents at the rectifier and inverter stations related to pre-fault measurements are used as inputs to the neural networks. In this research, most frequent kinds of bipolar HVDC TL power faults that may occur can be precisely detected and classified while the location of these faults can be determined with an acceptable percentage of error.

Analysis of neural networks with varying number of hidden layers and neurons per hidden layer has been provided to validate the choice of the neural networks in each step. Simulation results have been provided to demonstrate that artificial neural network based methods are efficient in detecting, classifying and locating faults on HVDC transmission lines and achieve acceptable performances.

ملخص الرسالة

هذا البحث هو عبارة عن دراسة لكيفية اكتشاف وتحديد نوع ومكان الأعطال في شبكات نقل الكهرباء عالية الجهد ذات التيار المستمر باستخدام تقنية الشبكات العصبية ذات التغذية الأمامية والانتشار الخلفي وهي إحدى تقنيات الذكاء الاصطناعي.

وقد تم اختيار شبكة نقل كهرباء هوائية عالية الجهد ثنائية الأقطاب ذات تيار مستمر بطول ٩٤٠ كم وجهد ± 500 كيلو فولت كنموذج للبحث وتم استخدام قيم الجهود والتيارات المستمرة والمتردة على جانبي محطات التحويل بعد حدوث العطل في الخط الناقل مقارنة بقيمها قبل حدوث العطل كمدخلات للشبكات العصبية المستخدمة لدراسة جميع أنواع الأعطال الممكن حدوثها على الشبكة ليصبح بالإمكان اكتشاف حدوثها من عدمه وتحديد نوع العطل ومسافة وقوع العطل عن محطة التحويل بنسبة خطأ مقبولة.

تم تحليل كفاءة الكثير من الشبكات العصبية الصناعية عن طريق تغيير عدد الطبقات المخفية للشبكة وكذلك تغيير عدد الخلايا العصبية في كل طبقة للوصول لأفضل تركيب لشبكة تحقق أعلى كفاءة ممكنة في اكتشاف وتحديد أنواع وأماكن الأعطال ضمن معايير مقبولة ومحددة.

Dedicated to my parents and my wife

ACKNOWLEDGEMENTS

Firstly, I would like sincerely to express my gratitude to my advisor and my thesis chair, Dr. Assad Abu-Jasser for all his support and cooperation without which this thesis would never have been possible. I thank him for his constant patience and the knowledge support he offered to me during the course of my research.

I would also like to thank my discussion committee for their invaluable suggestions that shaped this thesis to its best.

Finally, My sincere regards to the Department of Electrical Engineering in the Islamic University of Gaza for providing all the necessary resources and paving way to the successful completion of my Master's degree.

CONTENTS

Contents.....	vi
List of Tables.....	ix
List of Figures.....	x
Chapter One: Introduction.....	1
1.1 Background.....	2
1.1.1 Artificial Neural Networks.....	3
1.2 Motivation.....	4
1.3 Literature Review.....	5
1.4 Contribution.....	6
1.5 Outline of the Thesis.....	7
Chapter Two: HVDC System.....	8
2.1 Introduction.....	9
2.2 HVDC Converter Technologies.....	11
2.2.1 Line Commutated Current Source Converter.....	12
2.2.2 Self-Commutated Voltage Source Converter.....	13
2.3 LCC Converter Theory.....	14
2.4 HVDC System Configuration.....	16
2.4.1 Monopolar HVDC System.....	16
2.4.1.1 A Monopolar HVDC System with Ground Return.....	16
2.4.1.2 A Monopolar HVDC System with Metallic Return.....	16
2.4.2 Bipolar HVDC System.....	17
2.4.3 Tripole HVDC System.....	18
2.4.4 Back-To-Back HVDC System.....	19
2.5 HVDC Station Components.....	20
2.5.1 Thyristor Valves.....	20
2.5.2 Converter Transformer.....	21
2.5.3 Smoothing Reactor.....	22
2.5.4 Harmonic Filters.....	23
2.5.4.1 AC Harmonic Filters.....	24
2.5.4.2 DC Harmonic Filters.....	25
2.5.4.3 Quality Factor.....	26
2.5.4.4 HVDC Filter Types.....	26
2.6 HVDC TL Fault Types.....	27
2.6.1 Single Pole-to-Ground Fault.....	28
2.6.2 Pole-to-Pole Fault:.....	28
2.6.3 Pole-to-Pole-to-Ground Fault.....	29
2.6.4 Other Types of HVDC TL Faults.....	29
Chapter Three: Techniques Of Fault Detection and Location on Transmission Line	30
3.1 Introduction.....	31
3.2 Impedance Based Method.....	32
3.2.1 Simple Reactance Method.....	34
3.2.2 Method Without Using Source Impedances.....	35
3.2.3 Method Using Source Impedances.....	35
3.3 Travelling Wave Based Method.....	35
3.3.1 Travelling Wave Fault Location Theory.....	37
3.3.2 Travelling Wave Fault Location Data and Equipment Required.....	38

3.4 High Frequency Methods.....	39
3.4.1 Basic Principle and Fault Locator Design.....	40
3.5 Artificial Intelligence Methods.....	40
3.5.1 Artificial Neural Network (ANN)	40
3.5.2 Neuro Fuzzy.....	41
3.5.3 Adaptive Neuro-Fuzzy Inference System (ANFIS).....	43
3.5.4 Genetic Algorithms.....	44
Chapter Four: Neural Networks.....	46
4.1 Introduction.....	47
4.2 NN Neuron.....	48
4.3 Activation Functions.....	49
4.4 NN Structure.....	50
4.4.1 Feed-forward NN.....	50
4.4.2 Recurrent NN.	51
4.5 NN Learning Strategies.....	52
4.6 Training and Testing NN.....	54
4.6.1 Choosing the Number of Neurons.....	54
4.6.2 Choosing the Initial Weights.....	55
4.6.3 Choosing the Learning Rate.....	55
4.7 Training Functions.....	55
Chapter Five: Model Simulation.....	57
5.1 Building Model.....	58
5.2 Three Gorges - Changzhou Main Components.....	59
5.2.1 Filters.....	59
5.2.2 Valves.....	59
5.2.3 Converter Transformers.....	59
5.2.4 DC Smooth Reactors.....	59
5.3 Model Outputs.....	60
5.3.1 Model Outputs at Fault and No-Fault Conditions	61
5.3.2 Fault Location Effect on the Model Outputs.....	61
5.4 Simulator Levels.....	61
5.5 Neural Network Application.....	62
5.5.1 Training of Fault Detection Neural Network.....	63
5.5.2 Testing of Fault Detection Neural Network.....	64
5.5.3 Training of Fault Classifying Neural Network.....	64
5.5.4 Testing of Fault Classifying Neural Network.....	66
5.5.5 Training of Positive to Ground Fault Locator Neural Network.	66
5.5.6 Testing of Positive to Ground Fault Locator Neural Network...	67
5.5.7 Training of Negative to Ground Fault Locator Neural Network.....	68
5.5.8 Testing of Negative to Ground Fault Locator Neural Network..	68
5.5.9 Training of Positive to Negative Line Fault Locator Neural Network.....	69
5.5.10 Testing of Positive to Negative Line Fault Locator Neural Network.....	70
5.5.11 Training of Positive Line Open Circuit Fault Locator Neural Network.....	71
5.5.12 Testing of Positive Line Open Circuit Fault Locator Neural Network.....	72

5.5.13 Training of Negative Line Open Circuit Fault Locator Neural Network.....	73
5.5.14 Testing of Negative Line Open Circuit Fault Locator Neural Network.....	73
5.6 Simulation Summary.....	75
Chapter Six: Conclusion.....	77
Abbreviations.....	79
References.....	81

LIST OF TABLES

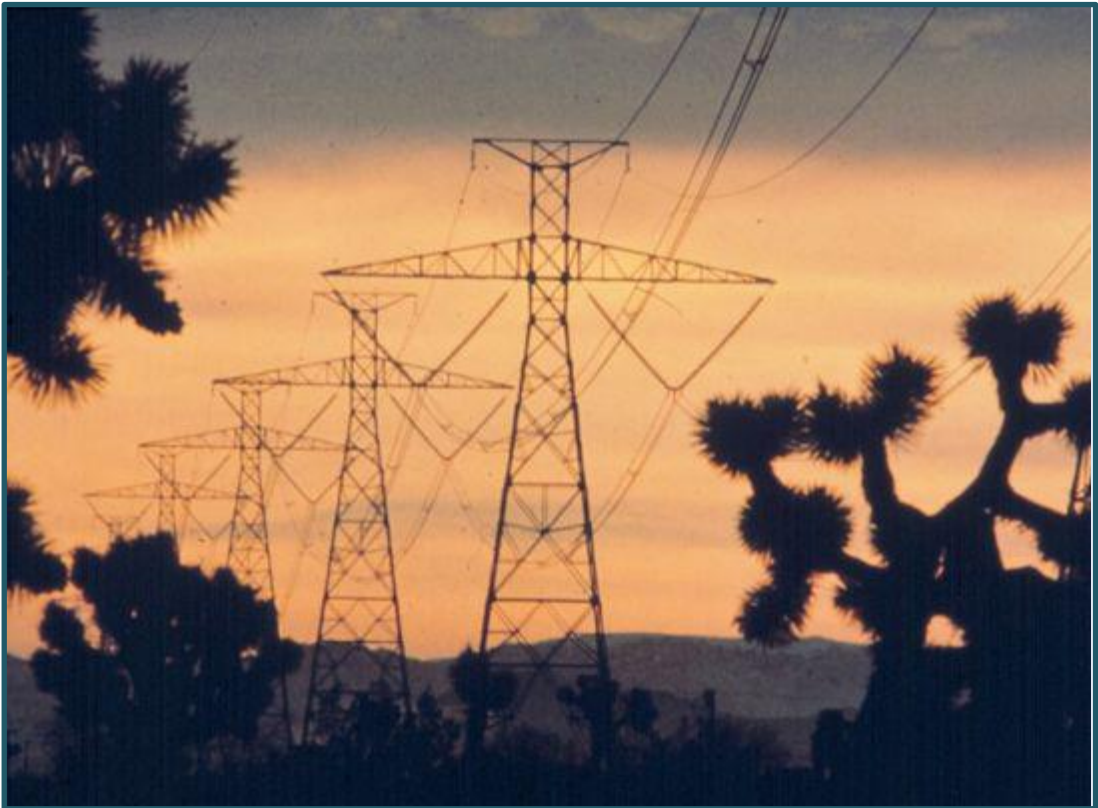
Table (4.1): Training Algorithms and their MATLAB Functions.....	55
Table (5.1): Summarized Specifications of the Simulated Model.....	60
Table (5.2): Comparison of Model Output for Fault and No-Fault Conditions at Distances of 340- and 600- km Away from the Rectifier side.....	62
Table (5.3): Fault Types and Their Codes.....	64
Table (5.4): Errors of Testing +Ve/GND Fault Locator NN	67
Table (5.5): Errors of Testing -Ve/GND Fault Locator NN	69
Table (5.6): Errors of Testing +Ve/-Ve Fault Locator NN	71
Table (5.7): Errors of Testing +Ve O.C Fault Locator NN.....	72
Table (5.8): Errors of Testing -Ve O.C Fault Locator NN.....	74
Table (5.9): Summary of the Used NNs.....	75

LIST OF FIGURES

Figure (1.1): A basic three-layer architecture of a feed-forward ANN.....	4
Figure (2.1): Total Cost Vs. Distance for HVAC & HVDC.....	10
Figure (2.2): Typical transmission line structures for 1000 MW.....	10
Figure (2.3): Conventional HVDC with current source converter.....	11
Figure (2.4): HVDC with voltage source converters.....	11
Figure (2.5): Thyristor valve arrangement for a 12-pulse converter with three quadruple valves, one for each phase.....	12
Figure (2.6): HVDC IGBT valve converter arrangement.....	13
Figure (2.7): Six-Pulse Converter and Current Switching Pattern.....	14
Figure (2.8): Effect of Commutation on Converter Operation.....	14
Figure (2.9): Effect of Firing Angle on Converter Operation.....	15
Figure (2.10): Effect of Firing Angle as it Approaches 90°.....	15
Figure (2.11): Effect of a Firing Angle of 140°.....	15
Figure (2.12): Monopolar HVDC System with Ground Return.....	16
Figure (2.13): Monopolar HVDC System with Metallic Return.....	17
Figure (2.14): Bipolar HVDC system.....	17
Figure (2.15): Bipolar HVDC System with Monopolar Metallic Return for Pole Outage.....	18
Figure (2.16): Tripole HVDC System	18
Figure (2.17): Back-To-Back HVDC System.....	19
Figure (2.18): 500MW Back-To-Back HVDC System Converter Station.....	19
Figure (2.19): Valve module , MVU and the representation of each in single diagram.....	20
Figure (2.20): A HVDC converter transformer	21
Figure (2.21): Typical Converter transformer arrangements.....	21
Figure (2.22): Air-insulated dc smoothing reactor, Inductance: 150 mH, Rated voltage: 500 kV DC, Rated current:1800 A DC.....	22
Figure (2.23): Three-Phase fundamental frequency sine-wave before and after the effect of 5th harmonic.....	23
Figure (2.24): A typical twelve-pulse converter bridge.....	24
Figure (2.25): HVDC converter station and location of filters.....	25
Figure (2.26): DC harmonic filter capacitors.....	25
Figure (2.27): Single Tuned Band Pass filter construction , design equations and response.....	26
Figure (2.28): High Pass filter construction , design equations and response of 24th harmonic.....	26
Figure (2.29): Double tuned filter construction and response of 11/13th harmonics.....	27
Figure (2.30): C-type filter construction, design equations and response.....	27
Figure (2.31): A single pole-to-ground fault on a bipolar system.....	28
Figure (2.32): A pole-to-pole fault on a bipolar system.....	28
Figure (2.33): A pole-to-pole to ground fault on a bipolar system.....	29
Figure (3.1): One-line diagram and equivalent circuit for a three-phase fault on a transmission line with two sources, G and H.....	33
Figure (3.2): Traveling voltage and current waves: lattice diagram for a fault at distance x from A.....	37
Figure (3.3): Structure of the simple FNN.....	41
Figure (3.4): Detailed fault-location scheme based on FNN.....	42

Figure (3.5): Flow chart of basic GA.....	45
Figure (4.1): The style of neural computation.....	47
Figure (4.2): Nonlinear model of a neuron.....	48
Figure (4.3): Different types of activation functions.....	49
Figure (4.4): General structure of feed-forward NN.....	50
Figure (4.5): Structure of recurrent NN.....	51
Figure (4.6): Scheme of supervised learning.....	52
Figure (4.7): Structure of back-error-propagation algorithm.....	54
Figure (5.1): Three Gorges – Changzhou Single Line Diagram	58
Figure (5.2): HVDC MATLAB model.....	59
Figure (5.3): Simulation levels.....	63
Figure (5.4): Performance of DC input fault detection NN	63
Figure (5.5): Performance of ten input fault detection NN.....	64
Figure (5.6): Performance of DC input fault classifying NN... ..	65
Figure (5.7): Performance of ten input fault classifying NN.....	65
Figure (5.8): Regression plot of training positive to ground fault locator NN....	66
Figure (5.9): Regression plot of testing positive to ground fault locator NN ..	69
Figure (5.10): Regression plot of training negative to ground fault locator NN .	68
Figure (5.11): Regression plot of testing negative to ground fault locator NN....	69
Figure (5.12): Regression plot of training positive to negative line fault locator NN.....	70
Figure (5.13): Regression plot of testing positive to negative line fault locator NN.....	70
Figure (5.14): Regression plot of training positive line open circuit fault locator NN.....	71
Figure (5.15): Regression plot of testing positive line open circuit fault locator NN	72
Figure (5.16): Regression plot of training negative line open circuit fault locator NN.....	73
Figure (5.17): Regression plot of testing negative line open circuit fault locator NN.....	74

CHAPTER 1 INTRODUCTION



1.1 Background

An electric power system comprises of generation, transmission and distribution of electric energy. Transmission lines (TL) are used to transmit electric power to distant large load centers. The rapid growth of electric power systems over the past few decades has resulted in a large increase of the number of lines in operation and their total length. These lines are exposed to faults as a result of lightning, short circuits, faulty equipment, miss-operation, human errors, overload and aging. Many electrical faults manifest in mechanical damages, which must be repaired before returning the line to service. The restoration can be expedited if the fault location is either known or can be estimated with a reasonable accuracy. Faults cause short to long term power outages for customers and may lead to significant losses especially for the manufacturing industry. Fast detecting, isolating, locating and repairing of these faults are critical in maintaining a reliable power system operation[1]. The subject of fault location has been of considerable interest to electric power utility engineers and researchers for many years. Most of the research done to date has been aimed at finding the locations of transmission-line faults. This is mainly because of the impact of transmission-line faults on the power systems and the time required to physically check the lines is much larger than the faults in the sub-transmission and distribution systems [2]. Fault location is a process aimed at locating the occurred fault with the highest possibly accuracy. A fault locator is mainly the supplementary protection equipment, which apply the fault-location algorithms for estimating the distance to fault [2]. Transmission lines experience temporary and permanent faults. Temporary faults, which are the most dominant faults on overhead lines, are self-cleared. In consequence, the power-supply continuity is not permanently affected, which is advantageous. In turn, after the permanent fault occurrence, the related protective relaying equipment enables the associated circuit breakers to de-energize the faulted sections. In the case of permanent faults, the restoration of power supply can be done after the maintenance crew finishes the repair of the damage caused by the fault. For this purpose, the fault position has to be known; otherwise the whole line has to be inspected to find the damaged place. Thus, it is important that the location of a fault is either known or can be estimated with reasonably high accuracy. This allows saving money and time for the inspection and repair, as well as to provide a better service due to the possibility of faster restoration of power supply. This also enables the blackouts to be avoided. Temporary faults are self-cleared and do not affect permanently the supply continuity, however, the location of such faults is also important. In this case the fault location can help to pinpoint the weak spots on the line. As a result, the plans of maintenance schedules can be fixed for avoiding further problems in the future [2].

Transmission lines can carry either alternate current (AC) or direct current (DC), each has its properties and advantages. AC TL is the popular type where the distribution networks are AC and the consumed power at customers is also AC, so using AC TL reduce the costs of inverters and rectifiers which used to convert the current from the direct form to alternate form and vice versa. When the amount of power needed to transmit increases and the distance of transmission become longer the need of using DC TL appears. In some cases when two AC systems with different frequencies need to be interconnected the only method is using DC system as a connection between them. High voltage direct current (HVDC) technology has been considered as a viable alternative to AC for long-distance power transmission and interconnection of power systems. HVDC technology allows power transmission between AC networks with different frequencies or networks which may not be synchronized. Since there is no skin

effect on DC transmission line, inductive and capacitive parameters do not restrict the transmission capacity of HVDC systems. Besides, according to fast DC power modulation configured in a HVDC project's control system, the power oscillation in its related AC power grids can be restrained timely, and that is helpful to enhance the transient stability of power system [3].

In a natural way a fault location can be done by foot patrols or by patrols equipped with different transportation means and binoculars. Such means of faulted-line inspection is considered as time consuming. Recent years have seen an increase in the number of algorithms designed to locate faults to improve protection in electrical power systems and to facilitate supervision and maintenance. Existing fault location methodology involves mainly the following methods:

1. Technique based on fundamental-frequency currents and voltages, mainly on impedance measurement;
2. Methods based on the travelling wave theory, these methods send an electrical pulse along the line and record the signals reflected at both ends. The return time of the pulse from the fault point indicates the distance to that point [1, 2].
3. Methods based on assessing electrical magnitudes at fundamental frequencies: these methods record the voltage and/or current signals at the ends of the line under consideration and find its periodic fundamental component both before and immediately after the fault. When processed suitably, these fundamental components enable the fault to be located.
4. knowledge-based approaches (Artificial Intelligence Methods (AI)).

Artificial Intelligence is a subfield of computer science that investigates how the thought and action of human beings can be mimicked by machines [4]. Both the numeric, nonnumeric and symbolic computations are included in the area of AI.

The mimicking of intelligence includes not only the ability to make rational decisions, but also to deal with missing data, adapt to existing situations and improve itself in the long time horizon based on the accumulated experience.

Three major families of AI techniques are considered to be applied in modern power-system automation and control:

- Expert System Techniques (XPSs).
- Artificial Neural Networks (ANNs).
- Fuzzy-Logic Systems.

At present, there is great scope for research in the field of neural networks in areas such as control systems, fault diagnosis, pattern classification, load forecasting in power systems and elsewhere. It has a capability of learning, generalization, fault tolerance and it is suitable for on line environment [5].

1.1.1 Artificial Neural Networks

An Artificial Neural Network (ANN) can be described as a set of elementary neurons that are usually connected in biologically inspired architectures and organized in several layers [6]. The structure of a feed-forward ANN is shown in Figure (1.1). There are N_i numbers of neurons in each I^{th} layer and the inputs to these neurons are connected to the previous layer neurons. The input layer is fed with the excitation signals. Simply put, an

elementary neuron is like a processor that produces an output by performing a simple non-linear operation on its inputs [7]. A weight is attached to each and every neuron

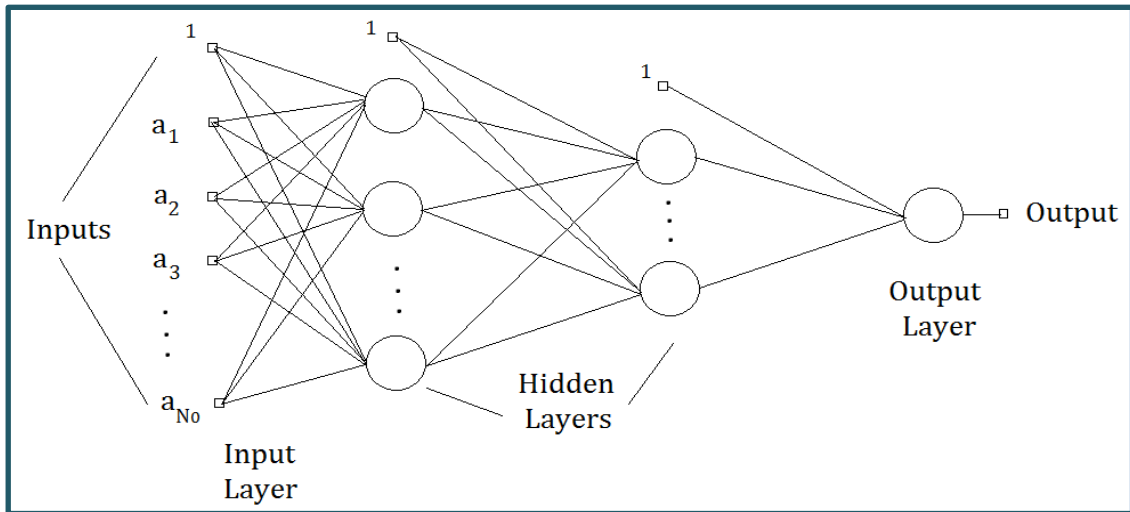


Figure (1.1): A basic three-layer architecture of a feed-forward ANN [6]

and training an ANN is the process of adjusting different weights tailored to the training set. An Artificial Neural Network learns to produce a response based on the inputs given by adjusting the node weights. Hence we need a set of data referred to as the training data set, which is used to train the neural network.

There are many techniques and algorithms used to determine the weights of layered ANN, the most common techniques are [8]:

1. Back-propagation Algorithm.
2. Radial Basis Function.
3. Support Vector Machines.
4. Committee Machines.

In this work we will focus on Back-propagation Algorithm to solve the model of HVDC Transmission Line. Back-propagation was created by generalizing the Widrow-Hoff learning rule to multiple-layer networks and nonlinear differentiable transfer functions. Input vectors and the corresponding target vectors are used to train a network until it can approximate a function, associate input vectors with specific output vectors, or classify input vectors in an appropriate way. Standard back-propagation is a gradient descent algorithm, as is the Widrow-Hoff learning rule, in which the network weights are moved along the negative of the gradient of the performance function [9].

1.2 Motivation

The prime motive behind this thesis was the significant impact of a very accurate fault locator could make if employed in a HVDC power transmission system, in terms of the amount of money and time that can be saved where the most HVDC TL are used to transmit power over a very long distances. The main goal of Fault Location is to locate a fault in the power system with the highest achievable accuracy.

One of the important aspects, that this thesis concentrates on, is the analysis of the transmission line's voltages and currents at inverter and rectifier sides of HVDC transmission system with the voltages and currents at the alternate current (AC) sides

during various fault conditions and how they can be effectively utilized in the design of an efficient fault locator. This thesis drew its initial motivation from [10], which demonstrates a method that could be used for location of faults in AC transmission lines. However, when extensively studied, it can be noted that a fault locator with acceptable accuracy can be easily achieved with the help of artificial neural networks by using large amount of data set for training and the learning process. This data simulated many times in different fault locations and the results used to approximate the results of unknown fault locations and for different types of faults.

1.3 Literature review

Due to the simplicity and the existence of a well-defined learning of feed-forward multilayer perceptron technique, most of the previous works have to study it. For example, Kulicke and Dalstein used neural networks for the detection of faults on transmission lines [9], a new technique for the detection and location of high speed faults using neural networks had been proposed by Rikalo, Sobajic and Kezunovic [11]. Neural network based single ended fault location techniques have been widely researched by Chen and Maun [12] while Song used neural networks for fault location on series compensated lines [13].

Because of the few numbers of HVDC Transmission lines over the world in comparison with AC TL, the topic of Power Fault Detection on HVDC TL have a small number of researches and most of them focus on classifying HVDC faults using wavelet techniques.

In 1992, the using of NN to identify faults of AC-DC system with back to back HVDC construction was studied [14]. That paper focused on identifying faults of HVAC TL with probability of fault in back to back HVDC section. Therefore, there's no long HVDC TL to study. The researchers found a way to detect and classify faults but they don't care in the dc faults and they only point to it with (dc fault) without classifying.

In 1993, using NN in HVDC system faults diagnosis was studied [15]. A 20-12-4 NN structure was used to classify 16 different fault types for a six-pulse HVDC system. Using twenty different inputs; voltage across and current through each thyristor (9-inputs), DC voltage and current at the rectifier end (2-input), three phase voltages and currents through the transformer (6-inputs), three inputs to represent the conduction pattern of the thyristors over one period. This paper focuses on detecting and classifying faults in AC-DC section with faults in the converter. Don't determine the fault location and not specialized on the HVDC TL.

In 1998, radial basis function NN was used for fault diagnosis in a HVDC system. The researchers here used eight different inputs and classify five types of faults (four of them to classify AC faults). The researchers decrease inputs by using ground current instead of three currents of AC system [16]. As mentioned in previous papers the researchers didn't care in HVDC TL section they only referred to the faults in HVDC by (DC fault) without classifying.

In 2000, A new method to reduce the needed training data at the cost of time delay by using expert systems with NN to classify –only- HVDC faults. They use the same way that was used in 1998 to reduce inputs by using ground current. Expert knowledge was used to reduce training data. In this paper, inputs took as patterns with window length covers both pre/post fault regions [17].

In 2001, researchers used wavelet modulus maxima technique in analysis and identification of HVDC system [18]. A12-pulse unipolar HVDC system model was simulated with this technique to classify three types of faults; DC line short circuit fault, commutation failure at the inverter station, single-phase short circuit fault at AC side of inverter. This paper does not interest in HVDC TL nor the fault position determination.

In 2010, researchers introduced a new method in determining HVDC TL fault location [19]. This method depends on using both mathematical equations and wavelet technique to determine the fault location in bipolar HVDC TL. Maximum of 0.55% error in one pole to ground fault, 0.78% error in bipole to ground fault and maximum of 0.75% error in pole to pole fault - in related to the overall length of 1000 km HVDC TL-. The good results are in cost of time because the introduced function needed to be calculates each km of TL and the equation itself takes a long time to be calculated.

June 2011, Fault location in extra-long HVDC TL using continuous wavelet transformation method was studied on 6-pulse HVDC system [20]. This method suffers in two main problems; it works at off-line environment and needs to special instruments to calculate the fault position. According to the paper it's possible to achieve fault location prediction error of $\pm 400\text{m}$ for the test system with 2400 km overhead HVDC TL.

November 2011, reverse travelling wave was used with a new mathematical analysis and equations to locate faults in a HVDC TL [10]. Sampling frequency of 80 KHz and signal processing methods were used to get accuracy of 98.56%. The need for special equipment and working in off-line environment are the main problems in this method.

In 2012, the wavelet based multi-resolution analysis was used to classify both AC and DC faults [21]. Researchers here tried to find a new method to classify HVDC faults by studying the percentage variation of phase voltages and currents in each fault case.

In 2014, IEEE researchers used ANN for fault classification on HVDC systems and succeeded to diagnose HVDC faults. Here NN output can predict the change in the firing angle required for the HVDC rectifier unit and each value of the firing angle refers to special type of fault [22].

1.4 Contribution

The contribution of this thesis can be concluded in the following points:

1. The focus of this work is on the faults on the HVDC TL link and not on the AC grid of the power system nor on the rectifier or the inverter stations while most previous researches have studied the HVDC TL as a part of a complete HVDC system.
2. In addition to detection and classification tasks, this thesis discusses the determination of fault location using NN technology. Most of the previous related works focus only on classifying and detecting of faults.
3. Using NN in HVDC gives the ability to get results in the on-line environment contrary to using travelling wave method where you must work in off-line

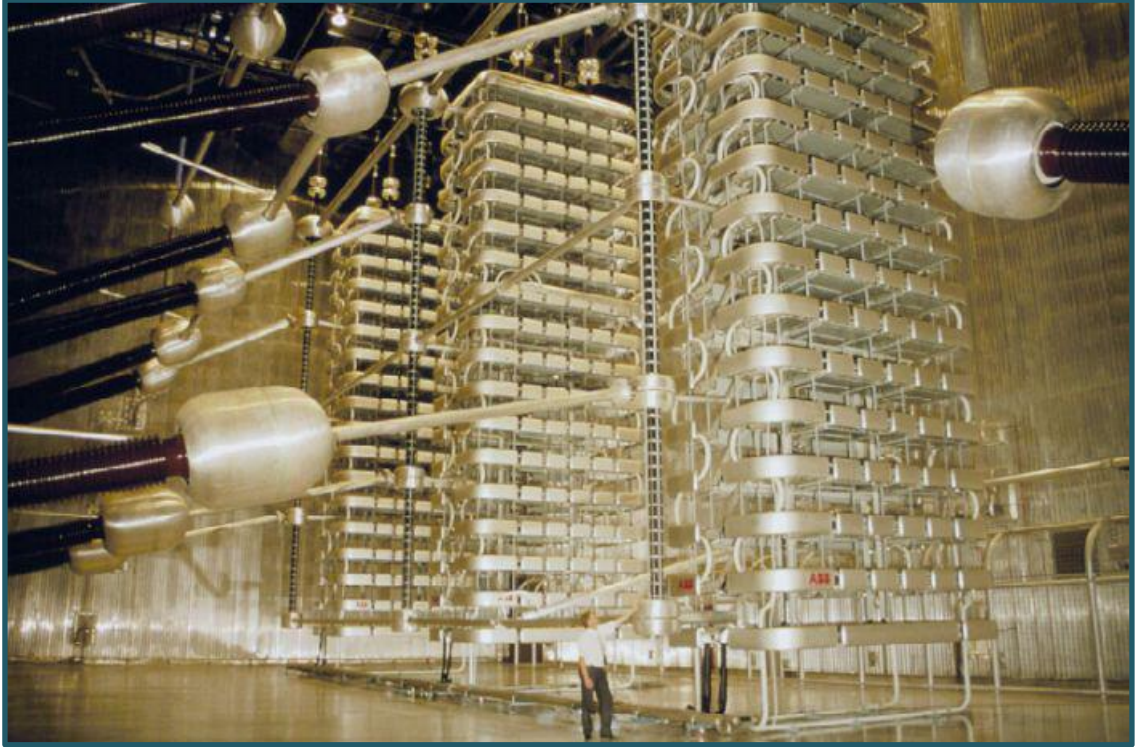
environment. Therefore, using NN to diagnose HVDC faults can detect the instantaneous and permanent faults where using any other method in off-line environments detects only permanent faults.

4. Using neural networks need no additional equipment where any HVDC system must have monitoring equipment for voltages and currents at converter stations.

1.5 Outline of the Thesis

The second chapter will describe HVDC system, system component, and types of the faults that can face HVDC TL will be studied briefly. Chapter three studies the used techniques to detect and locate faults at power transmission lines, four methods will be studied; Impedance Based method, Travelling wave, high frequency and Artificial Intelligent methods. Chapter four deals with one method of artificial intelligent methods that uses to detect, classify and locate HVDC faults. This method is the Artificial Neural Network (ANN), which will be studied in details where it is the thesis used method. Chapter five presents HVDC system model, series of simulation results that have been obtained using MATLAB, SimPowerSystems, and the Artificial Neural Networks Toolboxes in Simulink to emphasize the efficiency and accuracy factors of the proposed fault locator. Several neural networks with varying configurations have been trained, tested and their performances have been analyzed in this chapter. Finally, chapter six concludes the entire research and the work that's looked forward in future to be done.

CHAPTER 2 HVDC SYSTEM



Electrical power is generated as an alternating current (AC). It is also transmitted and distributed as AC and apart from certain traction and industrial drives and processes, it is consumed as AC. In many circumstances, however, it is economically and technically advantageous to introduce direct current (DC) links into the electrical supply system. In particular situations, it may be the only feasible method of power transmission. DC transmission is used when two AC systems cannot be synchronized or when the distance by land or cable is too long for stable and/or economic AC transmission. At one “converter station” the AC is converted to DC, which is then transmitted to a second converter station, converted back to AC, and fed into another electrical network [23].

In this Chapter, an overview of HVDC system, history and uses will be described in section 2.1. Section 2.2 discusses HVDC converting technologies like voltage source converter (VSC) and line commutated current (LCC) technology. Section 2.3 describes LCC converter theory where it is the thesis used technology. HVDC system connection types and differences between each other are studied in section 2.4. HVDC converter station components discussed in section 2.5 and finally, HVDC TL fault types are discussed in section 2.6.

2.1 Introduction

The transmission and distribution of electrical energy started with direct current in 1882, a 50-km-long 2-kV DC transmission line was built between Miesbach and Munich in Germany. At that time, conversion between reasonable consumer voltages and higher DC transmission voltages could only be realized by means of rotating DC machines. In an AC system, voltage conversion is simple. An AC transformer allows high power levels and high insulation levels within one unit, and has low losses. It is a relatively simple device, which requires little maintenance. Further, a three-phase synchronous generator is superior to a DC generator in every respect. For these reasons, AC technology was introduced at a very early stage in the development of electrical power systems. It was soon accepted as the only feasible technology for generation, transmission and distribution of electrical energy [24].

However, high-voltage AC transmission links have disadvantages, which may compel a change to DC technology, HVDC is preferred to use in four broad categories and any scheme usually involves a combination of two or more of these. The categories are [23]:

1. Transmission of bulk power where AC would be uneconomical, impracticable or subject to environmental restrictions.
2. Interconnection between systems, which operate at different frequencies, or between non-synchronized or isolated systems, which, although they have the same nominal frequency, cannot be operated reliably in synchronism.
3. Addition of power in-feed without significantly increasing the short circuit level of the receiving AC system.
4. Improvement of AC system performance by the fast and accurate control of HVDC power.

For a given transmission task, feasibility studies are carried out before the final decision on implementation of an HVAC or HVDC system can be taken.

Figure (2.1) shows a typical cost comparison curve between AC and DC transmission considering:

- AC vs. DC station terminal costs
- AC vs. DC line costs
- AC vs. DC capitalized value of losses

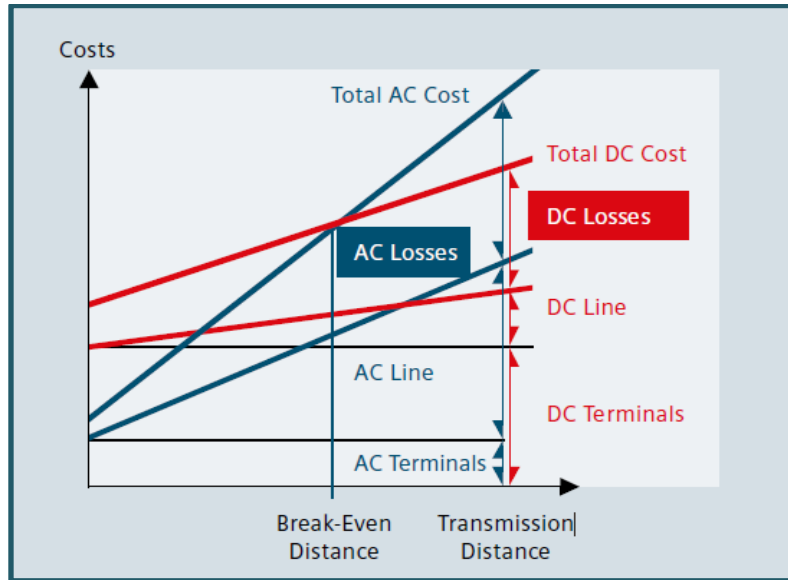


Figure (2.1): Total Cost Vs. Distance for HVAC & HVDC [24]

The DC curve is not as steep as the AC curve because of considerably lower line costs per kilometer. For long AC lines the cost of intermediate reactive power compensation has to be taken into account. The break-even distance is in the range of 500 to 800 km depending on a number of other factors, like country-specific cost elements, interest rates for project financing, loss evaluation, cost of right of way, etc.

The land coverage and the associated right-of-way cost for a HVDC overhead transmission line is not as high as that of an AC line. This reduces the visual impact and saves land compensation for new projects. It is also possible to increase the power transmission capacity for existing rights of way. A comparison between a DC and an AC overhead line is shown in Figure (2.2) [24].

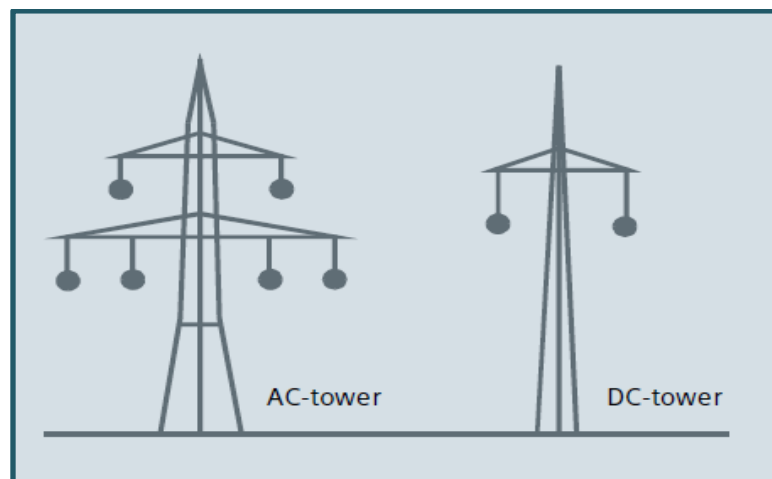


Figure (2.2): Typical transmission line structures for 1000 MW [24]

2.2 HVDC Converter Technologies

Two basic converter technologies are used in modern HVDC transmission systems. These are conventional line-commutated current source converters (CSCs) or (LCC) and self-commutated voltage source converters (VSCs). Figure (2.3) shows a conventional HVDC converter station with CSCs while Figure (2.4) shows a HVDC converter station with VSCs [25].

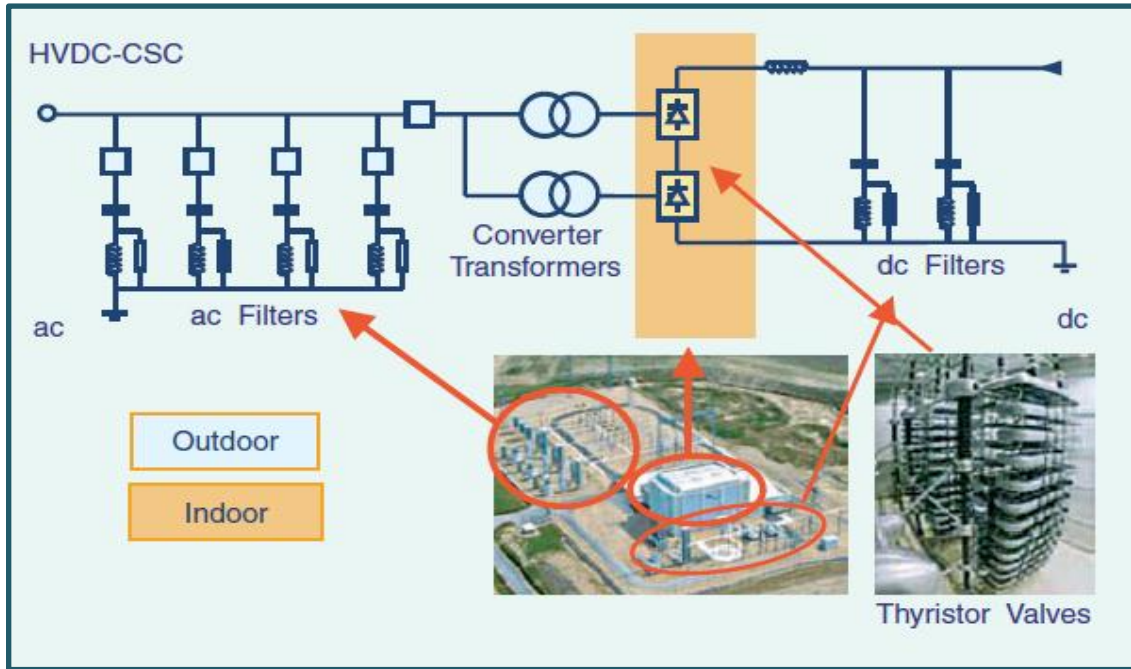


Figure (2.3): Conventional HVDC with current source converter [25]

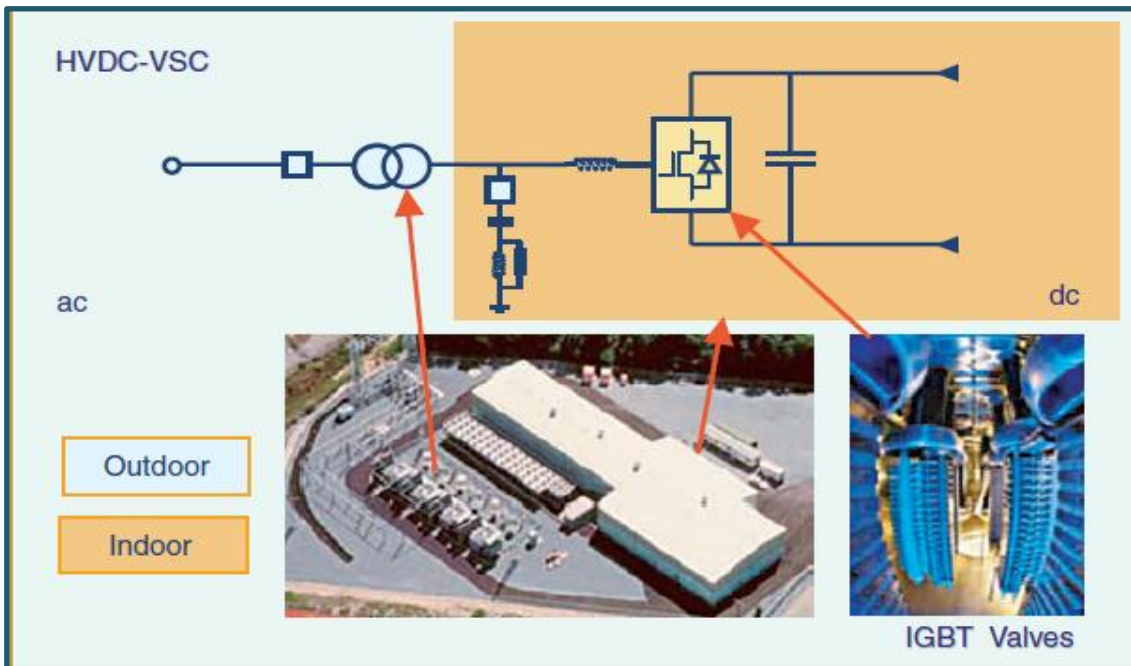


Figure (2.4): HVDC with voltage source converters [25]

2.2.1 Line Commutated Current Source Converter

Conventional HVDC transmission employs line-commutated CSCs with thyristor valves. Such converters require a synchronous voltage source in order to operate. The basic building block used for HVDC conversion is three phase, full-wave bridge referred to as a six-pulse or Graetz bridge. The term six-pulse is due to six commutations or switching operations per period resulting in a characteristic harmonic ripple of six times the fundamental frequency in the dc output voltage. Each six-pulse bridge is comprised of six controlled switching elements or thyristor valves. Each valve is comprised of a suitable number of series-connected thyristors to achieve the desired dc voltage rating. The dc terminals of two six-pulse bridges with ac voltage sources phase displaced by 30° can be connected in series to increase the dc voltage and eliminate some of the characteristic ac current and dc voltage harmonics. Operation in this manner is referred to as 12-pulse operation. In 12-pulse operation, the characteristic ac current and dc voltage harmonics have frequencies of $12n+1$ and $12n$, respectively. The 30° phase displacement is achieved by feeding one bridge through a transformer with a wye-connected secondary and the other bridge through a transformer with a delta-connected secondary. Most modern HVDC transmission schemes utilize 12-pulse converters to reduce the harmonic filtering requirements required for six-pulse operation; e.g., fifth and seventh on the ac side and sixth on the dc side. This is because, although these harmonic currents still flow through the valves and the transformer windings, they are 180° out of phase and cancel out on the primary side of the converter transformer. Figure (2.5) shows the thyristor valve arrangement for a 12-pulse converter with three quadruple valves, one for each phase. Each thyristor valve is built up with series-connected thyristor modules [25].

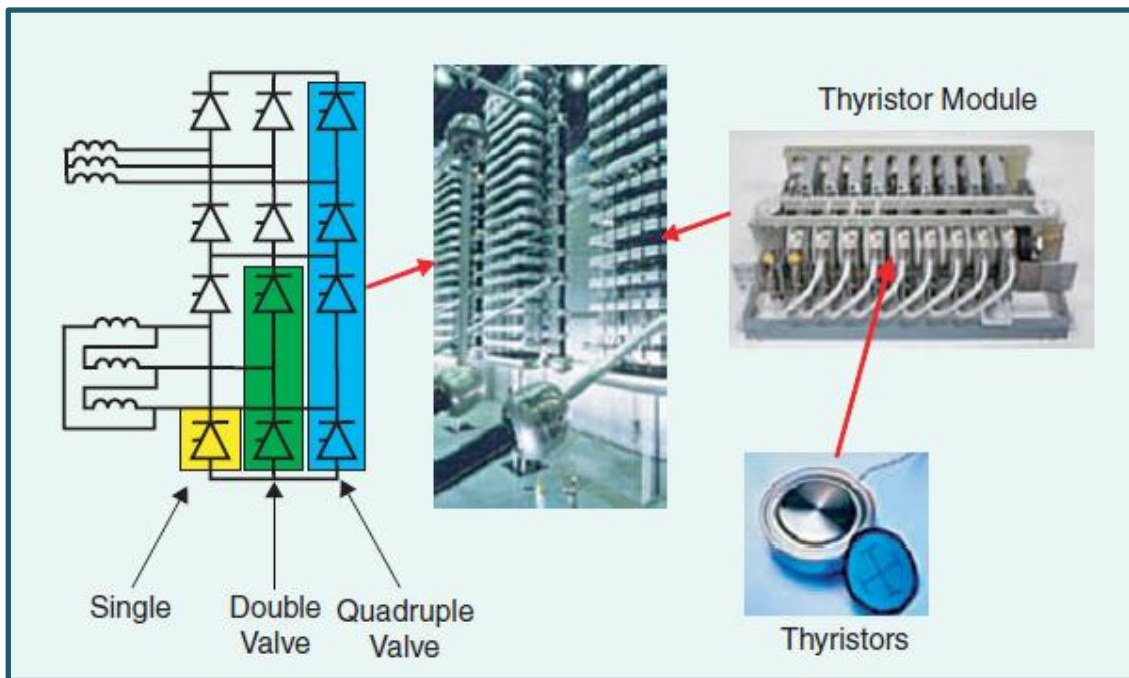


Figure (2.5): Thyristor valve arrangement for a 12-pulse converter with three quadruple valves, one for each phase [25]

2.2.2 Self Commutated Voltage Source Converter

HVDC transmission using VSCs with pulse-width modulation (PWM), commercially known as HVDC Light, was introduced in the late 1990s. Since then the progression to higher voltage and power ratings for these converters has roughly paralleled that for thyristor valve converters in the 1970s. These VSC-based systems are self-commutated with insulated-gate bipolar transistor (IGBT) valves and solid-dielectric extruded HVDC cables. VSC technology can rapidly control both active and reactive power independently of one another. Reactive power can also be controlled at each terminal independent of the dc transmission voltage level. This control capability gives total flexibility to place converters anywhere in the AC network since there is no restrictions on minimum network short-circuit capacity. Self-commutation with VSC even permits black start; i.e., the converter can be used to synthesize a balanced set of three phase voltages like a virtual synchronous generator. The dynamic support of the ac voltage at each converter terminal improves the voltage stability and can increase the transfer capability of the sending- and receiving-end ac systems, thereby leveraging the transfer capability of the dc link. Figure (2.6) shows the IGBT converter valve arrangement for a VSC station. Unlike conventional HVDC transmission, the converters themselves have no reactive power demand and can actually control their reactive power to regulate ac system voltage just like a generator [25].

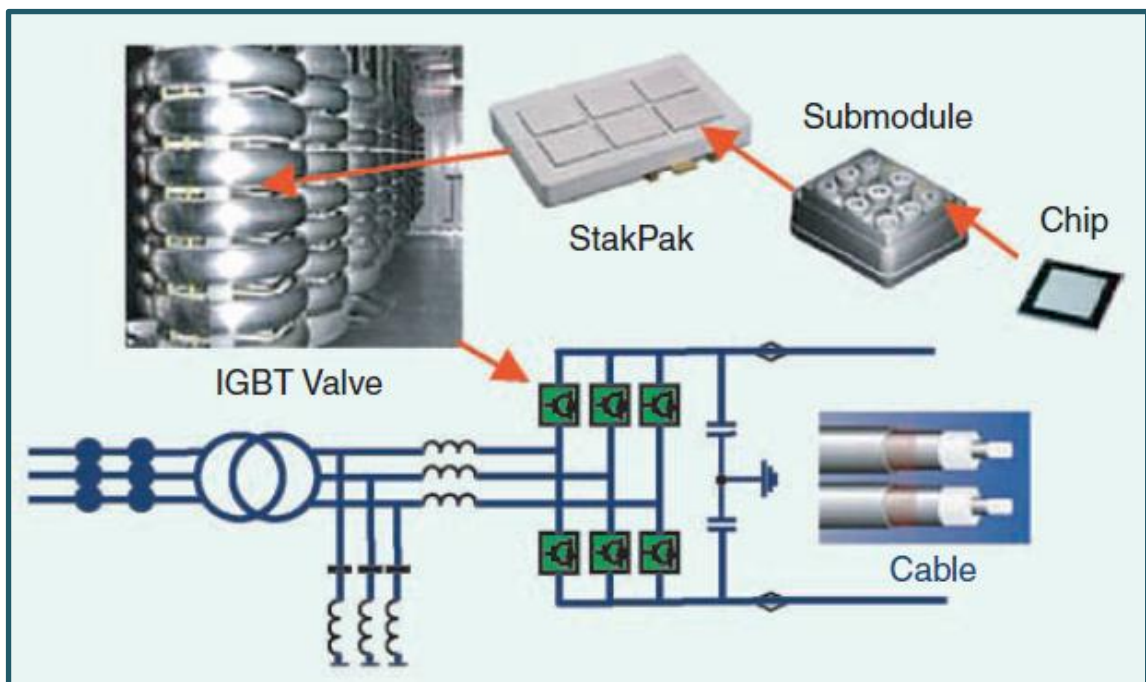


Figure (2.6): HVDC IGBT valve converter arrangement [25]

2.3 LCC Converter Theory

Six-pulse converters are the building block of HVDC systems. An example of a six-pulse converter, which employs diodes, is shown in Figure (2.7). Diodes conduct in the sequence 1,2,3,4,5,6, so the transitions between one diode and the next occur alternately in the upper and lower half-bridges. Each diode conducts for 120° , in every 360° cycle, so that the successive conducting pairs of diodes are 1 and 2, 2 and 3, 3 and 4, 4 and 5, 5 and 6, and 6 and 1. The conducting pair is always that pair of diodes which have the largest instantaneous AC voltage between them. The other diode pairs are connected to an instantaneously smaller voltage and hence are subjected to a reverse voltage across their terminals. As time passes, the relative amplitudes of the converter's three AC supply phases (valve-winding voltages) change, so in Figure (2.7) the voltage B-C becomes greater than the voltage A-C and valve 3 takes over the current which had been flowing in valve 1. This process is known as "commutation". In practice, the transfer of current from one diode to the next requires a finite time, since the current transfer is slowed down by the commutation reactance (made up of reactance in the converter transformer, the thyristor valve and a small amount in the HF filtering circuit). This produces an "overlap" between successive periods of conduction in one half of the six-pulse bridge. The time taken to commutate the current from one valve to the next is called the "overlap angle", μ and can be seen clearly in Figure (2.8) [24].

In a thyristor converter, shown in Figure (2.7), it is possible to vary the mean direct voltage by controlling the instant at which the thyristors are turned on. A thyristor is turned on (fired) by applying a short pulse to its gate terminal and turns off when the external circuit forces its anode current to zero. In this case, current zero is brought about by the commutation process when the next thyristor is fired. The firing delay angle α is defined as the angle between the phase voltage crossing of the valve-winding voltage and the instant when the thyristor is fired. This is illustrated in Figures (2.9), (2.10) and (2.11). This delay angle determines when the commutation process will commence and consequently determines the mean direct voltage (V_d). V_d is proportional to the cosine of α ; i.e. the greater the delay angle, the smaller the mean direct voltage. Zero voltage is reached as α approach 90° [23].

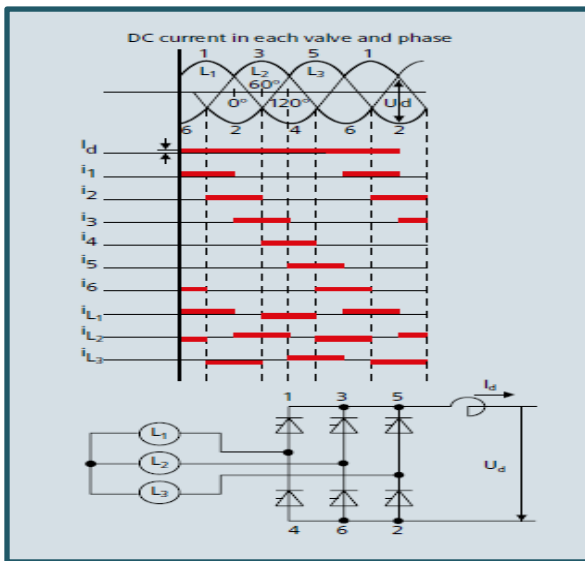


Figure (2.7): Six-Pulse Converter and Current Switching Pattern [24]

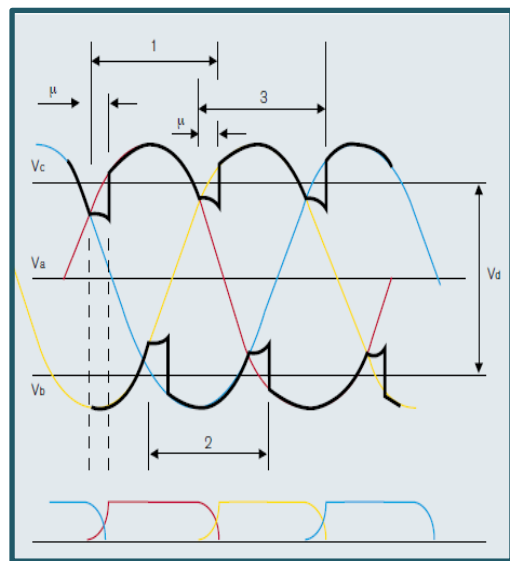


Figure (2.8): Effect of Commutation on Converter Operation [23]

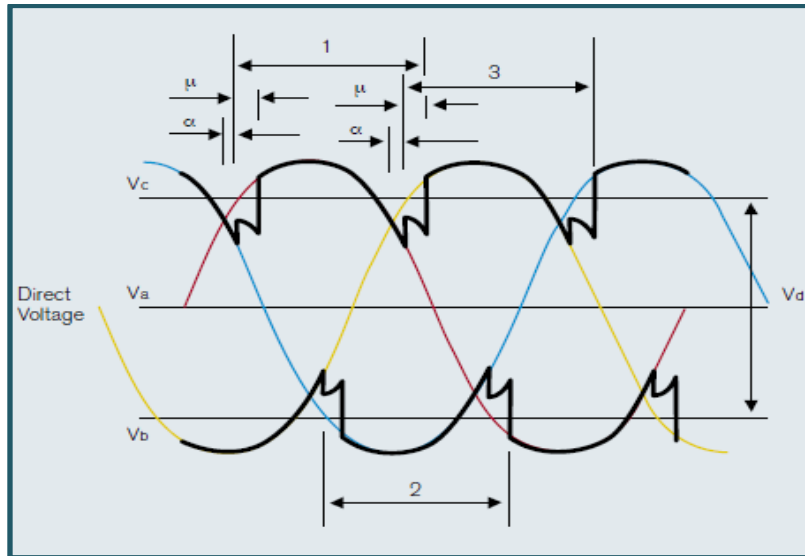


Figure (2.9): Effect of Firing Angle on Converter Operation [23]

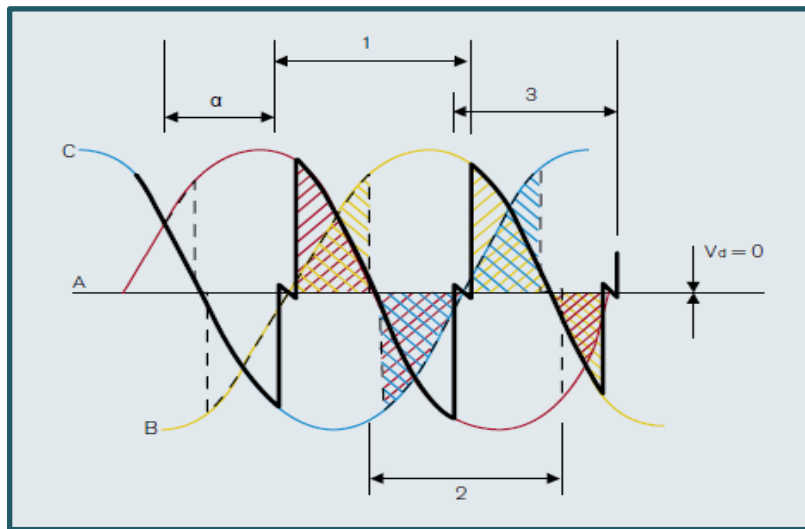


Figure (2.10): Effect of Firing Angle as it Approaches 90° [23]

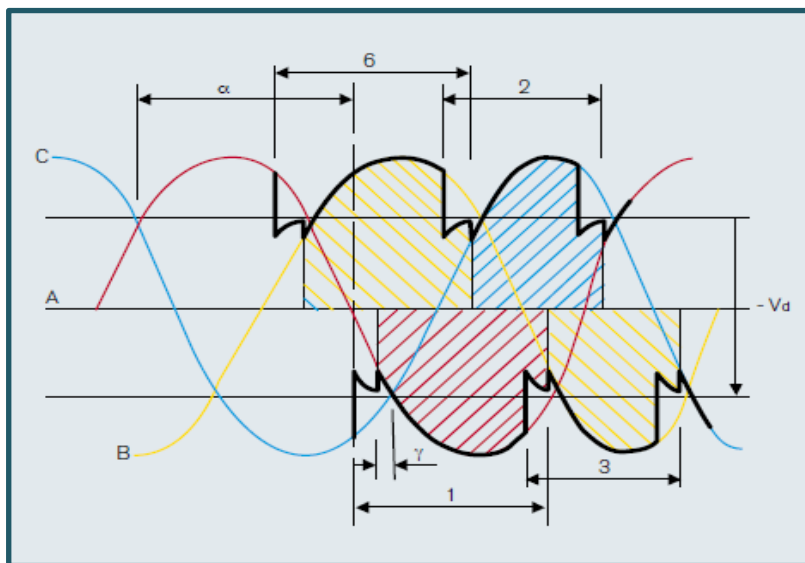


Figure (2.11): Effect of a Firing Angle of 140° [23]

By increasing the firing angle, α , beyond 90° , the voltage area of the phase-to-phase voltage connected to the DC terminals via the conducting thyristors will be predominantly negative; hence the DC terminal voltage will be negative. As, beyond 90° , the firing angle of the converter becomes large, it is more common to refer to the “extinction angle” or “gamma”, γ . This extinction angle represents the time between the end of the overlap period and the time when the phase voltage associated with the outgoing valve becomes more positive/negative than that of the next valve in sequence, and it is mathematically expressed as:

$$\gamma = 180^\circ - \mu - \alpha$$

It must be noted that the control of the output voltage of a six-pulse bridge is only achieved by the firing angle, α . The extinction angle, γ , is a measure of the available turn-off time for the valve following the point in time where the valve is fired [23].

2.4 HVDC System Configurations

HVDC system can be arranged by many different schemes depend on needed capacity and costs. These schemes can be divided as follow:

2.4.1 Monopolar HVDC System

Monopolar HVDC systems have either ground return or metallic return:

2.4.1.1 A Monopolar HVDC System with Ground Return

The ground return consists of one or more six-pulse converter units in series or parallel at each end, a single conductor and return through the earth or sea, as shown in Figure (2.12). It can be a cost-effective solution for a HVDC cable transmission and/or the first stage of a bipolar scheme [26]. At each end of the line, it requires an electrode line and a ground or sea electrode built for continuous operation.

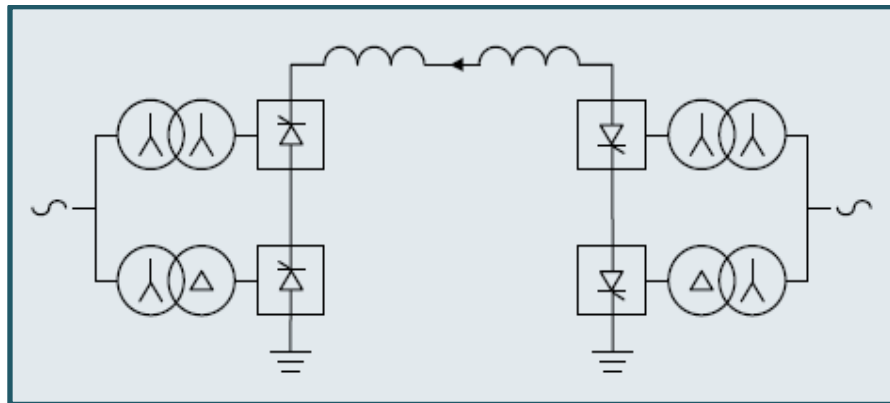


Figure (2.12): Monopolar HVDC System with Ground Return [23]

2.4.1.2 A Monopolar HVDC System with Metallic Return

Usually consists of one high voltage and one medium voltage conductor as shown in Figure (2.13). A monopolar configuration is used either as the first stage of a bipolar scheme, avoiding ground currents, or when construction of electrode lines and ground electrodes results in an uneconomical solution due to a short distance or high value of earth resistivity [23].

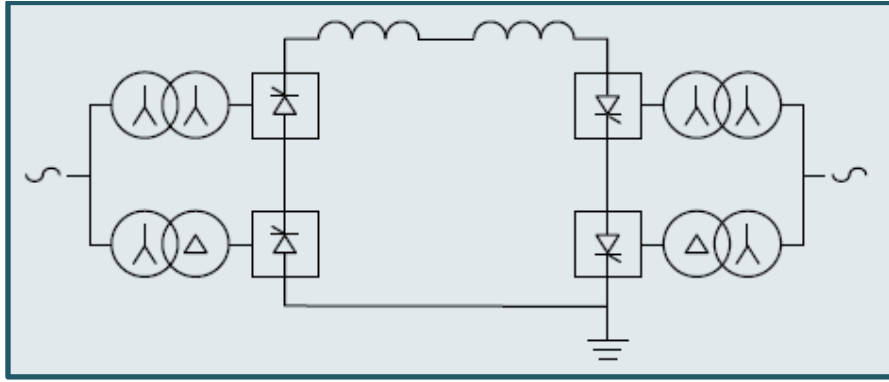


Figure (2.13): Monopolar HVDC System with Metallic Return [23]

2.4.2 Bipolar HVDC System

A Bipolar HVDC System consists of two poles, each of which includes one or more twelve-pulse converter units, in series or parallel. There are two conductors, one with positive and the other with negative polarity to ground for power flow in one direction. For power flow in the other direction, the two conductors reverse their polarities. A Bipole system is a combination of two monopolar schemes with ground return, as shown in Figure (2.14) [27].

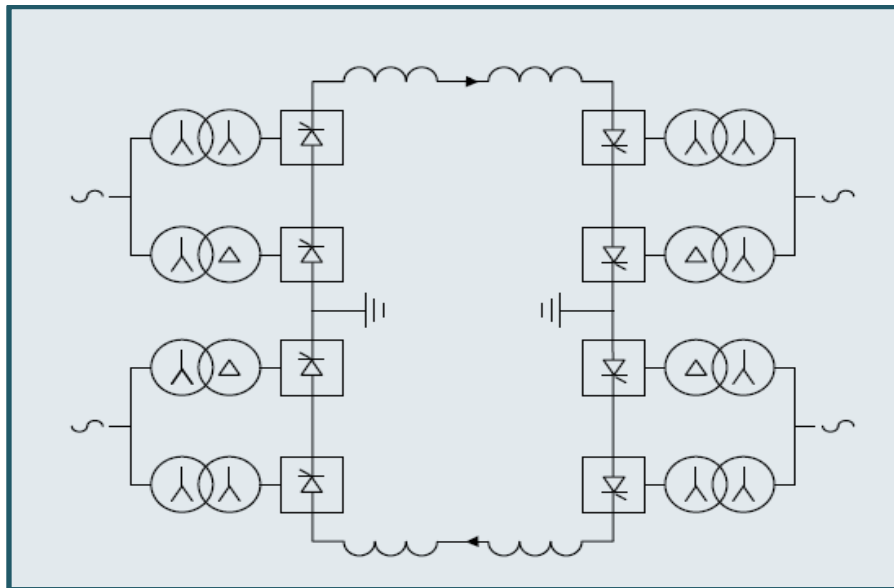


Figure (2.14): Bipolar HVDC System [23]

With both poles in operation, the imbalance current flow in the ground path can be held to a very low value. This is a very common arrangement with the following operational capabilities:

- During an outage of one pole, the other could be operated continuously with ground return.
- For a pole outage, in case long-term ground current flow is undesirable, the bipolar system could be operated in monopolar metallic return mode, if appropriate DC arrangements are provided, as shown in Figure (2.15).

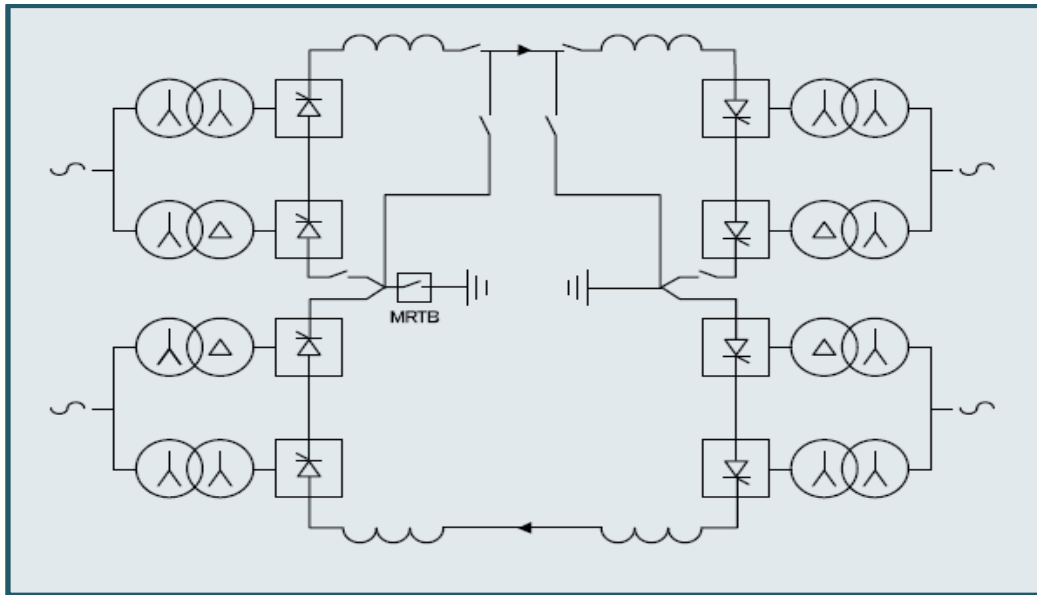


Figure (2.15): Bipolar HVDC System with Monopolar Metallic Return for Pole Outage [23]

- During maintenance of ground electrodes or electrode lines, operation is possible with connection of neutrals to the grounding grid of the terminals, with the imbalance current between the two poles held to a very low value.
- When one pole cannot be operated with full load current; the two poles of the bipolar scheme could be operated with different currents, as long as both ground electrodes are connected.
- In case of partial damage to DC line insulation, one or both poles could be continuously operated at reduced voltage [23].

2.4.3 Tripole HVDC System

It's new idea of transmission DC (since 2004). This structure based on a bipole and monopole systems fed from the same bus and supplying a common receiving-end bus. Monopole earth return current is eliminated by two modifications , The monopole is equipped with an additional bridge connected in anti-parallel to the first and all thyristors and their heat sinks are rated higher than normal. Transformers and other station equipment are standard, both in design and rating [28]. Figure (2.16) shows the arrangement of tripole HVDC system.

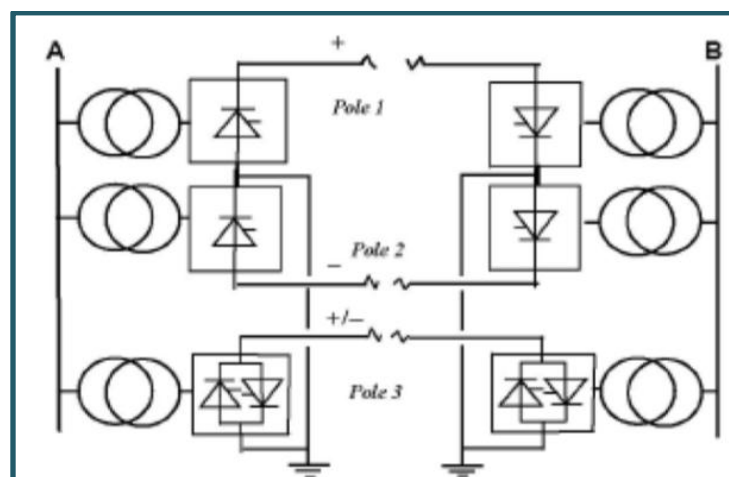


Figure (2.16): Tripole HVDC System [28]

2.4.4 Back-To-Back HVDC System

The expression Back-to-back indicates that the rectifier and inverter are located in the same station. Back-to-back converters are mainly used for power transmission between adjacent AC grids, which cannot be synchronized. They can also be used within a meshed grid in order to achieve a defined power flow [24]. Here there is no DC transmission line and both converters are located at the same site. For economic reasons each converter is usually a twelve-pulse converter unit and the valves for both converters may be located in one valve hall. The control system, cooling equipment and auxiliary system may be integrated into configurations common to the two converters. DC filters are not required, nor are electrodes or electrode lines, the neutral connection being made within the valve hall. Figure (2.17) shows two different circuit configurations used for back-to-back HVDC links and Figure (2.18) shows 500 MW Back-To-Back HVDC system converter station.

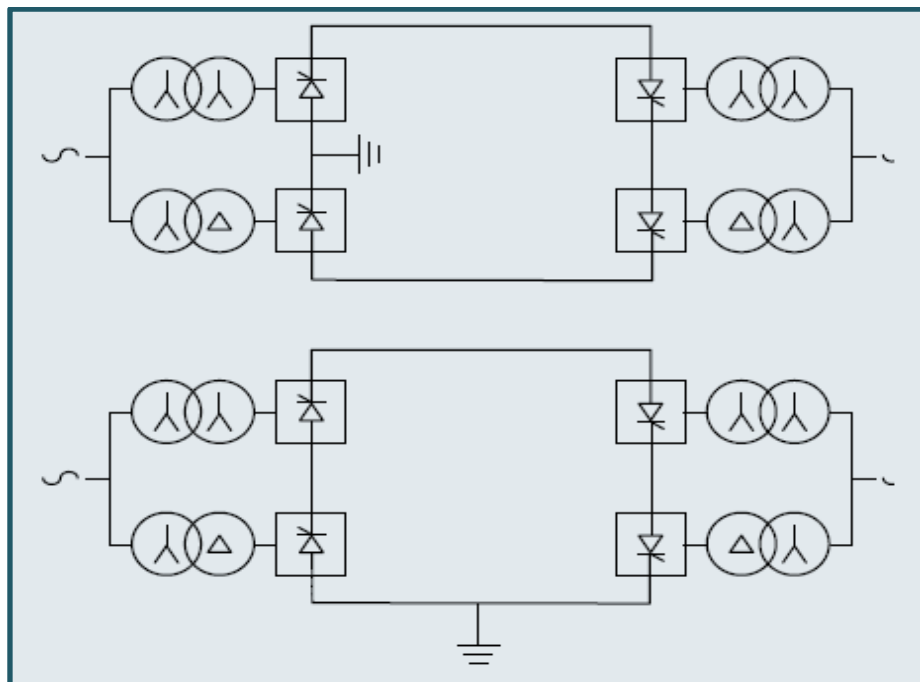


Figure (2.17): Back-To-Back HVDC System [23]



Figure (2.18): 500MW Back-To-Back HVDC System Converter Station [23]

2.5 HVDC Station Components

Any HVDC system must contain three major components; rectifier, inverter and the transmission line. In rectifier, AC current converted to DC form and then transmitted through the transmission line to the inverter to convert current again to AC form. Main components which needed to complete this process in converter station can be concluded as follows:

2.5.1 Thyristor Valves

The thyristor valves make the conversion from AC into DC and thus are the central component of any HVDC converter station. Thyristors are used as switches and thus the valve becomes controllable. The thyristors are made of highly pure mono-crystalline silicon. The high speed of innovation in power electronics technology is directly reflected in the development of the thyristor [24].

Thyristors which used for HVDC valves are amongst the largest semiconductors of any type produced for any industry. Such components are expensive and there may be many thousands of them in a HVDC station. Moreover, they are quite delicate and require a great many additional components to control and protect them. In fact, although it is the most obvious component of a thyristor valve, the thyristors account for a surprisingly low percentage of the total valve cost.

HVDC valves are almost never installed as individual units. Nearly always, several valves are combined together into a “Multiple Valve Unit”, or MVU. The MVU may either be mounted directly on the floor or, more commonly today, suspended from the ceiling. For economy of insulation, the valve design is often arranged so that the lower-voltage valves (usually those associated with the Delta connected six-pulse bridge) are used as part of the insulation on which the higher-voltage valves (usually those associated with the star-connected bridge) are mounted. Hence the low voltage end is the end at which the valve is attached to the floor or ceiling [23]. Figure (2.19) shows valve module and multiple valve units with the representation of MVU in single diagram.

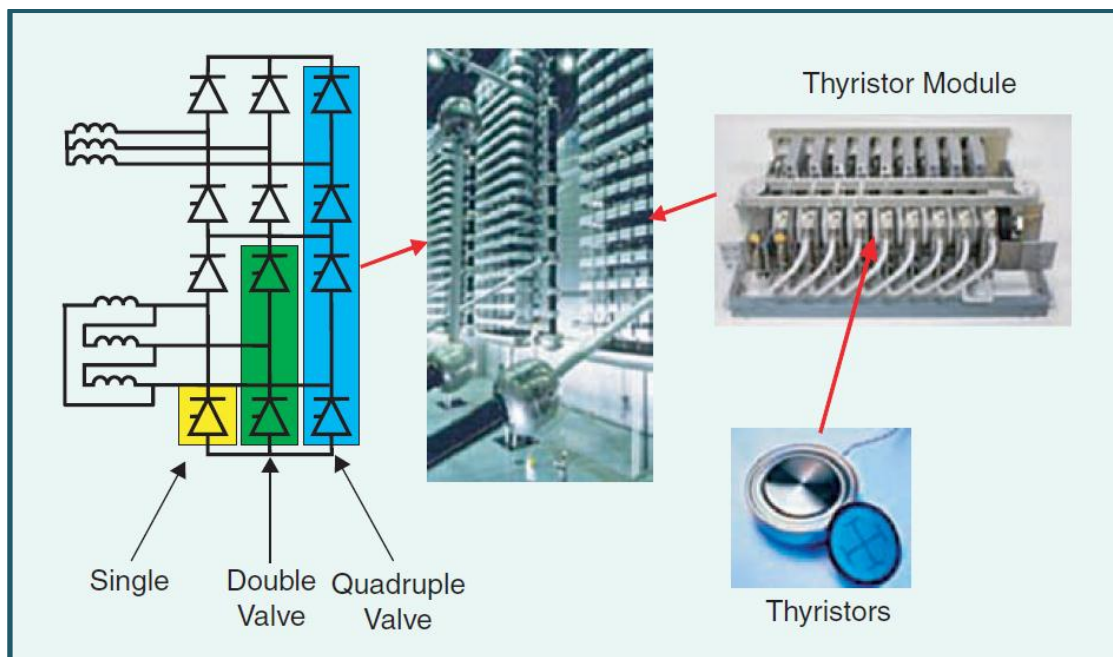


Figure (2.19): Valve module, MVU and the representation of each in single diagram [25]

2.5.2 Converter Transformer

The converter transformers transform the voltage of the AC bus-bar to the required entry voltage of the converter. The 12-pulse converter requires two 3-phase systems which are spaced apart from each other by 30 or 150 electrical degrees; Figure (2.20) shows a typical converter transformer [24]. The converter transformer acts as the interface between the HVDC converter and the AC system and provides several functions including:

- Providing galvanic isolation between the AC and DC systems.
- Providing the correct voltage to the converters.
- Limiting effects of steady state AC voltage change on converter operating conditions (tapchanger).
- Providing fault-limiting impedance.
- Providing the 30° phase shift required for twelve-pulse operation via star and delta windings.

Figure (2.21) illustrates the commonly recognized transformer arrangements in HVDC schemes. Lowest cost can normally be achieved by minimizing the number of elements the converter transformer is broken down into, hence the lowest cost is typically a 3-phase, 3-winding transformer. However, due to shipping limits, such a transformer may not be practical so another arrangement should be considered. Where a spare converter transformer is deemed necessary, based on an availability analysis of the scheme, then it is more cost-effective to use a 1-phase, 3-winding transformer arrangement, as one spare unit can replace any of the in-service units, whilst 2-winding arrangements require two spare units to be supplied.

An important consideration in the design of a converter transformer is the selection of the leakage reactance as this will constitute the major part of the converter's commutating reactance. The leakage reactance must primarily ensure that the maximum fault current that the thyristor valve can withstand is not exceeded. Typically the optimum leakage reactance will be in the range 0.12 pu to 0.22 pu [24].



Figure (2.20): A HVDC Converter transformer [24]

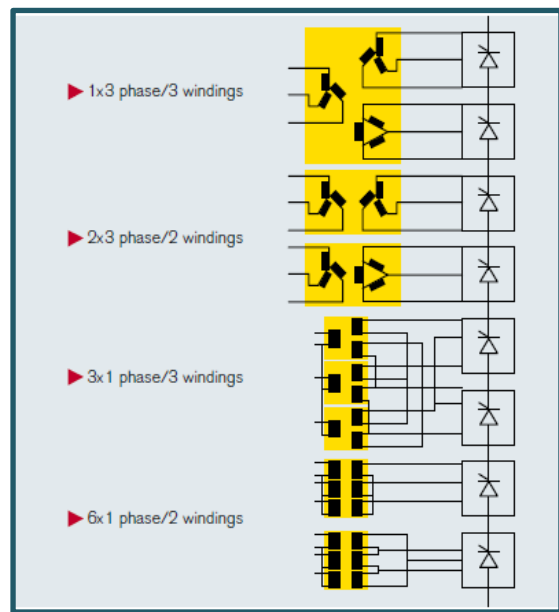


Figure (2.21): Typical Converter transformer arrangements [23]

2.5.3 Smoothing Reactor

For a HVDC transmission scheme, the DC smoothing reactor provides a number of functions but principally is used to:

- Reduce the DC current ripple on the overhead transmission line or cable.
- Reduce the maximum potential fault current that could flow from the DC transmission circuit into a converter fault.
- Modify the DC side resonances of the scheme to frequencies that are not multiples of the fundamental AC frequency.
- Protect the thyristor valve from fast front transients originating on the DC transmission line (for example a lightning strike).

The DC smoothing reactor is normally a large air-cored air-insulated reactor and is principally located at the high voltage terminal of the HVDC converter for schemes rated at, or below, 500 kVdc. Above 500 kV, the DC smoothing reactor is commonly split between the high voltage and neutral terminals [24].

While the current and voltage rating of the smoothing reactor can be specified based on the data of the DC circuit, the inductance is the determining factor in sizing the reactor. Taking all design aspects above into account, the size of smoothing reactors is often selected in the range of 100 to 300 mH for long distance DC links and 30 to 80 mH for back-to-back stations.

In an HVDC long-distance transmission system, it seems quite logical that the smoothing reactor will be connected in series with the DC line of the station pole. Figure (2.22) shows one kind of dc smoothing reactors.



Figure (2.22): Air-insulated dc smoothing reactor, Inductance: 150 mH, Rated voltage: 500 kV DC, Rated current: 1800 A DC [24]

2.5.4 Harmonic Filters

There are two main reasons to use filters in HVDC system; reactive power and harmonics. The reactive power consumption of an HVDC converter depends on the active power, the transformer reactance and the control angle. It increases with increasing active power. A common requirement to a converter station is full compensation or overcompensation at rated load. In addition, a reactive band for the load and voltage range and the permitted voltage step during bank switching must be determined. These factors will determine the size and number of filter and shunt capacitor banks [24].

Harmonics within a power system are defined as the modulation of the voltage or current at an integer multiple of the fundamental frequency. Hence, for example, on a 50 Hz system, the presence of 5th harmonic voltage means that there is an additional 250 Hz component added to the voltage waveform which will distort the voltage waveform as shown in Figure (2.23).

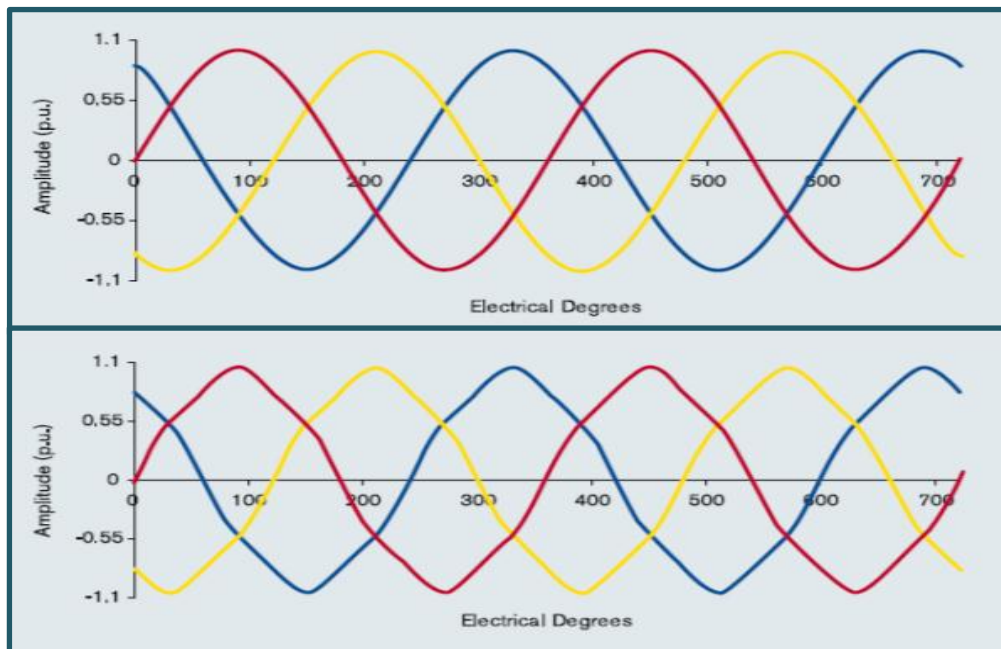


Figure (2.23): Three-Phase fundamental frequency sine-wave before and after the effect of 5th harmonic [23]

The presence of harmonics in the power system can result in some undesirable effects on connected power system equipment, for example, the presence of harmonics can result in:

- Overheating of capacitor banks.
- Overheating of generators.
- Instability of power electronic devices.
- Interference with communication systems.

The AC/DC converter is a source of harmonics. This is because the converter only connects the supply to the load for a controlled period of a fundamental frequency cycle and hence the current drawn from the supply is not sinusoidal. Seen from the AC side, a converter can be considered as a generator of current harmonics and from the DC side a generator of voltage harmonics. The actual level of harmonics generated by an AC/DC

converter is a function of the duration over which a particular phase is required to provide unidirectional current to the load. Hence, the higher the “pulse number” of the converter, which means the more switching between phases within a cycle, the lower the harmonic distortion in both the AC line current and the DC terminal voltage [23].

2.5.4.1 AC Harmonic Filters

The main components of a typical HVDC converter terminal are shown in Figure (2.24). If a Fourier analysis is performed on the idealized waveforms, the following results are obtained:

1) For Y/Y connection the generated current can be represented by equation (2.1) :

$$I = \frac{2 \times \sqrt{3} \times I_d}{\pi} \times \left[\cos \omega t - \frac{1}{5} \cos 5\omega t + \frac{1}{7} \cos 7\omega t - \frac{1}{11} \cos 11\omega t + \frac{1}{13} \cos 13\omega t - \dots \right] \quad (2.1)$$

2) For Y/Δ connection the generated current can be represented by equation (2.2):

$$I = \frac{2 \times \sqrt{3} \times I_d}{\pi} \times \left[\cos \omega t + \frac{1}{5} \cos 5\omega t - \frac{1}{7} \cos 7\omega t - \frac{1}{11} \cos 11\omega t + \frac{1}{13} \cos 13\omega t - \dots \right] \quad (2.2)$$

It can be seen from above equations that each six-pulse bridge generates harmonic orders $6n \pm 1$, $n = 1, 2, 3 \dots$, there are no tripled harmonics (3rd, 6th, 9th...) present and that for $n = 1, 3$, etc., the harmonics are phase shifted by 180° .

By combining two six-pulse bridges with a 30° phase shift between them, i.e. by using Y/Y and Y/Δ transformers as shown in Figure (2.24) and summing above equations, a twelve-pulse bridge is obtained and the current of overall connection will be as represented in equation (2.3):

$$I = \frac{4 \times \sqrt{3} \times I_d}{\pi} \times \left[\cos \omega t - \frac{1}{11} \cos 11\omega t + \frac{1}{13} \cos 13\omega t - \frac{1}{23} \cos 23\omega t + \frac{1}{25} \cos 25\omega t - \dots \right] \quad (2.3)$$

Thus, in a twelve-pulse bridge, the harmonic orders $6n \pm 1$, $n = 1, 3, 5 \dots$ are effectively cancelled in the common supply leaving only the characteristic twelve-pulse harmonics: i.e. $12n \pm 1$, $n = 1, 2, 3 \dots$

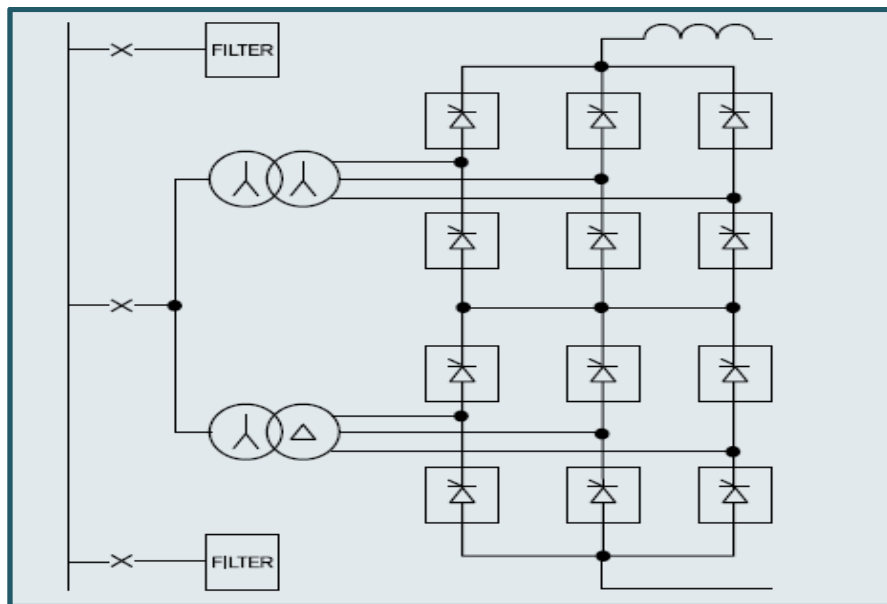


Figure (2.24): A typical twelve-pulse converter bridge [23]

2.5.4.2 DC Harmonic Filters

Harmonic voltages, which occur on the DC, side of a converter station cause AC currents which are superimposed on the direct current in the transmission line. These alternating currents of higher frequencies can create interference in neighboring telephone systems despite limitation by smoothing reactors. DC filter circuits, which are connected in parallel to the station poles, are an effective tool for combating these problems. The configuration of the DC filters very strongly resembles the filters on the AC side of the HVDC station. There are several types of filter design. Single and multiple-tuned filters with or without the high-pass feature are common. One or several types of DC filter can be utilized in a converter station. Figure (2.25) shows the place of DC filters in the converter station. For 12-pulse converter generates characteristic harmonics with order of $n = 12 \times K$ and $K = 1, 2, 3 \dots$. Figure (2.26) shows DC harmonic filters [24].

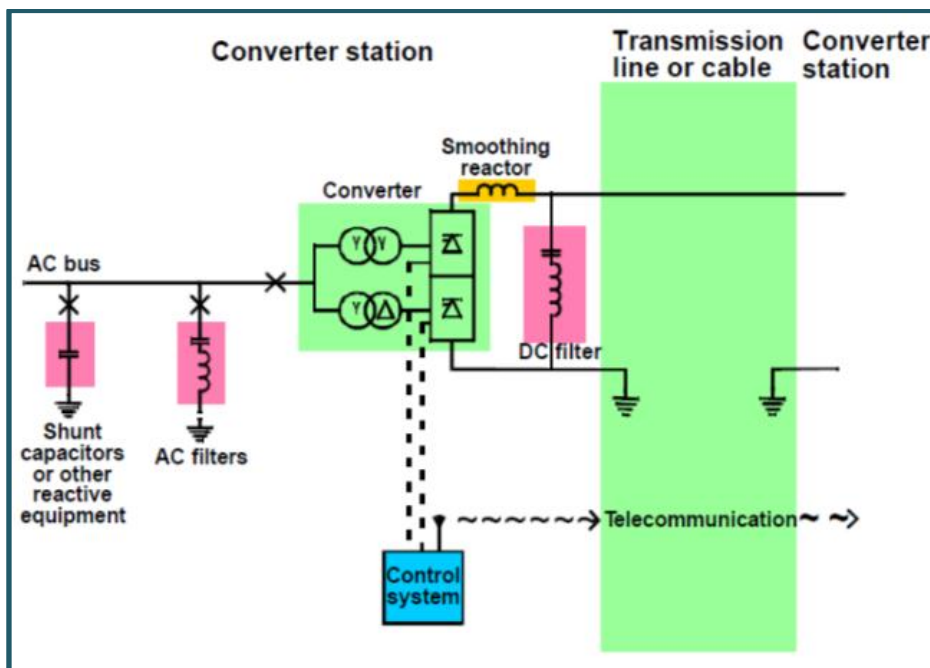


Figure (2.25): HVDC converter station and location of filters [29]



Figure (2.26): DC harmonic filter capacitors [29]

2.5.4.3 Quality Factor

The Quality factor is a measurement of the sharpness of a filter; High Q-value filter is sensitive with the frequency variation (detuning) according to equation (2.4): [29]

$$Q = \frac{\omega_o L}{R} \quad (2.4)$$

2.5.4.4 HVDC Filter Types

Four different types of filters are used in HVDC stations:

1. Single Tuned Band Pass Filter

Has a Very low impedance in resonance frequency with efficient filtering in a narrow frequency band, normally used for the largest harmonics like 11th and 13th. Figure (2.27) shows the filter construction, response and design equations [29].

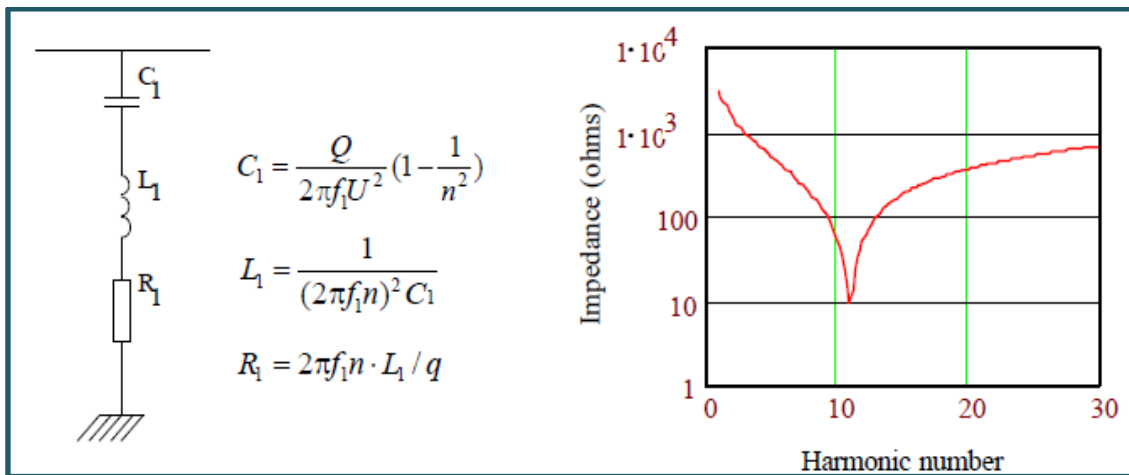


Figure (2.27): Single Tuned Band Pass filter construction , design equations and response [29]

2. High Pass Filter

Broadband filter used to take care of all harmonics from the 23rd and upwards, tuned to near the 24th harmonics with a Q-value normally lie within the range of 2-10. This type of filters can be designed with high Q-values for 11th and 13th with lower fundamental losses, but the parallel connected resistor is more expensive. Figure (2.28) shows the filter construction, response and design equations [29].

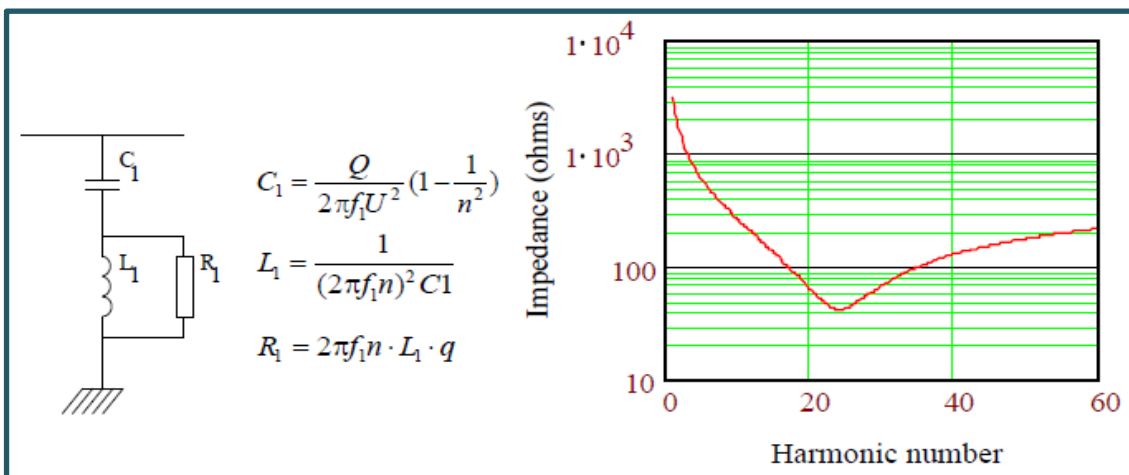


Figure (2.28): High Pass filter construction , design equations and response of 24th harmonic [29]

3. Double Tuned Filter

This type of filters is commonly used in modern HVDC station where at high system voltage the larger main capacitor is easier to optimize at lower cost/kvar. Each switched filter attenuates two harmonics to reduce filter branch types and facilitate filter redundancy. Figure (2.29) shows the double tuned filter construction and response [29].

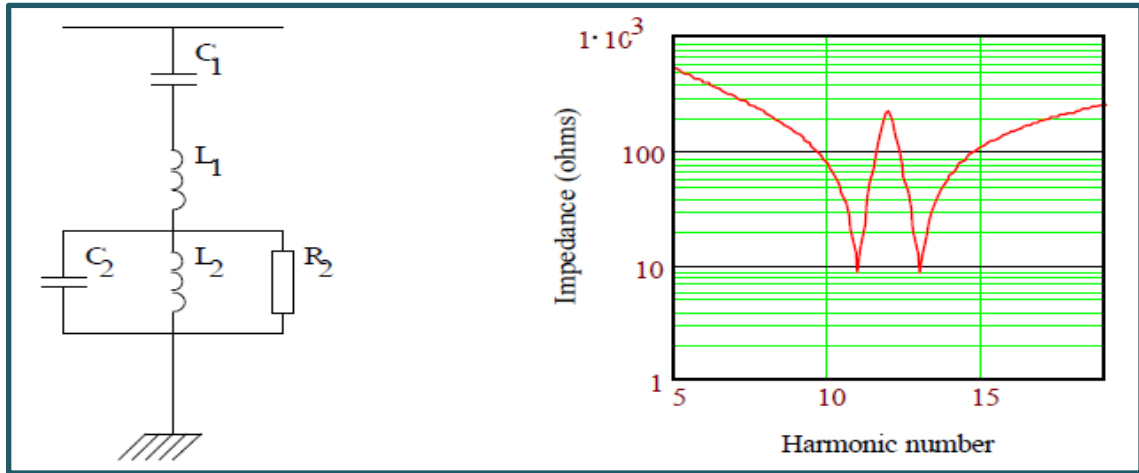


Figure (2.29): Double tuned filter construction and response of 11/13th harmonics [29]

4. C-Type Filter

Used as Low-order high-pass filter for 3rd, 5th and 7th harmonics. The lower L-C in filter construction is series resonant at the fundamental frequency and so bypassed the resistor to greatly reduce the filter losses. Figure (2.30) shows a C-type filter construction, design equations and response [29].

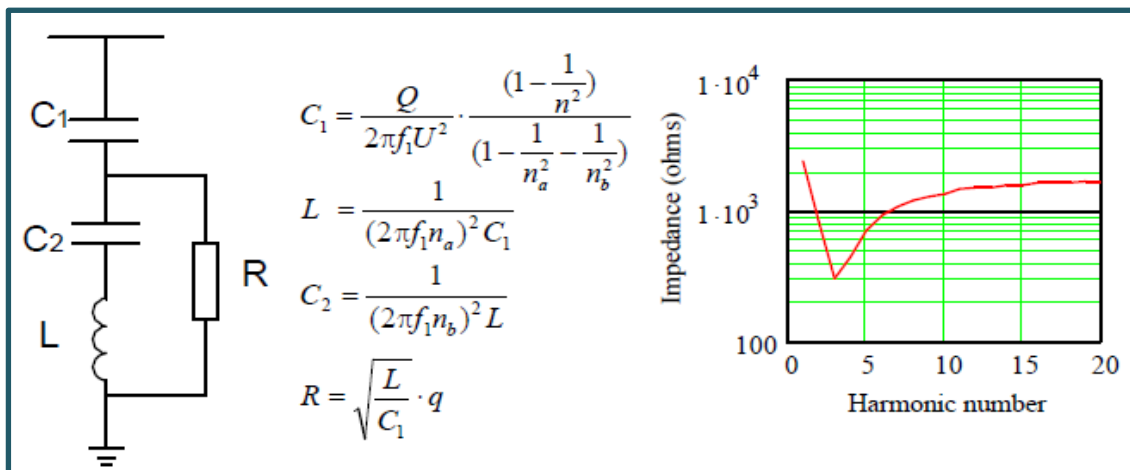


Figure (2.30): C-type filter construction, design equations and response [29]

2.6 HVDC TL Fault Types

Bipolar HVDC system is the type which we focus in this thesis. So, we interest in the faults that can occur in that system.

2.6.1 Single Pole-to-Ground Fault

A pole-to-ground fault occurs when one of the poles (positive or negative) is short circuited with the ground. When this occurs for a bipolar system, only the faulted pole is shut down, while the other pole continues conducting using the ground as a return. This allows the system to transfer half the power it was previously transferred. If the system is a mono-polar instead of a bipolar system, the system is shut down and no power is transferred. Figure (2.31) shows this type of fault on a bipolar system [30].

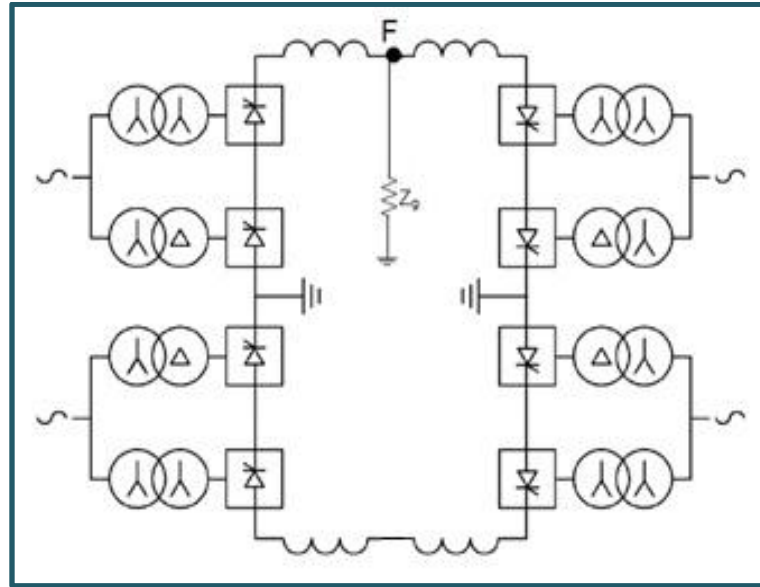


Figure (2.31): A single pole-to-ground fault on a bipolar system.

2.6.2 Pole-to-Pole Fault

This fault occurs only for a bipolar system and it occurs when the two poles are short circuited. A complete shutdown of the system is required when this happens. Figure (2.32) shows this type of fault [30].

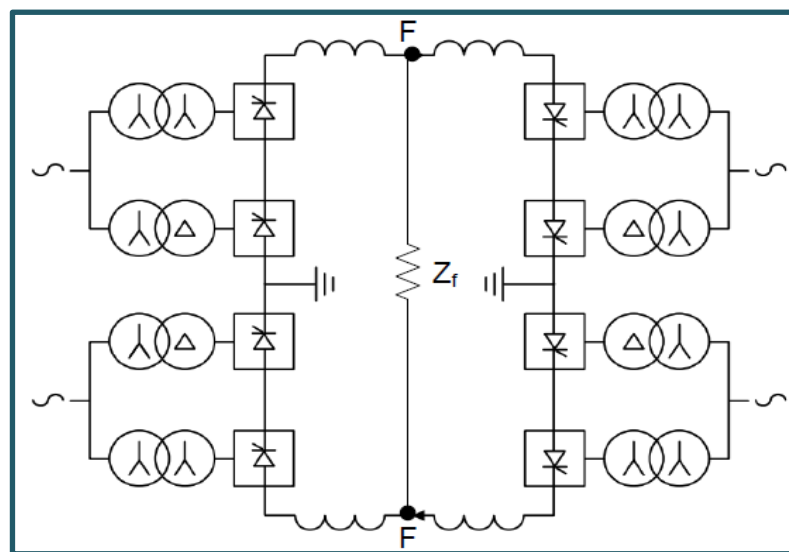


Figure (2.32): A pole-to-pole fault on a bipolar system [30]

2.6.3 Pole-to-Pole-to-Ground Fault

This type of fault occurs when the two poles of a bipolar system are short circuited through the ground. A complete shutdown of the system is required for this type of fault. Figure (2.33) shows this type of fault [30].

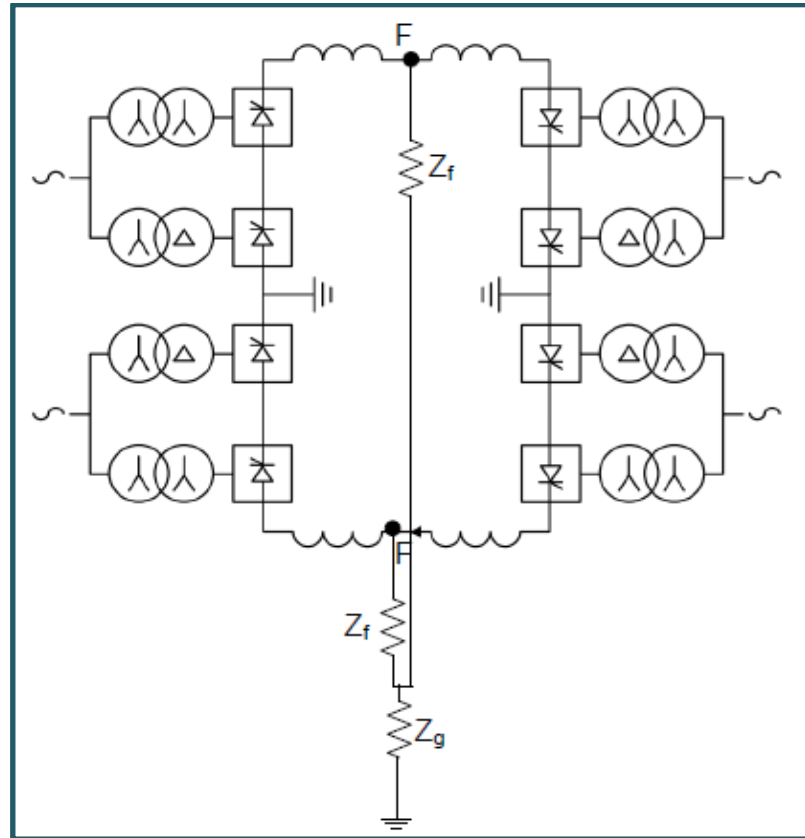


Figure (2.33): A pole-to-pole to ground fault on a bipolar system [30]

2.6.4 Other Types of HVDC TL Faults

Other types of HVDC faults can occur such as open circuit faults and flashover faults where Lighting strikes to a ground wire or tower cause this type of fault [30].

CHAPTER 3

TECHNIQUES OF FAULT DETECTION AND LOCATION ON TRANSMISSION LINE



Electric power systems, which are growing in size and complexity, will be always exposed to failures of their components. In the case of a failure, the faulty element should be disconnected from the rest of the sound system in order to minimize the damage of the faulty element and to remove the emergency situation for the entire system. This action should be taken fast and accurately and is accomplished by a set of automatic protective relaying devices. At the same time, when a fault occurs on a line, it is very important for the utility to identify the fault location as quickly as possible for improving the service reliability. If a fault location cannot be identified quickly and this produces prolonged line outage during a period of peak load, severe economic losses may occur and reliability of service may be questioned.

All these circumstances have raised the great importance of fault-location research studies and thus the problem has attracted widespread attention among researchers in power-system technology in recent years. Basic algorithms used in fault locators are intended to make distance to fault calculation as accurate as possible. The fault locator is mainly associated with protection relays. Distance relays for transmission-line protection provide some indication of the general area where a fault occurred, but they are not designed to pinpoint the location. Moreover, both the tasks: line protection and fault location are fulfilled by processing the same current and voltage signals that are obtained from the instrument transformers and recorded at the substation. Fault-location estimation is a desirable feature in any protection scheme. Locating the fault on the transmission line accelerates line restoration and maintains system stability. That is why these two subjects are closely related to each other. There are, however, different demands formulated for protection and fault location [2].

This chapter talks about methods and techniques used to detect and locate faults of TL. In section 3.1 HVDC TL fault types with both conventional and unconventional methods used in diagnosis faults in TL are discussed. Section 3.2 discusses the impedance based method, section 3.3 discusses travelling wave based method and high frequency methods are studied in section 3.4. Finally, section 3.5 studies the artificial intelligence methods.

3.1 Introduction

Normally, a fault location can be done by foot patrols or by patrols equipped with different transportation means and binoculars. Such means of faulted-line inspection is considered as time consuming. Also, calls from witnesses of damages on the power line, or customer calls, can provide the required knowledge about the fault position. However, such primitive ways do not satisfy the requirements imposed on fault location. Valuable information on fault location can be obtained also from fault indicators, installed either in substations or on poles (or towers) along the transmission or distribution line. Additional use of a radio link allows use of the information from indicators even during inclement weather. The other, unconventional fault-location system for monitoring transients of induced radiation from power system arcing faults, using both Very Low Frequency signals (VLF) and Very High Frequency signals (VHF) reception, has been tested in the experimental installation. In spite of various attempts to different unconventional techniques, automatic fault location is still considered as the most widely used. It is based on determining the physical location of a fault by processing the voltage and current waveform values.

Automatic fault location can be classified into the following main categories:[2]

1. Technique based on fundamental-frequency currents and voltages; mainly on impedance measurement.
2. Technique based on traveling-wave phenomenon.
3. Technique based on high-frequency components of currents and voltages generated by faults.
4. Knowledge-based approaches.

These techniques will be discussed briefly in next sections.

3.2 Impedance Based Method

Making use of the fundamental-frequency voltages and currents at the line terminal (or terminals), together with the line parameters, appears as the simplest way for determining the fault location. It is mainly considered that the calculated impedance of the faulted-line segment is a measure of the distance to fault. The methods belonging to this category are simple and economical for implementing. Depending on the utilized input signals of the fault locator, these methods as applied to the two terminal lines, can be further classified. Performing such classification one has to take into account an availability of measurements: whether from one or both ends, and also whether complete measurements (voltage and current) or incomplete measurements (voltage or current) from a particular line end are utilized. Various fault-location methods, with acceptable accuracy for most of the practical applications, have been developed using one-end impedance techniques. A major advantage for these techniques is that communication means are not needed and simple implementation into digital protective relays or digital fault recorders is possible. However, the fault-location algorithms will be more accurate, if more information about the system is available. Therefore, if communication channels are at the disposal, then the two-terminal fault-location methods may be used. Only low-speed communications are necessary for this application. If necessary, the data could be retrieved manually for estimation of the fault location. The two-end technique offers improved fault-location determination, without any assumptions and information regarding the external networks such as impedances of the equivalent sources [2].

For the implementation of the one-ended fault location methods, the following data are necessary: [31]

1. Phase-to-ground voltages and phase currents.
2. Identifying the fault type.
3. Pre-fault data are required for some methods.

This method uses the following equipment to obtain and process data [31]:

1. A microprocessor-based relay or other three-phase voltages and currents measurement device that could calculate fault location estimates.
2. Communication medium or SCADA interface for remote calculation of fault location estimates.

In order to determine an accurate fault location equation, the circuit in Figure (3.1) is examined.

Fault on a homogenous transmission line with fault resistance R_F and a line impedance Z_L between terminals G and H . The remote and local terminals are represented by their Thevenin equivalents.

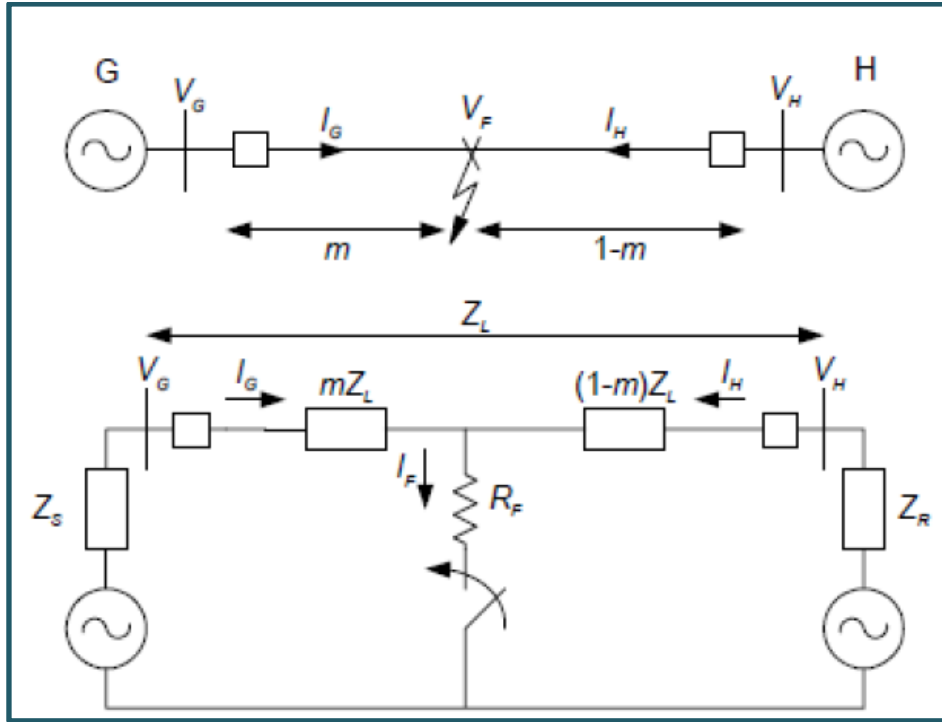


Figure (3.1) One-line diagram and equivalent circuit for a three-phase fault on a transmission line with two sources, G and H [31]

From Figure (3.1) it can be easily seen that the voltage drop from terminal G due to the fault occurring at location m per unit can be calculated by equation (3.1):

$$V_G = mZ_L I_G + R_F I_F \quad (3.1)$$

Where:

V_G is the voltage at terminal G .

m is the per unit distance to the fault.

Z_L is the line impedance between terminals G and H .

I_G is the line current from terminal G .

R_F is the fault resistance.

I_F is the total fault current.

The impedance measured from terminal G can be found by dividing equation (3.1) by I_G to be represented by equation (3.2):

$$Z_{FG} = \frac{V_G}{I_G} = mZ_L + R_F \frac{I_F}{I_G} \quad (3.2)$$

Where Z_{FG} is the apparent impedance measured from G to the fault. The fault impedance will have a reactive component if the ratio $\frac{I_F}{I_G}$ is complex. This reactive

component can be inductive or capacitive depending on the angle of the ratio. The reactive component will be zero when the angle is zero [30].

Now, In order to analyze the parameters affecting the error, the parameters affecting the angle of $\frac{I_F}{I_G}$ must be considered. To do that, the pre-fault system must be studied . Let the following equation (3.3) be defined.

$$\Delta I_G = I_G - I_L \quad (3.3)$$

Where:

ΔI_G is the difference current.

I_L is the pre-fault load current.

The equation (3.2) can be written as equation (3.4):

$$Z_{FG} = \frac{V_G}{I_G} = mZ_L + R_F \frac{1}{d_s n_s} \quad (3.4)$$

Where:

d_s is the current distribution factor in equation (3.5)

n_s is the circuit loading factor in equation (3.6).

$$d_s = \frac{\Delta I_G}{I_F} = \frac{Z_H + (1-m)Z_L}{Z_H + Z_L + Z_G} = |d_s| \angle \beta \quad (3.5)$$

$$n_s = \frac{I_G}{I_G - I_L} = \frac{I_G}{\Delta I_G} = |n_s| \angle \gamma \quad (3.6)$$

If the system is homogenous then β is zero. If there is load flow on the system then γ won't be zero. If the magnitude of the fault current I_G is much greater than the magnitude of the load current, I_L , then, γ will approach zero. The sum of the angles β and γ , determines the reactive component caused by the fault resistance R_F [31].

In order to implement fault location algorithms, some simplifying assumptions have to be made in order to reduce the effect of R_F . The performance of such an algorithm will depends on the underlying assumptions. The following section describes such an implementation of the algorithm [30]:

3.2.1 Simple Reactance Method

This method compensates for the fault resistance by taking only the imaginary part of the apparent impedance measurement. The fault locator uses the fact that the distance to the fault is proportional to the ratio of the measured reactance to the reactance of the entire line. The per-unit distance to the fault is represented by equation (3.7):

$$m = \frac{\text{Im}(V_G / I_G)}{\text{Im}(Z_L)} \quad (3.7)$$

Equation (3.8) describes the line-to-ground fault location (a-g) as follows:

$$m = \text{Im} \left[\frac{V_{Ga}}{I_{Ga} + K_0 I_R} \right] / \text{Im}(Z_L) \quad (3.8)$$

Where, K_0 and I_R are defined by equations (3.9) and (3.10) respectively .

$$K_0 = (Z_{0L} - Z_{1L}) / 3Z_{1L} \quad (3.9)$$

$$I_R = 3I_0 \quad (3.10)$$

I_R : Residual current

I_0 : Zero – sequence current

Z_{0L} : Zero- sequence line impedance

Z_{1L} : Positive sequence line impedance

3.2.2 Method Without Using Source Impedances

If the load current is eliminated by finding the change in current on the occurrence of a fault, the above method can be improved. Using the superposition current ΔI_G , equation (3.1) can be written as (3.11):

$$V_G = mZ_{1L}I_G + R_F \frac{\Delta I_G}{d_s} \quad (3.11)$$

Where; d_s is the voltage drop across the fault resistance [33]. Multiplying equation (3.11) by the complex conjugate, ΔI_G^* , using only the imaginary part, we obtain equation (3.12) [31]:

$$\text{Im}(V_G \Delta I_G^*) = m \cdot \text{Im}(Z_L I_G \Delta I_G^*) + R_F \cdot \text{Im}\left(\frac{1}{d_s}\right) \quad (3.12)$$

For a homogenous system, the angle is about zero for the current distribution factor ($\text{Im}(1/d_s)=0$), and the fault location is represented by (3.13):

$$m = \frac{\text{Im}(V_G \Delta I_G^*)}{\text{Im}(Z_L I_G \Delta I_G^*)} \quad (3.13)$$

For a non-homogenous system, an angle correction (β) derived from the source impedance to account for the non-zero current distribution factor in this type of system [31], and the fault location defined by (3.14):

$$m = \frac{\text{Im}(V_G I_R^* e^{-j\beta})}{\text{Im}(Z_{1L} I_G \Delta I_R^* e^{-j\beta})} \quad (3.14)$$

The fault location estimate is improved here by reducing the effect of the reactance error.

3.2.3 Method Using Source Impedances

Knowledge of the source impedance is required when the distribution factor is discounted and when using the positive-sequence model of the line. The fault location can be determined without assumptions using the following quadratic equation (3.15) [31]:

$$m^2 - mk_1 + k_2 - k_3 R_F = 0 \quad (3.15)$$

Where; k_1 , k_2 and k_3 are complex functions of voltage current and source impedances. Equation (3.15) is separated into real and imaginary components in order to have two equations with two unknowns' m and R_F and then the equation can be solved.

3.3 Travelling Wave Based Method

Traveling-wave theory has long been studied for the purpose of fault detection and location in transmission lines. The essential idea behind these methods is based on the correlation between the forward and backward traveling waves along the line. The principle of the fault-location techniques is based on the successive identification of the fault, initiated by traveling high-frequency voltage/current signal present where the

locator is installed. In particular, the first and few subsequent signals are used to identify the fault position. The propagation time of the high-frequency components is also used to determine the fault position. Recent developments in transducer technology enabled high sampling rate recording of transient signals during faults. The availability of such broad bandwidth sampling capability facilitates better and efficient use of traveling-wave-based methods for fault analysis. Another significant development in parallel with the advances in the transducer technology is the newly introduced signal-processing tools such as the discrete wavelet transform (DWT), which allows the analysis of sampled signals with localized transients. The attractive feature of wavelet transform in analyzing the traveling waves due to fault is the automatic adjustment of window width of the wavelets depending upon the duration of the transient under study. This is accomplished by time dilation of the chosen mother wavelet. As a result, accurate information on the arrival time of signals traveling at different speeds along the faulted line can be captured. This information is then used to calculate the distance to the fault point along the monitored line. Fault-location methods using traveling waves are independent of the network configuration and devices installed in the network. These techniques are very accurate, but require high sampling rate and their implementation is more costly than implementation of impedance-based techniques [2].

Nowadays, the currently used fault-location techniques for HVDC transmission lines are all based on traveling wave without exception. These traveling-wave-based methods have fast response and high accuracy, in which the time it takes for the traveling wave-head to propagate from the fault point to the terminals implies the fault distance. The results they give are not easily affected by the factors, such as bus configuration, fault types, ground resistance, and system parameters. However, they are also facing some insurmountable technical problems as follows:

- 1) The detection of the wave-head is the key to traveling-wave fault location. If the wave-head could not be captured successfully or the wave-head does not exist at all on the occurrence of a fault, the fault location will fail. For instance, when the line is grounded through a large resistance, the transient traveling -wave signals are too weak to be detected, disabling the fault location under these circumstances. Moreover, if a fault is caused by a gradual change in the transition resistance, the traveling wave may also be too weak to be discovered, resulting in the failure of fault location.
- 2) In the method, the time is measured for the wave-head to arrive at the point where the device is installed, and the fault distance is the product of the time and the wave speed. Therefore, the accuracy of fault location is dependent, to a great extent, on the wave speed which, in turn, depends on the parameters of the line.
- 3) Accuracy in fault location depends upon sampling frequency. Since the speed at which the wave travels over transmission lines is slightly lower than light speed, in order to achieve higher accuracy, a very high sampling frequency has to be used in the traveling-wave fault-location methods.
- 4) The wave-head must be identified in locating the fault, which is often carried out by experienced professionals and cannot be implemented automatically by computers.
- 5) The travelling-wave fault location is vulnerable to interference signals.

In a traveling-wave fault location, if the wave-head is not captured successfully or if it does not exist at all in some circumstances, the fault location cannot be implemented and all of the data that follow the traveling wave-head will be useless [19].

3.3.1 Travelling Wave Fault Location Theory

When a fault occurs along a transmission line, the voltage and current transients will travel towards the line terminals. These transients will continue to bounce back and forth between the fault point and the two terminals for the faulted line until the post-fault steady state is reached. Considering a single-phase lossless transmission line of length (l) connected between buses A and B with characteristic impedance Z_c and traveling-wave velocity of v . If a fault occurs at a distance x from bus A, this will appear as an abrupt injection at the fault point. This injection will travel like a surge along the line in both directions between the fault point and two terminals until the post-fault steady state is reached. A lattice diagram illustrating the reflection and refraction of traveling waves initiated by the fault transients is shown in Figure (3.2).

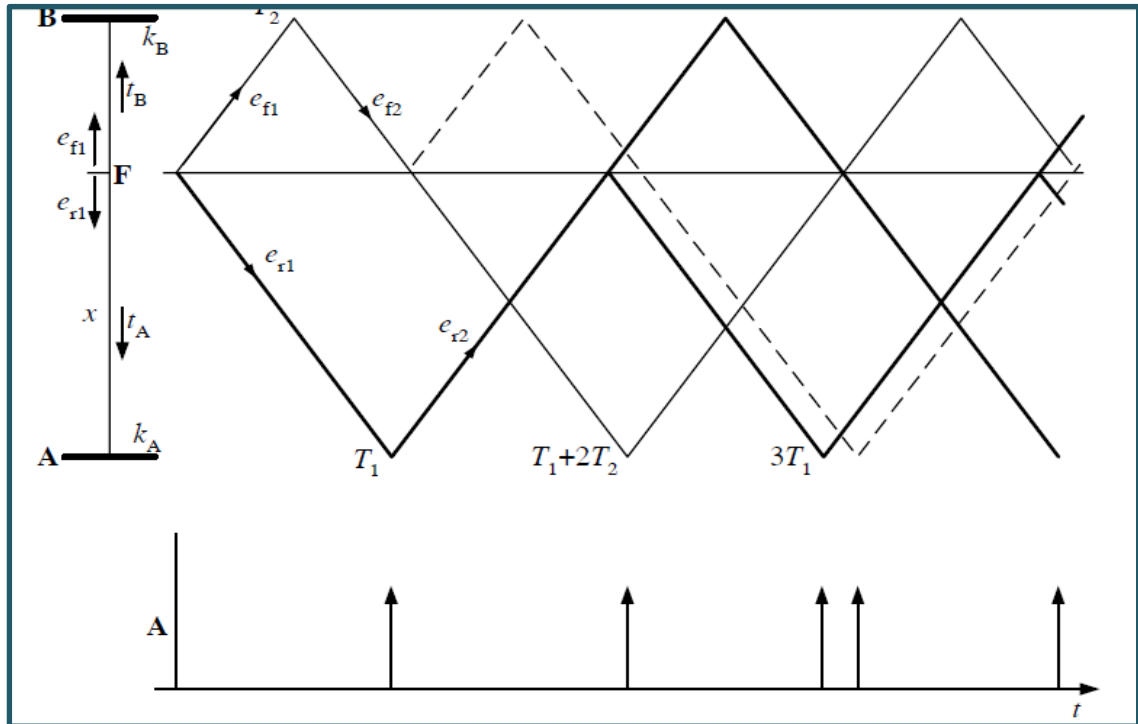


Figure (3.2) Traveling voltage and current waves: lattice diagram for a fault at distance x from A [2]

The voltage and current at any point x obey the differential equations (3.16) and (3.17):

$$\frac{\partial e}{\partial x} = -L' \frac{\partial i}{\partial t} \quad (3.16)$$

$$\frac{\partial i}{\partial x} = -C' \frac{\partial e}{\partial t} \quad (3.17)$$

where: L' and C' are the inductance and capacitance of the line per unit length. Resistance is assumed as to be negligible. The solutions of these equations are shown in equation (3.18) and (3.19):

$$e(x,t) = e_f(x-vt) + e_x(x+vt) \quad (3.18)$$

$$i(x,t) = \frac{1}{Z_c} e_f(x-vt) - \frac{1}{Z_c} e_x(x+vt) \quad (3.19)$$

Where: $Z_c = \sqrt{\frac{L'}{C'}}$ is the characteristic impedance of the transmission line and

$v = \sqrt{\frac{1}{L'C'}}$ is the velocity of propagation.

Forward (e_f) for voltage and similar for current (i_f) and reverse (e_r and i_r) waves, as shown in Figure (3.2), leave the disturbed area x traveling in different directions at v , which is a little less than the speed of light, toward the transmission-line ends. Transmission-line ends represent a discontinuity or impedance change where some of the wave's energy will reflect back to the disturbance. The remaining energy will travel to other power-system elements or transmission lines. The lattice diagram in Figure (3.2) illustrates the multiple waves (represented by subscripts 2 and 3) generated at line ends. Wave amplitudes are represented by reflection coefficients k_A and k_B , which are determined by characteristic impedance ratios at the discontinuities. τ_A and τ_B represent the travel time from the fault to the discontinuity.

With the GPS technology, τ_A and τ_B can be determined very precisely. By knowing the length (l) of the line and the time of arrival difference ($\tau_A - \tau_B$), one can calculate the distance (x) to the fault from substation A by:

$$x = \frac{l - c \cdot (\tau_A - \tau_B)}{2} \quad (3.20)$$

where: c – the wave propagation of 299.79 m/s.

Construction of the lattice diagram becomes computationally difficult if the attenuation and distortion of the signals are taken into account as they travel along the line. On the other hand, time-frequency resolution of the transient signals can be used to determine the travel times of these transients between the fault point and the line terminals. In three-phase transmission lines, if losses are taken into account, there are three modes of propagation, therefore for the analysis of the traveling-wave effect, phase values must be converted into modal values [2].

3.3.2 Travelling Wave Fault Location Data and Equipment Required

The traveling-wave method relies on calculation of time for the line disturbance to reach the end of the line. Essentially, when a disturbance occurs, very accurate time tagging must be done. Since the wave moves approximately at the speed of light, by comparing the wave arrival time difference at each end, one can determine the distance to the source of the disturbance. This requires extremely accurate timing for calculation of fault location. Either voltage or current wave data can be used. The voltage portion of the traveling waveform tends to be reduced as the result of buses with lower impedance. On the other hand, the current waveform tends to double as the result of a constant current source. The first data requirement is a standard time reference at both receiving terminals. Then, some method of distinguishing which waveform must be used is required. The appropriate current waveform (or time tag in the voltage method) must be known to accurately calculate a fault location. From this point, a fault location can be calculated based on the precise wave-arrival times on each end of the line. The main piece of data that must be known is the very precise time that the traveling wave reaches each end of the line. At this point, it is merely a matter of calculation.

The following equipment is necessary to locate faults using the traveling-wave method:

1. A very accurate time-stamping device (GPS) on both ends of the line.
2. An appropriate sensor to detect the voltage or current, depending on the parameter used. In the case of the current wave, normal relaying accuracy CTs are used. The secondary CT circuits then have the current pulses detected by clamp-on inductive sensors. In the case of detecting voltage pulses, capacitive potential transformers are utilized.
3. A communication circuit is required to transmit the time-stamped data back to a central location.
4. A computer capable of retrieving the remote data, distinguishing the appropriate waveform for the fault-location calculation, and providing the appropriate calculations to the fault [2].

3.4 High Frequency Methods

Contemporary methods for fault location on overhead lines and underground cables can be classified as two fundamental types: methods based on the measurement of post-fault line impedance and methods based on the measurement of the fault-generated traveling-wave component. There has been considerable research effort into the development of impedance-based methods for fault location. However, like any other power frequency-based measurement methods, they suffer from limitations due to fault-path resistance, line loading and source parameters, etc. As a result, the accuracy attained in fault location is rather limited. Theoretically, the pattern of the fault-generated traveling wave contains information about the fault location that can be used to accurately locate the fault. However, present traveling-wave-based fault-location methods exhibit shortcomings; a fault will not generate many traveling-wave components when it occurs at a voltage inception close to zero degree; for a close-up fault, the time difference between the arrival of an incident wave and the arrival of its reflection from the bus bar will be so short that the waves are unlikely to be detected separately. This could make the interpretation of the information available in the first few milliseconds after the arrival of the first wave front virtually impossible. Where the measurement involves voltage signals, then the bandwidth limitation of the capacitive voltage transformer (CVT) can be a serious impediment [32]. An approach to transmission-line protection has been developed based on the detection of fault-generated high-frequency transient signals, and the research shows that the technique can be applied to achieve very high accuracy in fault location [33]. The method has been shown to be immune to power frequency phenomena such as power swings and CT saturation. Similar techniques have been developed [34], where traveling-wave phenomena were used for fault detection. The use of wavelet transforms to extract the high frequency transients was introduced. Two basic systems were described; one using recordings from both ends of the line and synchronized using global positioning satellite receivers, and the second using recordings made at one end of the line. The technique based on high-frequency components of currents and voltages generated by faults, which travel between the fault and the line terminals, is still also not widely used. This method is considered as expensive and complex, since use of specially tuned filters for measuring high-frequency components is required [2].

3.4.1 Basic Principle and Fault-Locator Design

A sudden change in system voltage on a power line or cable will generate a wideband signal, which covers the entire frequency range [32]. The initial values of these waves are dependent, among other factors, on the fault position on the line, the fault-path resistance and, the most important of all, the instance of fault occurrence. These different frequency components propagate away from the fault point in both directions. In time, these signals reach other discontinuities on the line/cable and are reflected back towards the fault point. In the frequency domain, the magnitude of the individual signal components decreases as the frequency rises and traveling speed increases. The principle of the fault-location method is based on the successive identification arrival of traveling high-frequency voltage signals at the bus-bar where the locator is installed. In particular, the timing of the first received and subsequent signals referenced to that first signal are used to identify the fault position [2].

The voltages are monitored using high-voltage coupling capacitors. The signals from these are then digitized for processing. Modal mixing transforms are used to extract the aerial-mode and ground-mode signals. This process provides inherent filtering. Digital band-pass filters then extract the high-frequency components used for the fault location. In practice, the accuracy of the technique is mostly affected by noise interference, which arises mainly from two sources: noise on the power line/cable, such as corona and partial discharge; and background noise coupled into the equipment. The prevalent anti-noise techniques can be employed to reduce the effects of background noise. Moreover, the interference noise can be effectively reduced by controlling the gain of the input signals to maximize the accuracy of the fault location and reduce the effect of noise interference [2].

3.5 Artificial Intelligence Methods

Modern controls based on Artificial Neural Network, Fuzzy Logic and Genetic algorithm are found fast, reliable and can be used for protection against the line and converter faults and are gaining more interest in the field of HVDC transmission. Various artificial intelligence techniques that can be used for fault identification of HVDC transmission system are:

3.5.1 Artificial Neural Network (ANN)

ANNs have been extensively used for the fault diagnosis, load demand forecasting, system identification, state estimation etc., in power systems. The increasing use of AI paradigms (i.e. based on ANNs, Fuzzy logic, Expert Systems etc.) in recent years in the area of HVDC systems is indicative of the promising features associated with these new techniques. As Artificial Neural Network (ANN) has capability to map complex and highly nonlinear input-output behavior, this approach is widely used to recognize patterns in electrical circuits, fault identification in an AC-DC system, HVDC controller design etc. Expert system based on neural network or Fuzzy system, is now applied for power system functions to overcome limitations of digital techniques. Distributed representation and strong learning capabilities are the major features of neural network. Recently, incomplete method is developed to detect faults in HVDC converter using the concept of signature analysis. Limitation of the existing method is examined and new ANN based methods are proposed to provide discrete and unambiguous indication of converter fault. Proposed identifiers are very attractive for real time

implementation because of their simple architecture. Comparison between different methods is also made. The ANN has advanced methods such as optimal control adaptive control, multi-variable control and different approaches such as microprocessor based controllers and digital signal processing have been investigated or under investigation. Artificial Neural Networks (ANN) are gaining widespread application in several areas of engineering, especially where, due to non-linearity of the process, it is often too cumbersome to analyze the process or the plant under study. The ANN has the capability to learn and extract information in systems where the non-linearity and time dependency do not permit one to use methods such as frequency or modal analysis. Although it is airways possible to liberalize a system around an operating point and conduct same studies, thus derived models always remain valid only within the limited region [35]. ANN will be discussed extensively in next chapter.

3.5.2 Neuro Fuzzy

Fusion of ANN and fuzzy-logic systems is a result of the tendency to use the better features of both techniques: capability of non-linear mapping, learning of ANN and high immunity to errors in input data and flexibility to their inaccuracy or uncertainty, which is a characteristic property of a fuzzy-logic. Therefore, the neuro-fuzzy hybrid system combines the advantages of a fuzzy-logic system, which deals with explicit knowledge that can be explained and understood, and neural networks, which deal with implicit knowledge, which can be acquired by learning. This combination is referred to as a fuzzy neural network (FNN). There are several approaches to integrate ANN and fuzzy logic and very often it depends on the application. One of the simplest structures of FNN is presented in Figure (3.3).

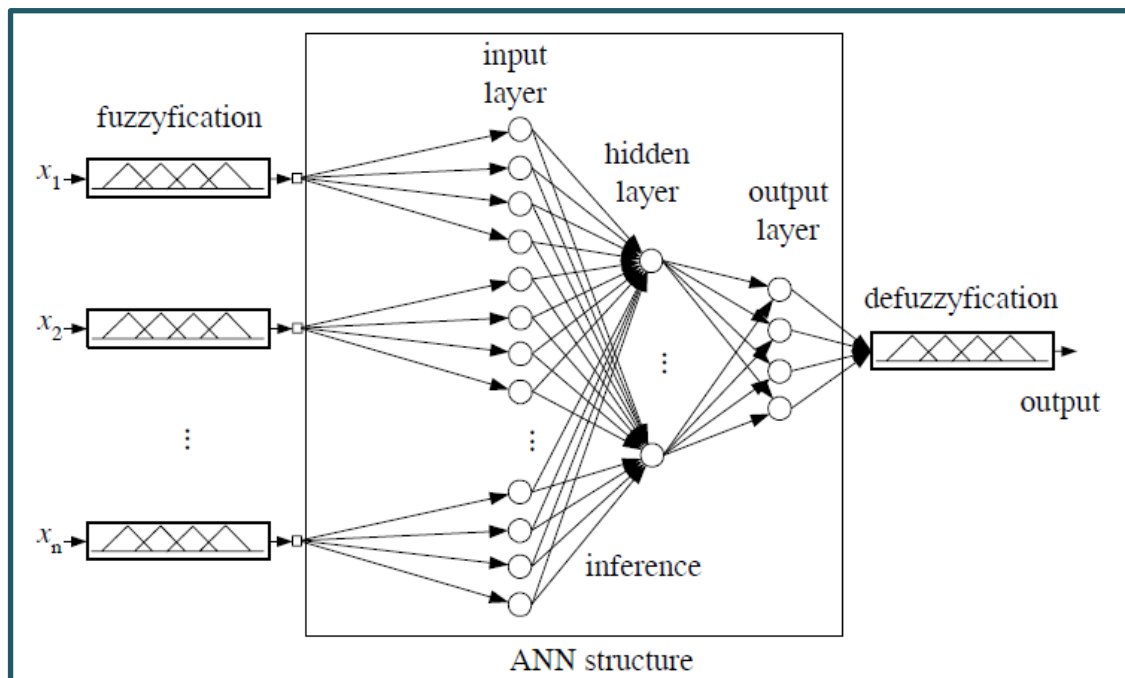


Figure (3.3) Structure of the simple FNN [2]

In fact, that is a combination of feed-forward ANN driven by fuzzy inputs. In that structure the ANN represents a fuzzy-inference system: each node in the inference layer multiplies the input signals and the output of the node becomes the result of fuzzy

inputs product (fuzzy intersection). In a fuzzy inference layer fuzzy rules are fired and the value at the end of each rule represents the initial weight of the rule, and will be adjusted to its appropriate level at the end of training. For determination of a crisp output a defuzzification procedure is applied. Before that, in the output layer all particular outputs are summed with adequate weights (fuzzy union operation). Training of the network can be realized with a back-propagation method. For fault-location application the input signals represent normalized voltage and current waveforms obtained from simulation of different disturbances in the considered network Figure (3.3). They are divided into groups with respect to place of fault or any other disturbances. Fuzzification of input signals is performed by taking into account different signal characteristics, such as for example: value of DC component (in current signals fuzzy fication), signal spectrum (classified to one of a few categories) and so on. The adequate signal characteristics are calculated in the pre-processing stage. The phase-coordinates or symmetrical-components approaches can be applied here. Designation of x_i in the input signals is related to the fault place in the training data. Details are presented in Figure (3.4) FNNs are designed to an adequate type of fault. If the line needs to be considered as an untransposed one the FNNs should be precisely adjusted to a specific type of fault. Recently, the neuro-fuzzy approach is becoming one of the major areas of interest because it has the benefits of neural networks as well as of fuzzy-logic systems and it removes the individual disadvantages by combining them on the common features [2].

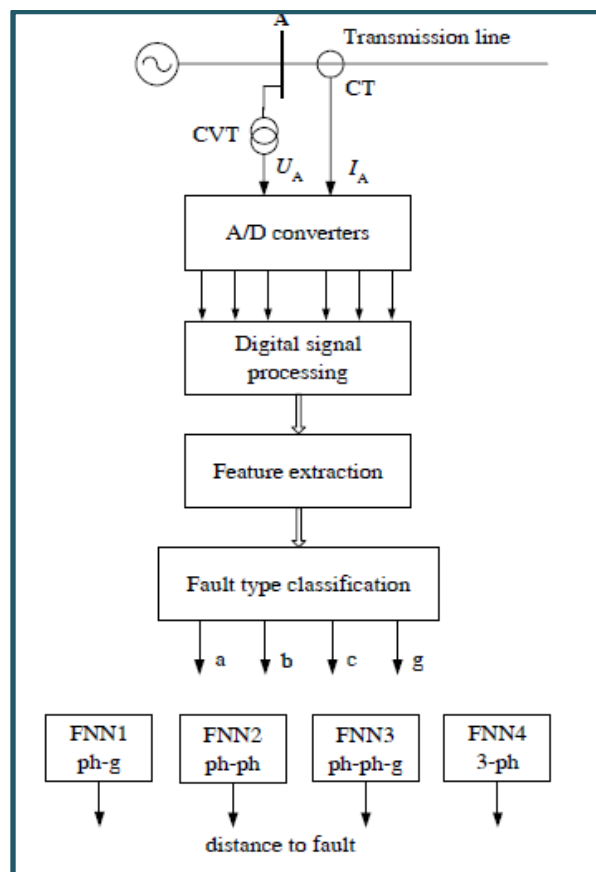


Figure (3.4) Detailed fault-location scheme based on FNN [2]

3.5.3 Adaptive Neuro-Fuzzy Inference System (ANFIS)

Fuzzy systems are generally used in cases when it is impossible or too difficult to define crisp rules that would describe the considered process or system, which is being controlled by a fuzzy control system. Thus, one of the advantages of fuzzy systems is that they allow describing fuzzy rules, which fit the description of real-world processes to a greater extent. Another advantage of fuzzy systems is their interpretability; it means that it is possible to explain why a particular value appeared at the output of a fuzzy system. In turn, some of the main disadvantages of fuzzy systems are that expert input or instructions are needed in order to define fuzzy rules, and that the process of tuning of the fuzzy system parameters (e.g., parameters of the membership functions) often requires a relatively long time, especially if there is a high number of fuzzy rules in the system. Both these disadvantages are related to the fact that it is not possible to train fuzzy systems. A diametrically opposite situation can be observed in the field of neural networks. User can train neural networks, but it is extremely difficult to use a priori knowledge about the considered system and it is almost impossible to explain the behavior of the neural system in a particular situation. In order to compensate the disadvantages of one system with the advantages of another system, several researchers tried to combine fuzzy systems with neural networks. A hybrid system named ANFIS (Adaptive- Network-Based Fuzzy Inference System or Adaptive Neuro-Fuzzy Inference System) has been proposed [10]. ANFIS is the fuzzy-logic based paradigm that grasps the learning abilities of ANN to enhance the intelligent system's performance using a priori knowledge. Using a given input/output data set, ANFIS constructs a Fuzzy Inference System (FIS) whose membership function parameters are tuned (adjusted) using either a back propagation algorithm alone, or in combination with a least squares type of method. This allows your fuzzy systems to learn from the data they are modeling. These techniques provide a method for the fuzzy modeling procedure to learn information about a data set, in order to compute the membership function parameters that best allow the associated fuzzy inference system to track the given input/output data. This learning method works similarly to that of neural networks. As the data in HVDC system are highly uncertain and the power disturbance monitoring is a pattern classification problem, therefore ANFIS based expert system is adopted for designing fault identifier. The existing method available for converter fault identification may give a very quick indication of the converter fault with the assumption that the overlap angle μ is limited up to 60 degrees. But the accuracy of the identifier totally relies on the proper selection of the delay time, i.e. the delay time exceeding the expected overlap angle μ may give false indication of fire through and false indication of commutation failure if the delay angle is not sufficient [35].

3.5.4 Genetic Algorithms

Genetic algorithms belong to the wide family of evolutionary computation methods. They are computational optimization algorithms that are inspired by Nature's evolutionary process. They primitively emulate (with great simplicity) the rules of natural selection, which favor the stronger species and force further evolution such that they remain alive in a given environment. GAs offer the attraction that all parts of the possible space are potentially available for consideration, so the global minimum should be attained if premature convergence can be avoided. The primary focus of such algorithms is the search for the global optimal state when for any reason the analytical methods cannot be used (e.g., for problems with multiple local optima, or even for problems where we do not know whether a single optimum is unique). Similarly as in

natural evolution, the process reproduced in GA delivers successive generations of individuals that are modified so as to approach an optimum form. Each descendant has different features from its parents, i.e., it is not a perfect but modified copy. If the new characteristics are favorable, the offspring is more likely to flourish and pass its characteristics to the next generation. However, an offspring with unfavorable characteristics is not reproduced, ending further development of the considered path. These concepts have been applied to mathematical optimization, where a population of candidate solutions develops toward an optimal point. Originating from the evolutionary inspiration, GA also uses biological terminology. The calculation procedure can be tracing by calling the natural process. Characteristics of a living organism (from the point of view of its fitness with respect to an environment) are determined by a set of chromosomes placed in each organism cell. The chromosomes are made up of genes, where each gene determines a particular attribute such as hair color. The complete set of genetic material is referred to as the genome, and a particular set of gene values constitutes a genotype. The resulting set of attributes is described as the phenotype [38]. Each individual in the population of candidate solutions is graded according to its fitness. The higher the fitness of a candidate solution, the greater are its chances of reproducing and passing its characteristics to the next generation. This simplified procedure constitutes the basis for genetic algorithms. In the computer program the process characteristics are represented by numbers. The searching algorithm optimizes the fitness function inside the search space that is defined by the set of chromosomes made up by genes. For example, in a simple case the chromosome can be composed of two genes: α , β , each defined by three binary numbers:

$$[\alpha \beta] = [\alpha_0 \alpha_1 \alpha_2 \beta_0 \beta_1 \beta_2]. \text{ e.g.: } [4 \ 3] = [1 \ 0 \ 0 \ 0 \ 1 \ 1]$$

The possible values for the genes are called alleles, so there are 8 alleles for each gene in this example. Each position along the chromosome is known as a locus; there are two decimal or six binary loci in the above example. It can be seen that the investigated problem involving many variables can be represented by the chromosome with as many as needed numbers of genes or with fewer numbers of genes and adequate numbers of loci in a single gene. For N binary numbers of loci there are $2N$ alleles in the chromosome. For each possible combination of genes in the search space there can be determined fitness function:

$$f(\alpha, \beta) = f(\alpha_0, \alpha_1, \alpha_2, \beta_0, \beta_1, \beta_2)$$

Each individual in the population has his specific chromosome. On the basis of this fitness function the selection process is performed: the fitter an individual, the more likely it is to be selected for further reproduction. The optimization process is performed iteratively by selection of the individuals with higher (less) fitness function belong to the consecutive created generations. The global optimization is assured thanks to two additional mechanisms performed in one after another generation (reproduction): *cross-over* and *mutation*. These operators define the method for creation of the next-generation individuals (candidate solution) by adequate modification of its chromosomes. *Cross-over* is the operation during which a new chromosome is created that typically shares many of the characteristics of its parents: mother and father. Different approaches can be applied here. For example, for a six-loci chromosome the new solutions can be generated as follows (m_i and f_i stand for: mother and father, respectively):

$$\begin{bmatrix} m_0 & m_1 & m_2 & m_3 & m_4 & m_5 \\ f_0 & f_1 & f_2 & f_3 & f_4 & f_5 \end{bmatrix} \rightarrow \begin{bmatrix} m_0 & f_1 & f_2 & f_3 & m_4 & m_5 \\ f_0 & m_1 & m_2 & m_3 & f_4 & f_5 \end{bmatrix}$$

Mutation involves changing the values of one or more loci. The classic example of a mutation operator involves a probability that an arbitrary bit in a chromosome will be changed from its original state. A common method of implementing the mutation operator involves generating a random variable for each bit in a sequence. This random variable indicates whether or not a particular bit will be modified. In this way parents are selected for each child, and the process continues until a new population of candidate solutions of appropriate size is generated. The general scheme of the GA is presented in Figure (3.5). GA starts with a randomly generated population (a set of solutions) and then moves from one population to another. This process continues until the stopping criteria are met. At each iteration, the new population is generated by applying various search operators.

Common terminating conditions are: solution is found that satisfies minimum criteria or fixed number of generations reached.

Genetic algorithms are a very effective way of quickly finding a reasonable solution to a complex problem. Moreover, the basic principle of the method is simple and clear. However, it is important to understand that the functioning of such an algorithm does not guarantee success because it has a stochastic nature and in some applications, a genetic pool may be too far from the solution [2].

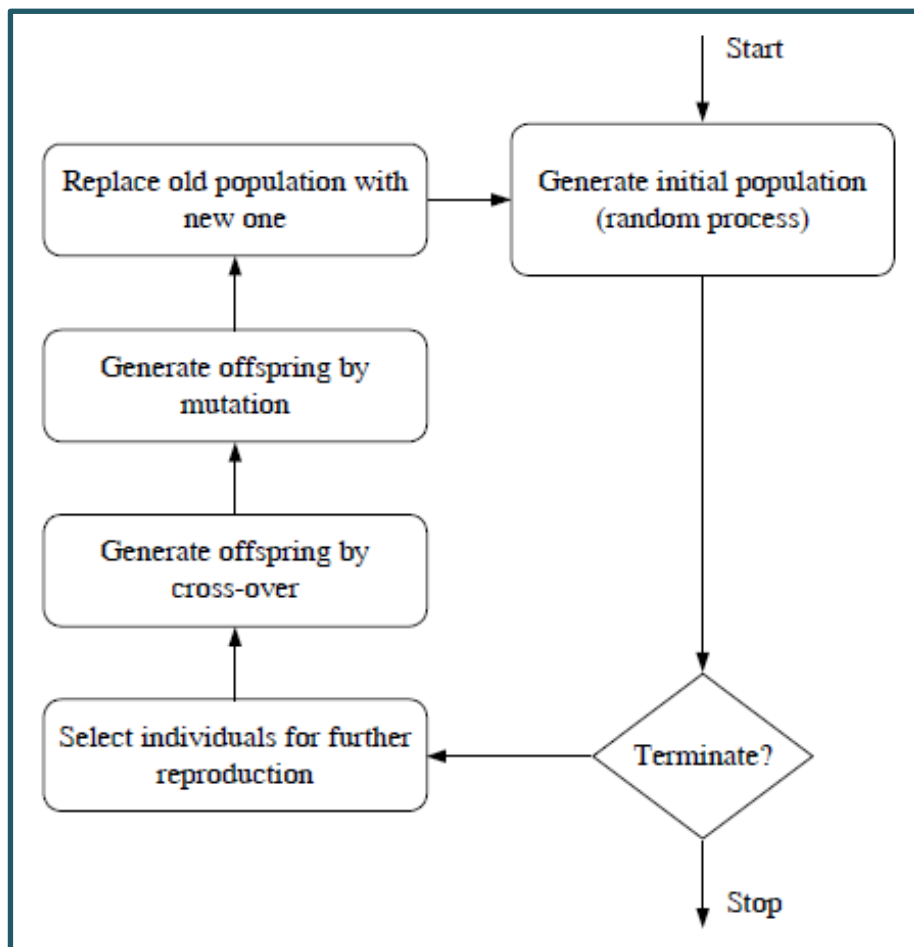
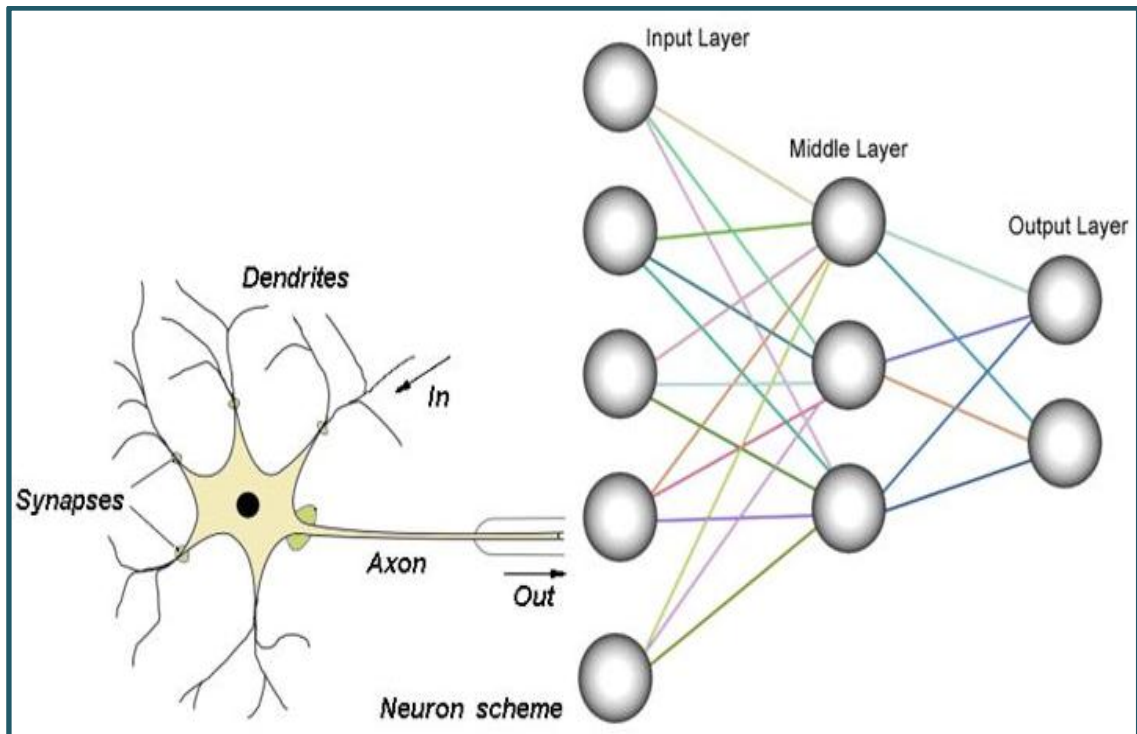


Figure (3.5) Flow chart of basic GA [2]

CHAPTER 4 ARTIFICIAL NEURAL NETWORKS



Working on artificial neural networks, commonly referred to "neural networks", has been motivated right from its inception by the recognition that the human brain computes in an entirely different way from the conventional digital computer. The brain is a highly complex, nonlinear and parallel computer (information processing system). It has the capability to organize its structural constituents, known as neurons. So as to perform certain computations (e.g. pattern recognition, perception and motor control) many times faster than the fastest digital computer in existence today [36].

In this chapter the intelligent copy of the brain, artificial neural networks (NN) will be studied. An introduction of how NN works is discussed in section 4.1. The neuron will be defined and studied in section 4.2. Section 4.3 explains activation function types and section 4.4 studies different structures of NN. In section 4.5 many types of NN learning strategies are introduced. Training and testing NN are discussed in section 4.6. Finally, training functions will be studied in section 4.7.

4.1 Introduction

An ANN is an adaptive, most often nonlinear system that learns to perform a function (an input/output map) from data. Adaptive means that the system parameters are changed during operation, normally called the training phase. After the training phase the ANN parameters are fixed and the system is deployed to solve the problem at hand (the testing phase). ANN is built with a systematic step-by-step procedure to optimize a performance criterion or to follow some implicit internal constraint, which is commonly referred to as the learning rule. The input/output training data are fundamental in neural network technology, because they convey the necessary information to “discover” the optimal operating point. The nonlinear nature of the neural network processing elements (PEs) provides the system with lots of flexibility to achieve practically any desired input/output map. There is a style in neural computation that is worth describing in Figure (4.1). An input is presented to the network and a corresponding desired or target response set at the output (when this is the case the training is called supervised). An error is composed from the difference between the desired response and the system output. This error information is fed back to the system and adjusts the system parameters in a systematic fashion (the learning rule). The process is repeated until the performance is acceptable. It is clear from this description that the performance hinges heavily on the data. If one does not have data that cover a significant portion of the operating conditions or if they are noisy, then neural network technology is probably not the right solution.

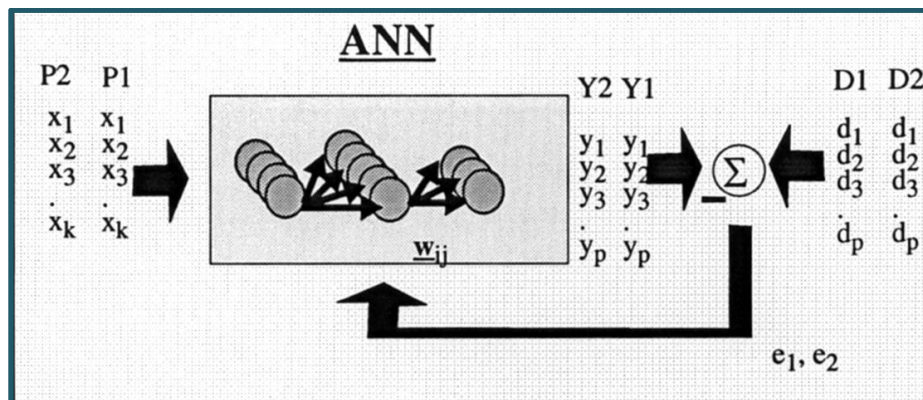


Figure (4.1): The style of neural computation [37]

On the other hand, if there is plenty of data and the problem is poorly understood to derive an approximate model, then neural network technology is a good choice. This operating procedure should be contrasted with the traditional engineering design, made of exhaustive subsystem specifications and intercommunication protocols. In ANNs, the designer chooses the network topology, the performance function, the learning rule, and the criterion to stop the training phase, but the system automatically adjusts the parameters. So, it is difficult to bring *a priori* information into the design, and when the system does not work properly it is also hard to incrementally refine the solution. But ANN-based solutions are extremely efficient in terms of development time and resources, and in many difficult problems ANNs provide performance that is difficult to match with other technologies [37].

4.2 NN Neuron

A neuron is an information processing unit that is fundamental to the operation of a neural network. The block diagram of Figure (4.2) shows the model of a neuron, which forms the basis for designing neural networks. Here we identify three basic elements of the neural model:

1. A set of synapses or connecting links, each of which is characterized by a weight or strength of its own.
2. An adder for summing the input signals, weighted by the respective synapses of the neuron.
3. An activation function for limiting the amplitude of the output of a neuron.

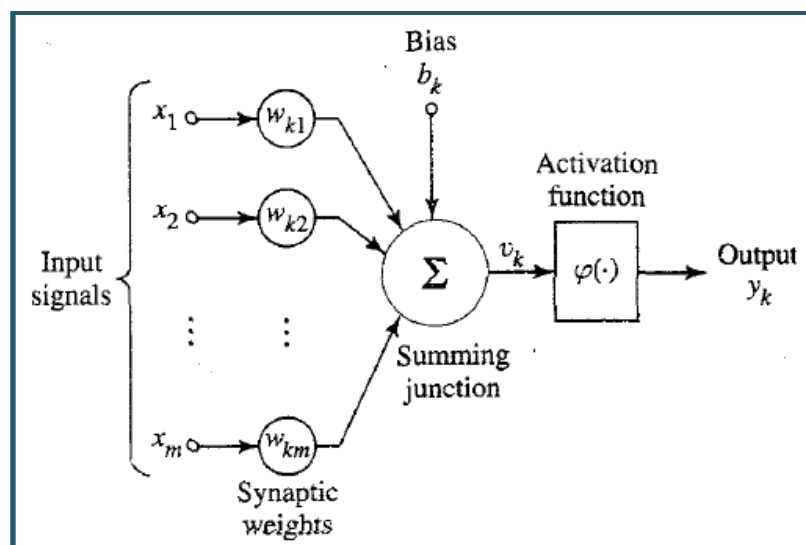


Figure (4.2): Nonlinear model of a neuron [36]

The neural model of Figure (4.2) also includes an externally applied bias, denoted by b_k . The bias b_k has the effect of increasing or lowering the network input of the activation function, depending on whether it is positive or negative, respectively [36].

In mathematical terms, we may describe a neuron k by writing the following pair of equations (4.1) and (4.2):

$$u_k = \sum_{j=1}^m w_{kj} x_j \quad (4.1)$$

$$y_k = \varphi(u_k + b_k) \quad (4.2)$$

where x_1, x_2, \dots, x_m are the input signals; $w_{k1}, w_{k2}, \dots, w_{km}$ are the synaptic weights of neuron k ; u_k is the linear combiner output due to the input signals; b_k is the bias; φ is the activation function; and y_k is the output signal of the neuron. The use of bias b_k has the effect of applying an affine transformation to the output u_k of the linear combiner in the model of Figure (4.2), as shown by equation (4.3) and (4.4): [36]

$$V_k = \sum_{j=0}^m w_{kj} x_j \quad (4.3)$$

$$y_k = \varphi(V_k) \quad (4.4)$$

4.3 Activation Functions

An activation function decides how powerful the output from the neuron should be, based on the sum of its inputs. Depending upon the application's requirements, the most appropriate activation function is chosen. The activation function φ can be in different forms, a few of which are described below:

1. Step function, equation (4.5):

$$\varphi(t) = \begin{cases} 1 & \dots t \geq 0 \\ 0 & \dots t < 0 \end{cases} \quad (4.5)$$

2. Piecewise linear function equation (4.6):

$$\varphi(t) = \begin{cases} 1 & \dots t > 1 \\ -1 & \dots t < -1 \\ t & \dots |t| < 1 \end{cases} \quad (4.6)$$

3. Sigmoid unipolar function, equation (4.7):

$$\varphi(t) = \frac{1}{1 + e^{-\beta t}} \quad (4.7)$$

4. Sigmoid bipolar function, equation (4.8):

$$\varphi(t) = \tanh(\beta t) = \frac{1 - e^{-2\beta t}}{1 + e^{-2\beta t}} \quad (4.8)$$

Figure (4.3) shows the above activation equations [6].

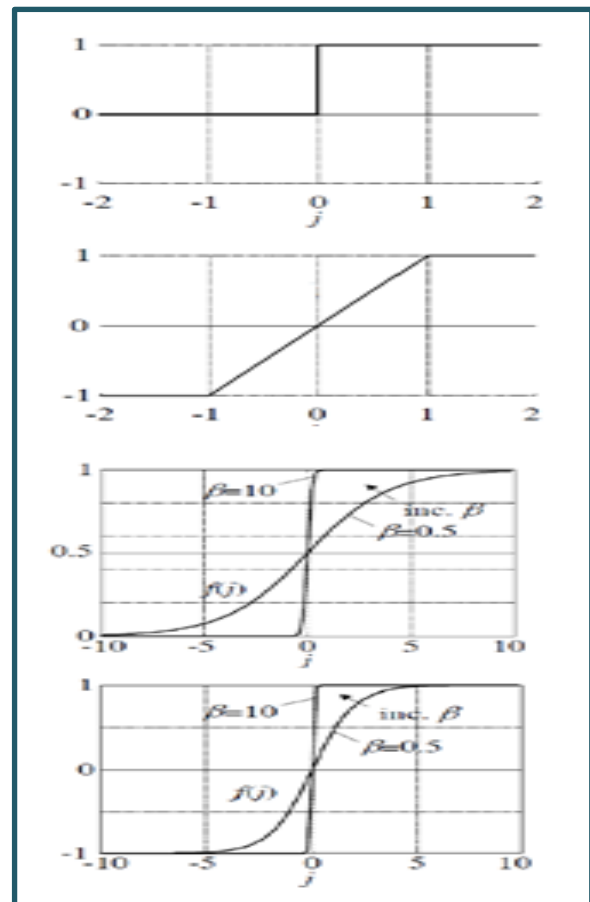


Figure (4.3): Different types of activation functions [6]

1. Step function.
2. Piecewise linear function
3. Sigmoid unipolar function
4. Sigmoid bipolar function

4.4 NN Structure

Based on the way the neurons are interconnected in a model, neural networks can be broadly classified into two types namely feed-forward and feedback networks. As the name suggests, feedback networks unlike feed-forward networks have a feedback connection fed back into the network along with the inputs.

4.4.1 Feed-forward NN:

Figure (4.4) shows the structure of a feed-forward multi-layer network with K_0 input and K_M output signals. Processing is realized in two final layers, so it is a two layer network. The intermediate layer is called hidden because their neurons have no connections with outside information. For simplicity, the polarizing signals frequently are not indicated in such schemes.

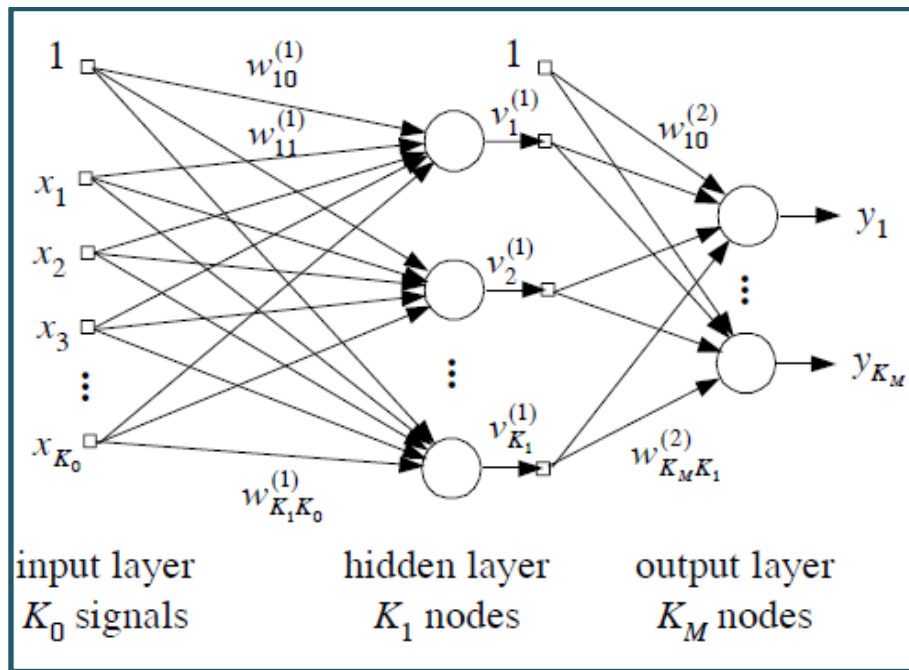


Figure (4.4): General structure of feed-forward NN [6]

Signal processing in the i^{th} network layer is performed according to the following relation (4.9):

$$v^{(i)} = f^{(i)}(W^{(i)} q^{(i-1)}) \quad (4.9)$$

Where:

$v^{(i)} = [v_1^{(i)} \ v_2^{(i)} \ v_3^{(i)} \ \dots \ v_k^{(i)}]^T$ Signal vector at the output of i^{th} layer.

$W^{(i)} = \begin{bmatrix} w_{10}^i & w_{11}^i & \dots & w_{1K_{i-1}}^i \\ w_{20}^i & w_{21}^i & \dots & w_{2K_{i-1}}^i \\ \vdots & \vdots & \vdots & \vdots \\ w_{K_i 0}^i & w_{K_i 1}^i & \dots & w_{K_i K_{i-1}}^i \end{bmatrix}$ Weighting matrix between $(i-1)^{\text{th}}$ and i^{th} layer.

\mathbf{x} : vector of input signals, $f^{(i)}(\cdot)$: activation function of neurons at the i^{th} layer, M: number of processing layers.

$$q^{(i-1)} = \begin{cases} x & \text{for } i=1 \\ \begin{bmatrix} 1 \\ v^{(i-1)} \end{bmatrix} & \text{for } i=2,3,\dots,M \end{cases}$$

It is assumed that all neurons of the i^{th} layer are the same. There may be more than one hidden layer. The result of the network processing is represented by the output vector in equation (4.10):

$$y = v^{(M)} = [y_1 \quad y_2 \quad \dots \quad y_{K_M}]^T \quad (4.10)$$

At present, the majority of problems use feed-forward architecture. Such networks are widely used in prediction, filtering, information selection and decision making.

Due to feed-forward simplicity and the existence of a well-defined learning algorithm [2], only feed-forward networks have been used in this thesis for the simulation.

4.4.2 Recurrent NN

Modification of a multi-layer perceptron that leads to feedback between the output and input of the network gives a recurrent network. Such networks may have a different structure depending on the depth and type of the connections between output (from the network output or any hidden layer) and input. An example is presented in Figure (4.5). That is a so-called real-time recurrent network. The processing layer is composed of the output and hidden neurons. Feedback is created by connection of neurons from the processing layer with input layer through the delaying lines. In the input layer there are input signals and feedback signals. Because of feedback such a network has its own dynamics: steady state is achieved after multiple input–output interactions. Changing of any neuron influences the entire network. Therefore, such a structure is suitable for simulation of dynamic processes. Unfortunately, the negative side of the introduced feedback is the possible appearance of unstable regions in the network operation [2].

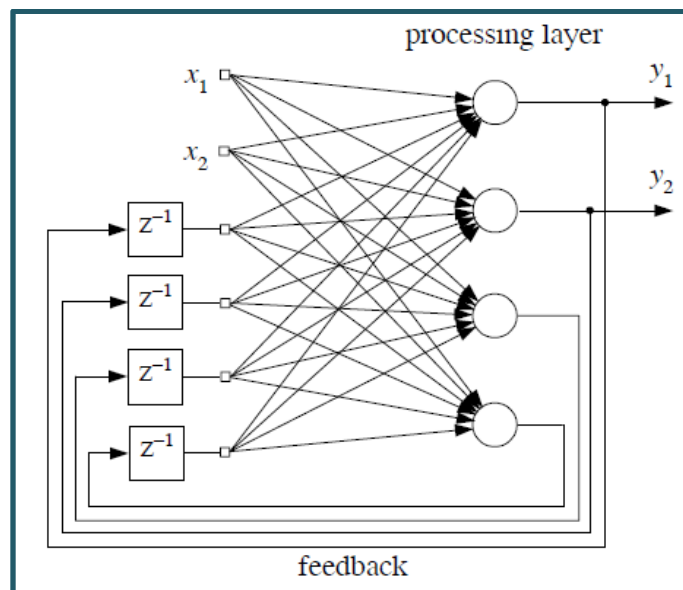


Figure (4.5): Structure of recurrent NN [2]

4.5 NN Learning Strategies

The basic problem in designing of ANN lies in determination of the weights in order to achieve the desired objective. This process is usually called learning or training. Generally, there are two strategies of ANN learning: supervised or unsupervised learning. Supervised learning consists in modification of the network weights with the intention of minimization of the difference (error) between the presented input examples and the target output values. This strategy may be considered as some form of ‘teaching’ in which the teacher has knowledge of the desirable input–output relations. The input signals are considered as a training vector and the desired response represents the optimum action to be performed by the network. The error signal is defined as the difference between the actual and desired network response [38, 8].

In unsupervised learning there is no external teacher and there are no defined relations between inputs and output. The learning is performed on the basis of a set of examples where only input conditions are known. In the learning process these examples are selected with respect to some similarity principle. Such a network may be considered as a self-organizing system that is learning on a competitive principle: the output neurons compete among themselves to be activated with the result that only one neuron is on at any time (a winner-takes-all competition rule). The learning strategy depends on an ANN structure. In the case of feed-forward multi-layer networks supervised learning is used [8]. Its structure is presented in Figure (4.6).

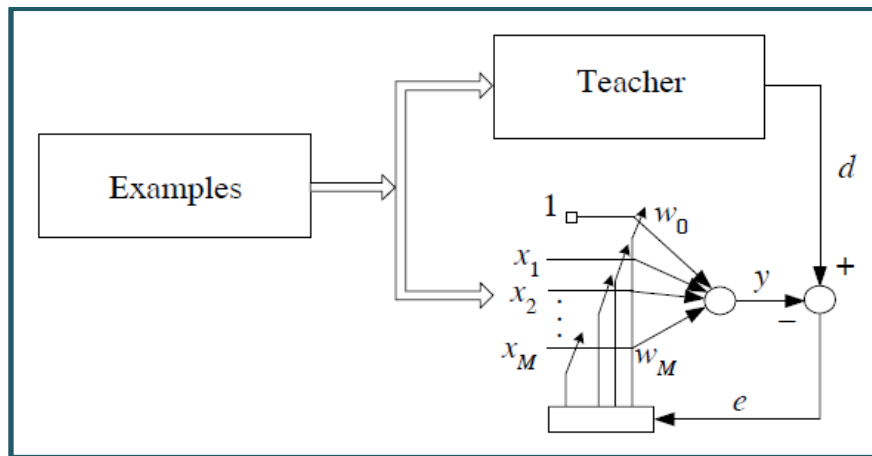


Figure (4.6): Scheme of supervised learning [2]

For simplicity, the considered example is connected with a one-neuron network.

The set of examples used in the learning process (with known input–output relations) are collected from measurements or are obtained from simulation. In the last case it is assumed that the system model is known. Successive correction of the neuron weighting coefficients is performed according to the following rule in equation (4.11):

$$w_{ji}(n+1) = w_{ji}(n) + \Delta w_{ji}(n) \quad (4.11)$$

Where:

$w_{ji}(n)$ and $w_{ji}(n+1)$ represent previous and corrected weights between the i^{th} and j^{th} adjoining layers; while $\Delta w_{ji}(n)$ is a correction value; n is the number of the iteration step. A stable learning process is assured by such choice of corrections $\Delta w_{ji}(n)$ that the previous iteration calculations are convergent.

Consider the j^{th} neuron in a single-layer network. The learning process is based on minimizing errors between the actual output of the considered j^{th} neuron: $y_j(n)$ and the value requested by the teacher $d_j(n)$ which can be represented by equation (4.12):

$$e_j(n) = d_j(n) - y_j(n) \quad (4.12)$$

These errors are collected in vector $\mathbf{e}(n)$. We can see that the vector $\mathbf{e}(n)$ is a function of weighting coefficients vector $\mathbf{w}(n)$ at the input to the considered layer. The correction value in equation (4.11) can be calculated as follows in equation (4.13):

$$\Delta w_{ji}(n) = \eta e_j(n) x_i(n) \quad (4.13)$$

Where:

x_i is the i^{th} input signal;

η : is the learning rate parameter determining the speed of iteration process.

The aim of learning is to obtain a minimum of error function equation (4.12). For a network composed of L neurons the error function can be defined as in equation (4.14):

$$S_2(w) = \frac{1}{2} \sum_{j=1}^L (d_j - y_j)^2 \quad (4.14)$$

If the training set contains P learning pairs of $(\mathbf{x}(n), \mathbf{d}(n))$ with input vector $\mathbf{x}(n)$ and vector $\mathbf{d}(n)$ of desired outputs then for the n^{th} iteration step of learning the error function can be described as in equation (4.15):

$$S_2(w(n)) = \frac{1}{2} \sum_{n=1}^P \sum_{j=1}^L (d_j(n) - y_j(n))^2 \quad (4.15)$$

Minimization of equation (4.15) is a non-linear problem because of non-linear activation functions. Fortunately, there are known effective numerical algorithms for minimization of that function, which is based on the steepest-descent method. They are an analytical base for the back-error-propagation learning strategy. The back-error-propagation algorithm consists in calculation of correction values equation (4.13) as functions of errors estimated from minimization of equation (4.15). The process is performed layer by layer across the network in the reverse direction starting from the output layer. The structure of the algorithm is presented in Figure (4.6). Corrected weighting vectors are determined in blocks $A^{(M)}, A^{(M-1)}, \dots, A^{(1)}$ and errors 'propagated' to low layers are calculated in blocks $B^{(M-1)}, B^{(M-2)}, \dots, B^{(2)}$. There are many kinds of different implementation of the back-error propagation algorithm. They differ in methods of determination of new weighting coefficients, which can be successfully upgraded when errors are passed back from layer to layer, or in parallel after finalizing a given iterative step. The grade of network 'learning' can be evaluated by checking the value of corrections equation (4.13) in successive stages. The number of iterative steps (that is equivalent to the size of prepared learning set) needed to achieve satisfactory convergence depends on the network size, their structure, kind of investigated problem, details of used learning algorithm and so on. Sometimes, the learning set should have the size of many thousand cases [2].

Correctness of the chosen ANN structure and learning process can be controlled by evaluation of the network outputs on some test excitation (with known answers). A testing set of input-output pairs is a part of all learning sets of cases, which, however,

was not used in the learning. Although the back-error propagation is the most frequently used method for training feed-forward ANN, it is neither the only nor necessarily the unique approach. First, the technique has no adaptive feature so all learning examples should be used every time the weighting coefficients are updated, even if a subset is not pertinent to the subject under consideration (the importance of some learning examples is not easy to determine). The method could not be easily adopted to optimize an ANN size and structure. Moreover, such an algorithm can be very slow in the vicinity of the final solution [39].

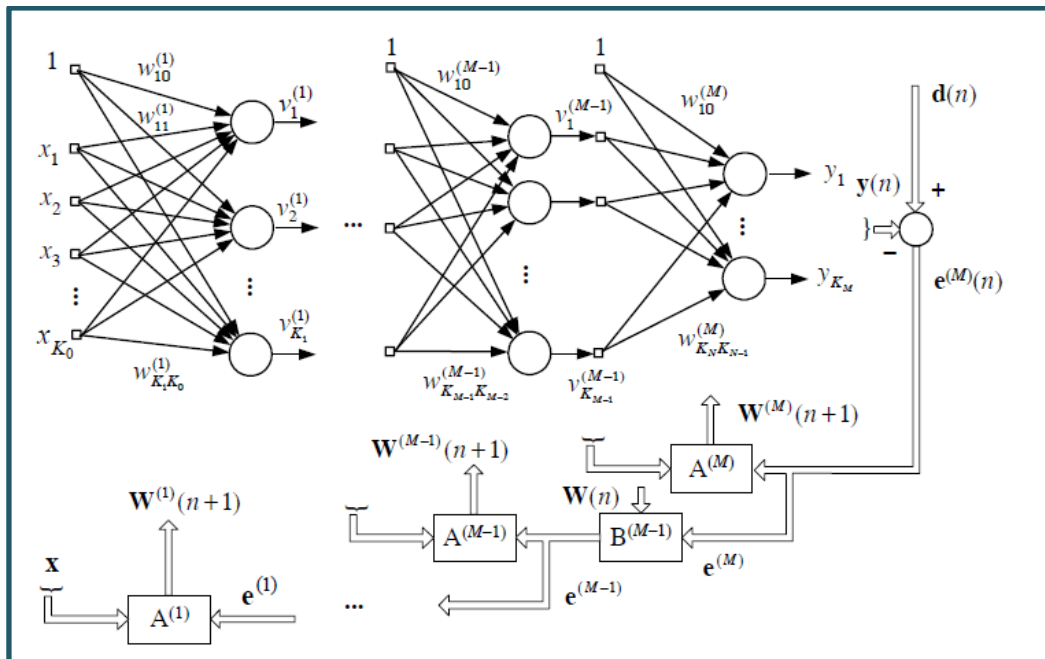


Figure (4.7): Structure of back-error-propagation algorithm [2]

4.6 Training and Testing NN

The best training procedure is to compile a wide range of examples (for more complex problems, more examples are required), which exhibit all the different characteristics of the problem. To create a robust and reliable network, in some cases, some noise or other randomness is added to the training data to get the network familiarized with noise and natural variability in real data. Poor training data inevitably leads to an unreliable and unpredictable network. Usually, the network is trained for a prefixed number of epochs or when the output error decreases below a particular error threshold. Special care is to be taken not to over train the network. By overtraining, the network may become too adapted in learning the samples from the training set, and thus may be unable to accurately classify samples outside of the training set [40].

4.6.1 Choosing the Number of Neurons

The number of hidden neurons affects how well the network is able to separate the data. A large number of hidden neurons will ensure correct learning, and the network is able to correctly predict the data it has been trained on, but its performance on new data, its ability to generalize, is compromised. With few hidden neurons, the network may be unable to learn the relationships amongst the data and the error will fail to fall below an acceptable level. Thus, selection of the number of hidden neurons is a crucial decision.

4.6.2 Choosing the Initial Weights

The learning algorithm uses a steepest descent technique, which rolls straight downhill in weight space until the first valley is reached. This makes the choice of initial starting point in the multidimensional weight space critical. However, there are no recommended rules for this selection except trying several different starting weight values to see if the network results are improved [40].

4.6.3 Choosing the Learning Rate

Learning rate effectively controls the size of the step that is taken in multidimensional weight space when each weight is modified. If the selected learning rate is too large, then the local minimum may be overstepped constantly, resulting in oscillations and slow convergence to the lower error state. If the learning rate is too low, the number of iterations required may be too large, resulting in slow performance [40].

4.7 Training Functions

As an illustration of how the training works, consider the simplest biases in the direction in which the performance function decreases most rapidly, the negative of the gradient. An iteration of this algorithm can be written as:

$$\mathbf{x}_{k+1} = \mathbf{x}_k - \alpha_k \mathbf{g}_k \quad (4.16)$$

where \mathbf{x}_k is a vector of current weights and biases, \mathbf{g}_k is the current gradient, and α_k is the learning rate. This equation is iterated until the network converges.

A list of the training algorithms which use gradient- or Jacobian-based methods is shown table (4.1) [41].

Table (4.1): Training Algorithms and their MATLAB Functions

No.	MATLAB Function	Algorithm
1	trainlm	Levenberg -Marquardt
2	trainbr	Bayesian Regularization
3	trainbfg	BFGS Quasi-Newton
4	trainrp	Resilient Backpropagation
5	trainscg	Scaled Conjugate Gradient
6	traincgb	Conjugate Gradient with Powell/Beale Restarts
7	traincgf	Fletcher-Powell Conjugate Gradient
8	traincgp	Polak-Ribière Conjugate Gradient
9	trainoss	One Step Secant
10	traingdx	Variable Learning Rate Gradient Descent
11	traingdm	Gradient Descent with Momentum
12	traingd	Gradient Descent

The fastest training function is generally trainlm, and it is the default training function for feed-forward net. The quasi-Newton method, trainbfg, is also quite fast. Both of these methods tend to be less efficient for large networks (with thousands of weights), since they require more memory and more computation time for these cases. Also, trainlm performs better on function fitting (nonlinear regression) problems than on pattern recognition problems. When training large

networks, and when training pattern recognition networks, `trainscg` and `trainrp` are good choices. Their memory requirements are relatively small, and yet they are much faster than standard gradient descent algorithms [41].

It is very difficult to know which training algorithm will be the fastest for a given problem. It depends on many factors, including the complexity of the problem, the number of data points in the training set, the number of weights and biases in the network, the error goal, and whether the network is being used for pattern recognition (discriminant analysis) or function approximation (regression) [41].

In general, for networks that contain up to a few hundred weights, the Levenberg-Marquardt algorithm will have the fastest convergence. This advantage is especially noticeable if very accurate training is required. In many cases, `trainlm` is able to obtain lower Mean Square Errors than any of the other algorithms. However, as the number of weights in the network increases, the advantage of `trainlm` decreases. In addition, `trainlm` performance is relatively poor on pattern recognition problems. The storage requirements of `trainlm` are larger than the other algorithms tested. The `trainrp` function is the fastest algorithm on pattern recognition problems. However, it does not perform well on function approximation problems. Its performance also degrades as the error goal is reduced. The memory requirements for this algorithm are relatively small in comparison to the other algorithms considered. The conjugate gradient algorithms, in particular `trainscg`, seem to perform well over a wide variety of problems, particularly for networks with a large number of weights. The SCG algorithm is almost as fast as the LM algorithm on function approximation problems (faster for large networks) and is almost as fast as `trainrp` on pattern recognition problems. Its performance does not degrade as quickly as `trainrp` performance does when the error is reduced. The conjugate gradient algorithms have relatively modest memory requirements. The performance of `trainbfg` is similar to that of `trainlm`. It does not require as much storage as `trainlm`, but the computation required does increase geometrically with the size of the network because the equivalent of a matrix inverse must be computed at each iteration. The variable learning rate algorithm `traingdx` is usually much slower than the other methods, and has about the same storage requirements as `trainrp`, but it can still be useful for some problems. There are certain situations in which it is better to converge more slowly. For example, when using early stopping you can have inconsistent results if you use an algorithm that converges too quickly. You might overshoot the point at which the error on the validation set is minimized [41]. For more information about how the training functions work look to [42].

CHAPTER 5 MODEL SIMULATION



This chapter includes all the thesis work and simulation. Conditions and properties of the chosen model for HVDC system are discussed in (5.1). Chosen model Components are described in (5.2). Model simulation outputs are presented in (5.3). Section (5.4) covers the used methodologies for simulation of NNs and then the testing and training of used NNs are analyzed in (5.5). Finally, section (5.6) summarizes the results of simulation.

5.1 Building Model

This thesis focuses on fault detecting, classifying and locating on overhead, bipolar HVDC TL. Therefore, studied power network has been chosen to meet the following conditions:

1. The network must exist in the world to make benefit of the result.
2. It has to be HVDC Network.
3. It has to be Overhead and bipolar transmission line.
4. It has to be long enough to study fault location precisely

Few numbers of TL satisfy the above conditions. By studying the existed networks around the world, the most compatible network was constructed in China, in 2003, to connect the land of Three Gorges with Changzhou (3GC). It is a 940-kilometre (580 mi) long, 3000 MW capacity and bipolar 12-pulse HVDC transmission line. The (3GC), ± 500 -kV DC Transmission project is an integral part of the Three Gorges Hydroelectric Power Project. The DC transmission used to transmit the bulk power generated by this project to the Changzhou area in East China. The project interconnects the central power region of China to the eastern power region of China. The 3000 MW rated power will be transmitted to a distance of 940 km on one single bipolar DC line at ± 500 kV. Figure (5.1) shows the single line diagram of 3GC [43].

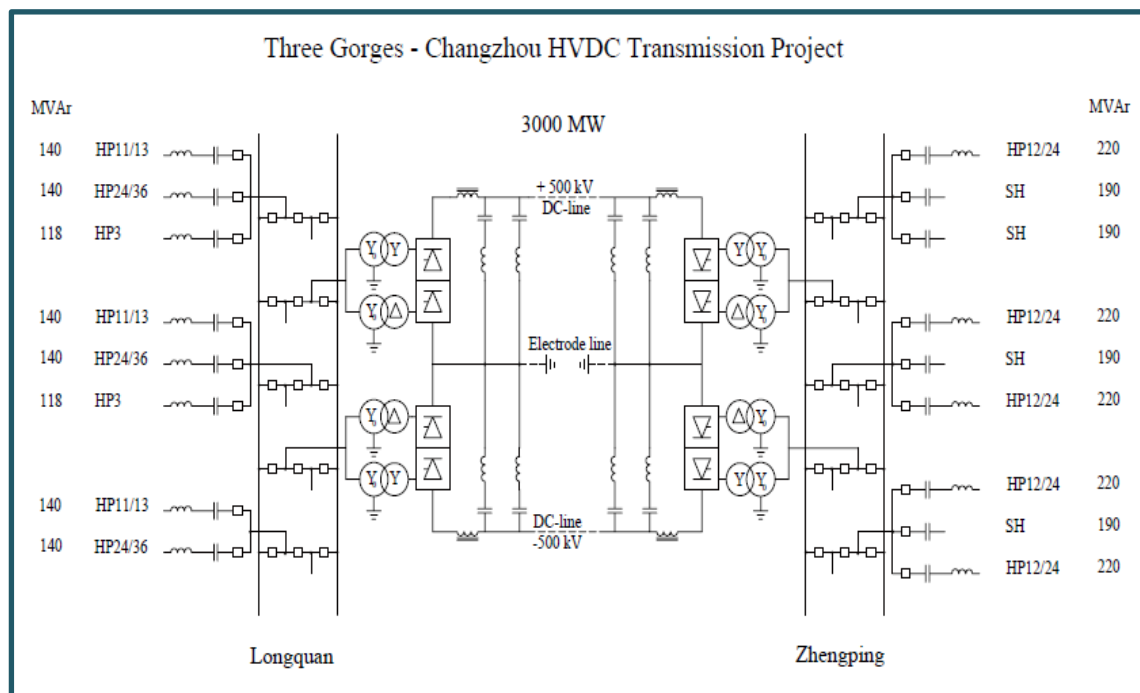


Figure (5.1): Three Gorges – Changzhou Single Line Diagram [43]

5.2 Three Gorges - Changzhou Main Components

To construct any research model, its components and their specifications must be known. Three Gorges-Changzhou network consists of the following main components:

5.2.1 Filters

Switchable filter/capacitor banks on the converter station AC buses are used as compensation equipment. At Longquan there are eight switchable sub-banks with a total capacity of 1076 Mvar. Three of those are HP11/13 (140 Mvar), three HP24/36 (140 Mvar) and remaining two as HP3 (118 Mvar).

A total of 1860 Mvar is provided in Zhengping, divided into nine switchable sub-banks; four of which are pure shunt capacitors, each rated for 190 Mvar. The remaining five are HP12/24 filter sub-banks, each rated for 220 Mvar [43].

5.2.2 Valves

Each converter is built up of twelve (air insulated, water-cooled) single valves arranged in six units. Each suspended unit consists of two single valves combined into one mechanical unit called a double valve. There are 90/84 thyristors per valve at Longquan/Zhengping respectively. The thyristors used are 5" (YST90) and are identical for the two stations [43].

5.2.3 Converter Transformers

The converter transformers are of the single phase two-winding type with two wound legs. The nominal parameters of the Longquan transformers are 297.5 MVA, 525/210.4 kV, 16% reactance.

The nominal parameters of the Zhengping transformers are 283.7 MVA, 500/200.4 kV, 16% reactance [43].

5.2.4 DC Smooth Reactors

Oil insulated smoothing reactors with a reactance of 290/270 mH are used in each pole at Longquan/Zhengping respectively [43].

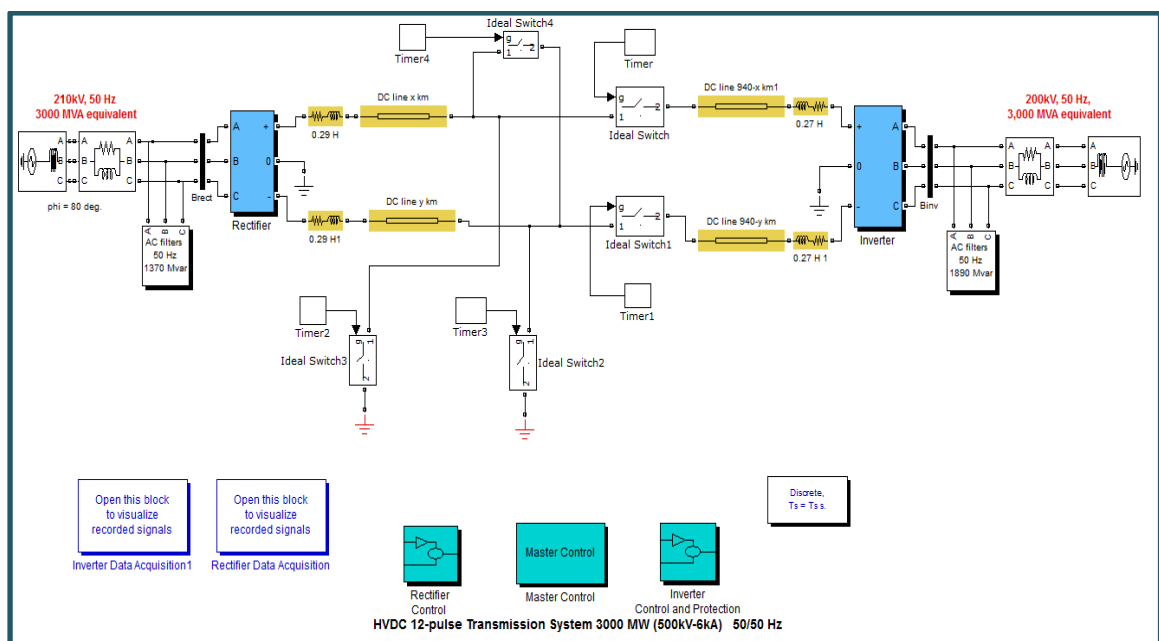


Figure (5.2): HVDC MATLAB model

The model specifications in table (5.1) were used to construct the Matlab model using SimPowerSystem toolbox, which is one of MATLAB program toolboxes. Figure (5.2) shows the HVDC Matlab model. This model was developed from Thyristor-Based HVDC Transmission System MATLAB example model [43,44].

Table (5.1) Summarized Specifications of the Simulated Model

Rectifier side							
AC Source				Converter Transformers			Smooth Reactors
Ph-Ph voltage	Internal resistance	Internal Inductance	Frequency	Type	Capacity	Voltages	Value
210KV	0 Ω	98.03mH	50 Hz	Single phase	297.5 MVA	525/210.4 KV	290 mH
Transmission Line							
Length		Resistance		Inductance		Capacitance	
940 km		0.015 Ω/km		.792 mH/km		14.4 μF/km	
Inverter Side							
AC Source				Converter Transformers			Smooth Reactors
Ph-Ph voltage	Internal resistance	Internal Inductance	Frequency	Type	Capacity	Voltages	Value
200.4KV	0 Ω	28 mH	50 Hz	Single phase	283.7 MVA	500/200.4 KV	270 mH

5.3 Model Outputs

Many outputs can be noticed from the studied Matlab model to distinguish between faulty and no-fault conditions; however, the focus was on the measurements of AC and DC voltages and currents at the rectifier side. The same measurements at the inverter side can also be used. The network will be simulated with a sampling time of 5×10^{-5} seconds for five types of faults each 5-km of the TL starting at the 15th km to 925th km and will be simulated many times for no fault conditions.

In each simulation, the needed measurements will be recorded to use them as input to the neural networks. To study a certain fault, the voltages and currents at the instant of fault does not give clear vision to make the neural network work properly. Therefore, a comparison between the post- and pre-fault measurements have to be employed. For the time being, there is no protection system can deal with faults in less than a duration of one cycle after fault occurrence. So, the measurements of voltages and currents after a duration of one cycle of fault occurrence are compared to their measurements before a duration of one cycle of the fault occurrence.

Based on a sampling time of 5×10^{-5} and a network frequency of 50 Hz each cycle is represented by 400 impulses. The network outputs are depicted in equation (5.1).

$$Outputs = \begin{bmatrix} V_a * \\ V_b * \\ V_c * \\ I_a * \\ I_b * \\ I_c * \\ V_{dc1} * \\ V_{dc2} * \\ I_{dc1} * \\ I_{dc2} * \end{bmatrix} = \begin{bmatrix} (V_a + 400)/(V_a - 400) \\ (V_b + 400)/(V_b - 400) \\ (V_c + 400)/(V_c - 400) \\ (I_a + 400)/(I_a - 400) \\ (I_b + 400)/(I_b - 400) \\ (I_c + 400)/(I_c - 400) \\ (V_{dc1} + 400)/(V_{dc1} - 400) \\ (V_{dc2} + 400)/(V_{dc2} - 400) \\ (I_{dc1} + 400)/(I_{dc1} - 400) \\ (I_{dc2} + 400)/(I_{dc2} - 400) \end{bmatrix} \dots(5.1)$$

Where:

$x+400$ represents the value of x at 400 impulses after the instant of fault occurrence.
 $x-400$ represents the value of x at 400 impulses before the instant of fault occurrence.

400 impulses represent a complete cycle in 50 Hz frequency and 5×10^{-5} sampling time.

V_a : AC Voltage of phase a at the rectifier side

V_b : AC Voltage of phase b at the rectifier side.

V_c : AC Voltage of phase c at the rectifier side.

I_a : AC Current of phase a at the rectifier side.

I_b : AC Current of phase b at the rectifier side.

I_c : AC Current of phase c at the rectifier side.

V_{dc1} : DC voltage of positive line at the rectifier DC side.

V_{dc2} : DC voltage of Negative line at the rectifier DC side.

I_{dc1} : DC Current of positive line.

I_{dc2} : DC Current of negative line.

5.3.1 Model Outputs at Fault and No-Fault Conditions

The first level in this work is to detect faults; this mission requires studying the differences between the data of faults and no faults. Table (5.2) shows different data of each type of faults at a distance of 340 and 600 km away from the rectifier side and data in no fault conditions. From table (5.2) each type of faults has a special data. The no fault case is the normal case which has data of approximately ones. Using the AC data only is not enough while there is no important change between AC data at each fault type. By studying DC data we can compare between each type of faults and detecting the fault. The using of AC and DC data is required in this work in fault location level, using all data will make the results stronger in all research levels.

5.3.2 Fault Position Effect On The Model Outputs

From table (5.2) the model output data of voltages and currents changes according to the fault position; this property can be used in neural network to determine the fault location.

5.4 Simulator Levels

This research has three levels of simulation; first, the research detect existence of fault. While the network works normally without any fault the simulator will stop. When the simulator detect fault the simulator moves to the second level.

The second level means that a fault has occurred, the simulator starts to classify the type of that fault. It can classifies five different fault types; positive line to ground (+ve/GND) fault, negative line to ground (-ve/GND) fault, positive line to negative line (+ve/-ve) fault, positive line open circuit (+ve O.C) fault and negative line open circuit (-ve O.C) fault.

In the third level the simulator starts to determine the location of the fault related to the distance from the rectifier side. Each type has a special NN to determine its location. Figure (5.3) shows the simulation levels used in this thesis.

Table (5.2): Comparison of model output for fault and no-fault conditions at distances of 340- and 600- km away from the rectifier side

Station	Fault Dist.	+ve/GND		-ve/GND		+ve /-ve		+ve O.C		-ve O.C		No Fault	
		340	600	340	600	340	600	340	600	340	600	x	x
Rectifier Station	V_a^*	2.14	1.65	2.03	1.55	0.45	0.90	1.90	1.92	1.82	1.81	1.02	1.02
	V_b^*	0.75	0.76	0.74	0.75	0.25	0.33	1.11	1.10	1.08	1.06	1.00	1.00
	V_c^*	0.45	0.57	0.45	0.57	0.21	0.21	0.94	0.92	0.91	0.90	1.00	1.00
	I_a^*	2.51	2.48	2.53	2.49	2.92	3.36	0.63	0.62	0.70	0.72	1.00	1.00
	I_b^*	-3.3	-2.4	-3.2	-2.36	-3.2	-3.3	0.53	0.57	0.54	0.55	0.99	0.99
	I_c^*	0.54	0.81	0.59	0.84	0.83	1.10	0.60	0.60	0.65	0.66	1.00	1.00
	V_{dc1}^*	0.14	-0.1	0.70	0.74	0.07	-0.2	2.53	1.79	1.00	0.97	0.99	0.99
	V_{dc2}^*	0.73	0.78	0.14	-0.09	0.07	-0.2	1.02	1.00	2.52	1.79	0.99	0.99
	I_{dc1}^*	3.28	3.26	0.21	0.23	2.46	2.40	-0.02	0.01	1.29	1.32	1.00	1.00
	I_{dc2}^*	0.12	0.14	3.28	3.26	2.46	2.40	1.19	1.21	-0.02	0.01	1.00	1.00
Inverter Station	V_a^*	-0.6	-0.2	-0.6	-0.2	-1.0	-0.6	0.18	0.34	0.12	0.28	0.98	0.98
	V_b^*	0.97	0.98	0.97	0.98	0.95	0.97	0.99	1.00	0.97	0.99	1.00	1.00
	V_c^*	1.11	1.08	1.11	1.08	1.12	1.10	1.06	1.06	1.05	1.05	1.00	1.00
	I_a^*	0.06	0.09	0.08	0.11	0.00	0.00	0.42	0.45	0.53	0.53	1.00	1.00
	I_b^*	0.04	0.07	0.06	0.09	0.00	-0.0	0.56	0.56	0.58	0.59	0.99	0.99
	I_c^*	0.01	0.03	0.03	0.04	-0.0	-0.0	0.83	0.77	0.69	0.70	0.99	0.99
	V_{dc1}^*	0.00	-0.0	0.14	0.19	0.00	-0.0	0.01	-0.0	1.17	1.18	0.99	0.99
	V_{dc2}^*	0.09	0.15	0.00	-0.0	0.00	-0.0	1.12	1.13	0.01	-0.0	0.99	0.99
	I_{dc1}^*	-0.1	-0.5	0.86	0.82	-0.1	-0.5	0.16	-0.6	0.97	1.00	1.00	1.00
	I_{dc2}^*	0.88	0.83	-0.1	-0.5	-0.1	-0.5	0.98	0.99	0.16	-0.6	1.00	1.00

5.5 Neural Networks Application

Neural network is the tool employed to detect, classify and locate the faults in this thesis. By taking the simulation outputs and feeding them as inputs of a neural network we can approach the promising results.

Neural network structures have to be modified by changing number of layers, number of neurons, training functions, weights and biases to get the best performance and least mean square error.

Each level in detection and classifying fault has a special structure of neural networks and each position locator of each fault type has its topology differs from another.

The neural network must be trained using outputs of the model before using to achieve the needed performance. After the choosing of a neural network, different groups of model outputs are applied to the neural network to test its performance.

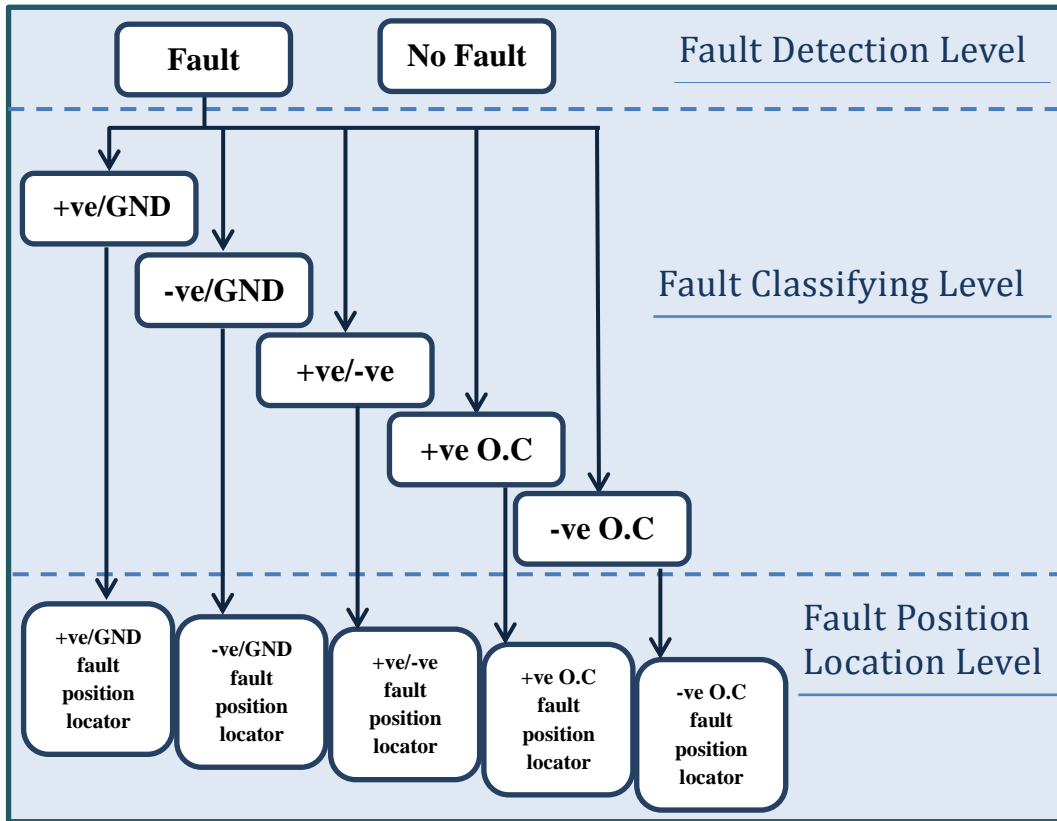


Figure (5.3): Simulation levels

5.5.1 Training of Fault Detection Neural Network

To train neural network to detect the existence of the fault, measurements of 952 different conditions for different types of faults at different locations, and some of no fault cases were used as inputs for the neural network. The output of the neural network states whether a fault exists or not: a value of '1' means a faulty condition while a value of '0' indicates an unfaulty condition. Many NN topologies have been trained to get the best performance; when the DC measurements at the rectifier station were used only in **4-4-8-1** NN topology, best validation MSE of 1×10^{-11} is

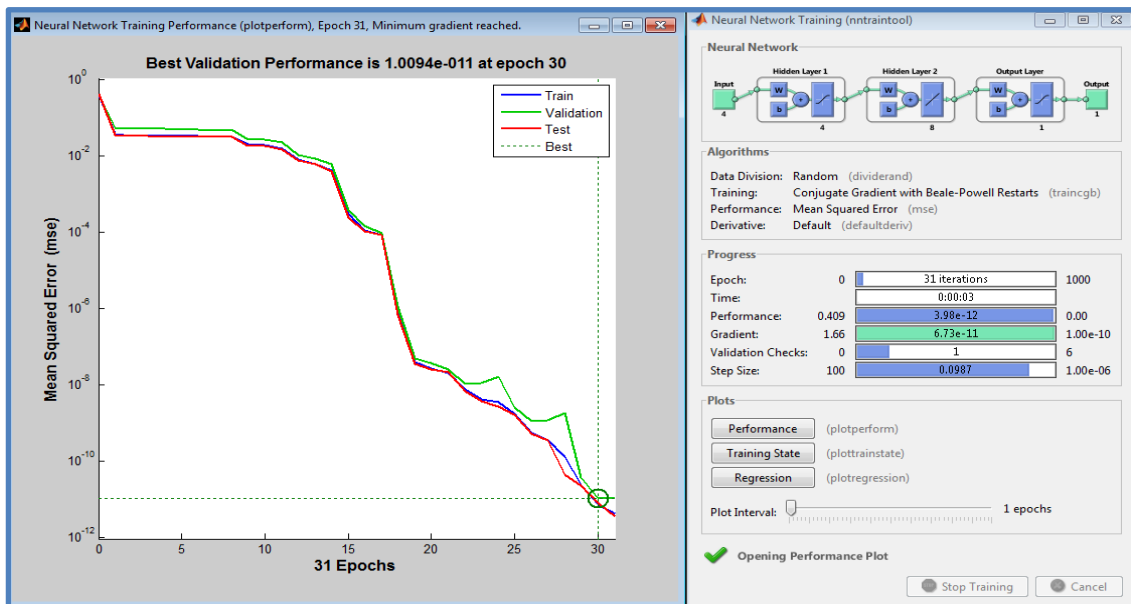


Figure (5.4): Performance of DC input fault detection NN

achieved. This value is acceptable and gives good results. Figure (5.4) shows the NN topology with the fault detection performance with DC inputs .To increase accuracy, the number of inputs have been increased by including the AC voltage and current measurements at the converter side. The 10 inputs represent all the measurement data studied in section 5.3 at rectifier station. Figure (5.5) shows the chosen 10-10-10-1 NN topology and its performance when employing the Conjugate Gradient with Beale Powell Restarts training function. With the chosen topology best validation MSE of 6.18×10^{-13} and gradient of 1.4×10^{-11} were achieved.

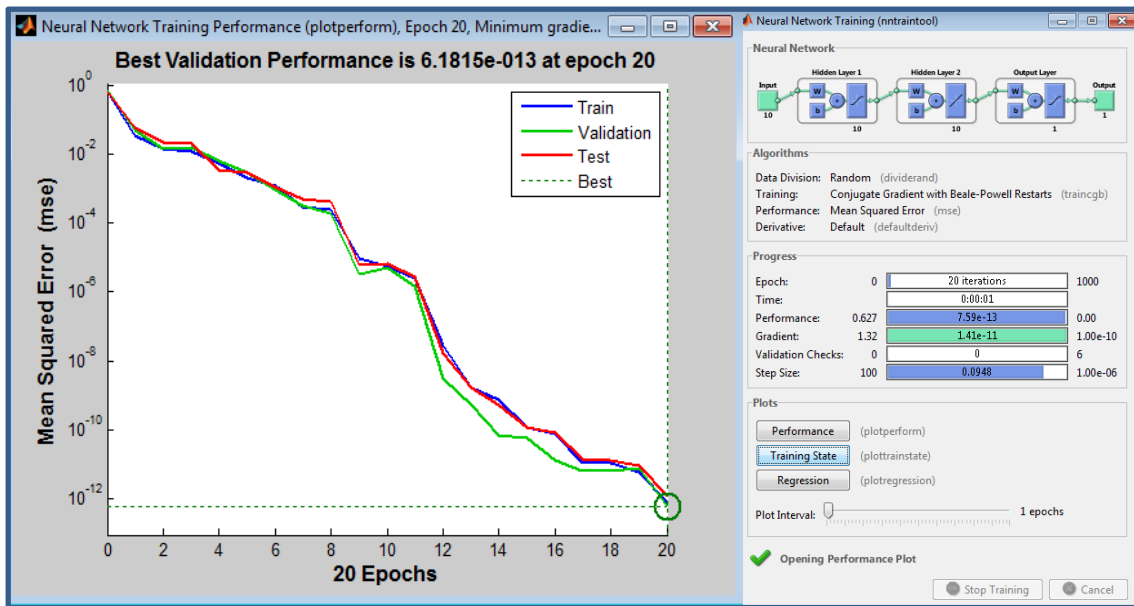


Figure (5.5): Performance of ten input fault detection NN

Note that

MATLAB program divides NN training data to three groups; training data; to train and found appropriate NN weights and biases , validation data; used to validate the trained NN, and Test data; used to test NN performance (represents by 70%, 15% and 15% of total data, respectively, by default).

5.5.2 Testing of Fault Detection Neural Networks

To test the chosen neural networks, data of 393 model outputs for conditions differ than the training conditions are used as input for the trained 4-4-8-1 NN. The maximum error value between NN output and the target values was 7.3×10^{-7} while by using ten input NN of 10-10-10-1 topology, the maximum error value between NN output and the target values was 6.7×10^{-6} . Where the NN output is zero or one, NN output can be approximated to make NN get zero error in all tested cases. So, both NNs can be used to detect faults with an accurate result.

5.5.3 Training of Fault Classifying Neural Network

After detecting fault the next task of classifying that fault starts. Five types of Overhead Bipolar HVDC TL faults (in section 5.4) are studied, each has a special code represents it. Table (5.3) shows the fault types and their represented codes.

Table (5.3): Fault types and their codes.

Fault	+ve/GND	-ve/GND	+ve /-ve	+ve O.C	-ve O.C
Code	001	010	011	100	101

Each digit in the code represents an output of NN. The used NN will be with 4 inputs and 3 outputs if we use only the DC measurements of model outputs at the rectifier station and will be with 10 inputs and 3 outputs if we use all model simulation outputs. If we use only DC outputs of the model at the rectifier station to classify faults, a NN of 4-10-20-10-3 is used to get best validation MSE of 8.8×10^{-12} which is an acceptable result. Figure (5.6) shows the performance of classifying fault NN with inputs of DC measurements only.

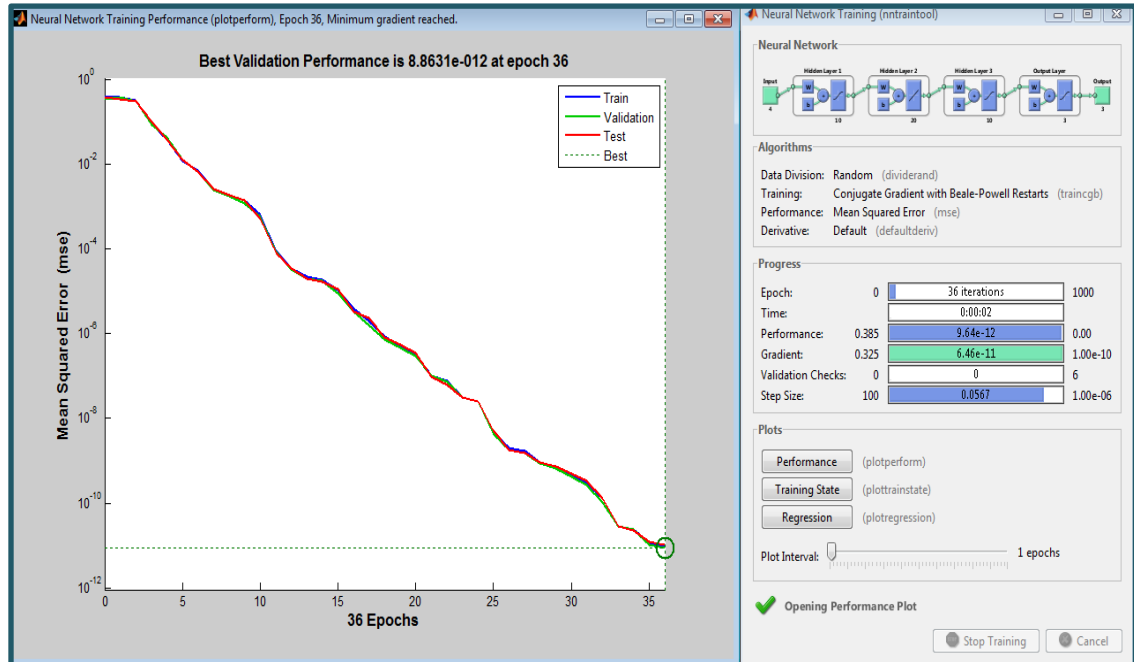


Figure (5.6): Performance of DC input fault-classifying NN

In the other hand and after too many attempts to increase accuracy, using ten inputs that represent all the measurements mentioned in section 5.3 at the rectifier station, the NN of 10-10-20-3 topology with Conjugate Gradient with Beale Powell Restarts training function gives the best validation MSE with a value of 1.62×10^{-12} . Figure (5.7) shows the 10-10-20-3 NN topology and its performance.

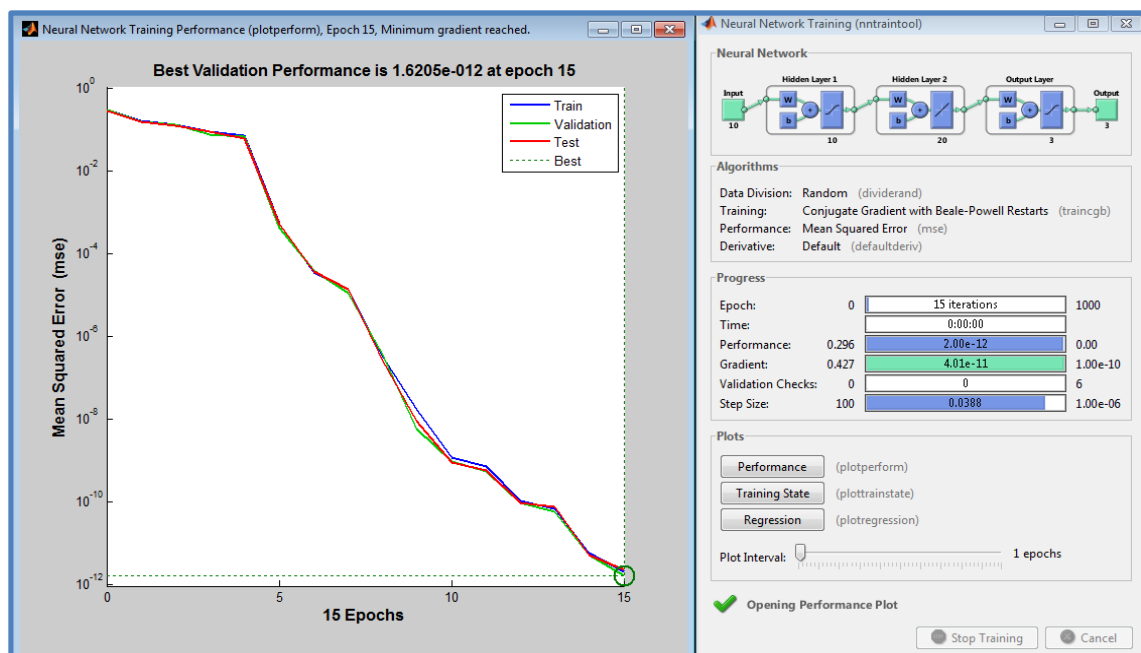


Figure (5.7): Performance of ten input fault classifying NN.

5.5.4 Testing of Fault Classifying Neural Network

To be sure, that we construct a powerful NN, model outputs of 355 cases for different faults at locations differ from the locations used in training the NN were used to test the trained classifying NN of 4-10-20-10-3 topology. The maximum error value was 2.8×10^{-6} between NN outputs and targets. While by using 10-10-20-3 topology, the maximum error in digits value of NN simulation related to the target outputs was 7.2×10^{-6} . All outputs of these NNs have values of zeros or ones. Therefore, by approximating these outputs to the nearest integer; NN get no errors in all tested cases.

5.5.5 Training of Positive to Ground Fault locator Neural Network

In case of positive to ground fault occurs another level starts. The target of this level is to determine the fault distance from the rectifier side. The model is simulated in this level each 3 km between the 15 km and the 925 km and the simulation outputs at the rectifier side and the inverter side are taken as inputs for a new NN to get the best performance. In fault locators, twenty different inputs represent the measurements mentioned in section 5.3 from both rectifier and inverter stations are used. The increasing in inputs is to improve NN performance. Figure (5.8) shows the used 20-50-10-5-1 NN topology to locate the +ve/GND fault location and its regression plot. This NN has best validation MSE of 6.7×10^{-5} .

From regression plot, all the outputs (in circles) have values near their targets (the diagonal line), the simulation maximum errors occur in the first 100 km from the rectifier, the total outputs can be represented with the following equation (5.2):

$$\text{Output} \approx \text{Target} + 0.84 \text{ km} \quad (5.2)$$

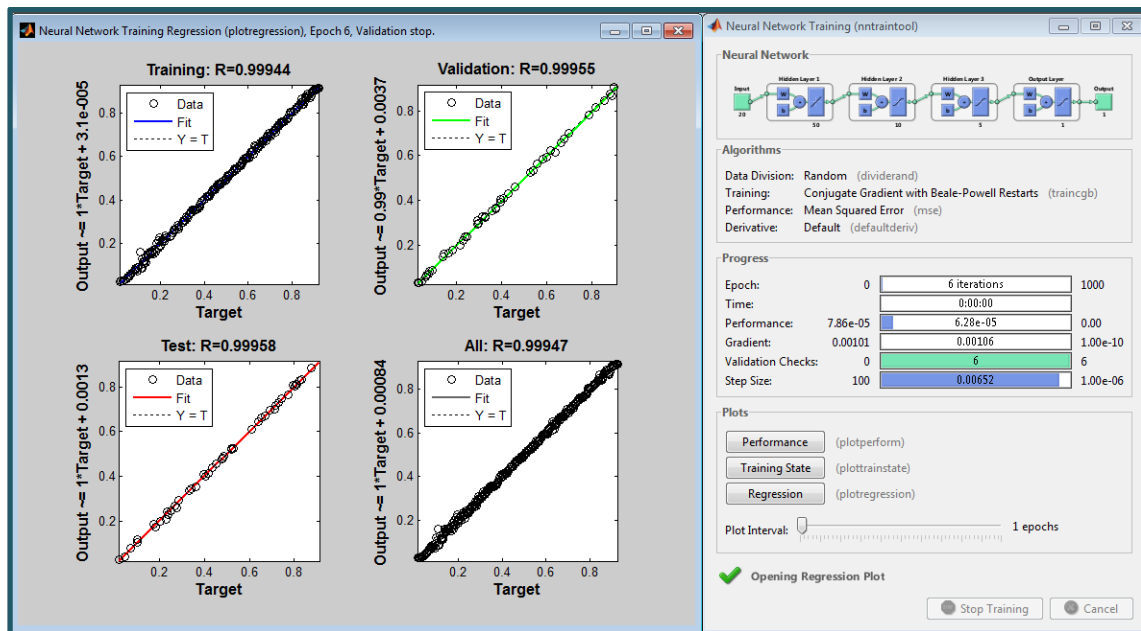


Figure (5.8): Regression plot of training positive to ground fault locator NN

Note that

Regression plot is a MATLAB Figure that shows the relation between NN outputs and targets, where NN outputs are represented by circles. This Figure gives the ability to represent outputs by equation of targets.

5.5.6 Testing of Positive to Ground Fault Locator Neural Network

To test the chosen +ve/GND fault locator, measurements of 71 different locations of positive to ground fault are used. Table (5.4) shows sample of these outputs and targets for different positions. The errors vary from 0.1 km to 36.8 km with an average of 7.34 km. Figure (5.9) shows the regression plot of the relation between targets and outputs of the testing +ve/GND fault locator NN.

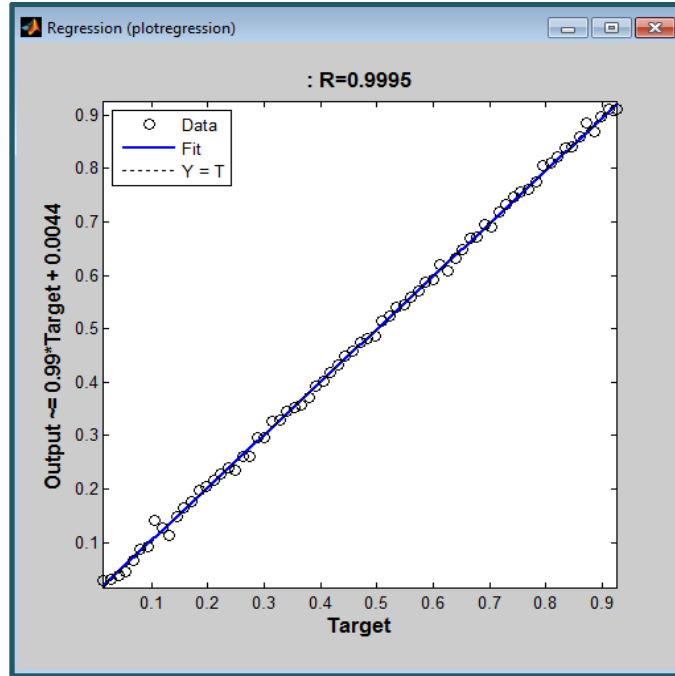


Figure (5.9): Regression plot of testing positive to ground fault NN

From Figure (5.9), the outputs of NN testing data can be represented by the following equation (5.3):

$$\text{Output} \approx 0.99 \times \text{Target} + 4.4 \text{ km} \quad (5.3)$$

Outputs in this Figure approaches their targets and worse case appears in range of 100-150 km away from the rectifier station. These results are acceptable while the errors are very small related to the HVDC TL length.

Table (5.4): Errors of testing +ve/GND fault locator NN

Target output	NN output	Error	Target output	NN output	Error	Target output	NN output	Error
28	31.6	3.6	314	327.9	13.9	665	669.7	4.7
41	37.5	3.5	340	344.6	4.6	704	691.1	12.9
67	66.3	0.7	379	371.1	8.9	743	746.4	3.4
80	87	7	418	419.4	1.4	782	774.1	7.9
106	142.8	36.8	457	459.4	2.4	821	821.1	0.1
119	128.7	9.7	470	474.8	4.8	834	837.1	3.1
145	148.6	3.6	509	514.1	5.1	886	868.8	17.2
184	197.2	13.2	530	539.3	9.3	899	897.2	1.8
223	228.9	5.9	587	586.5	0.5	912	910.1	1.9
262	261.1	0.9	626	608.9	17.1	925	910.7	14.3

5.5.7 Training of Negative to Ground Fault Locator Neural Network

As before in training positive to ground fault locator, the HVDC model simulation outputs for both rectifier and inverter sides of 304 different positions of negative to ground fault have been simulated with 20-50-10-5-1 NN – which is the best found NN- to find the fault location. Figure (5.10) shows the used NN and its performance and the relation between NN outputs and targets. From Figure (5.10), the NN outputs have values near the target values, the total outputs can be represented as in equation (5.4):

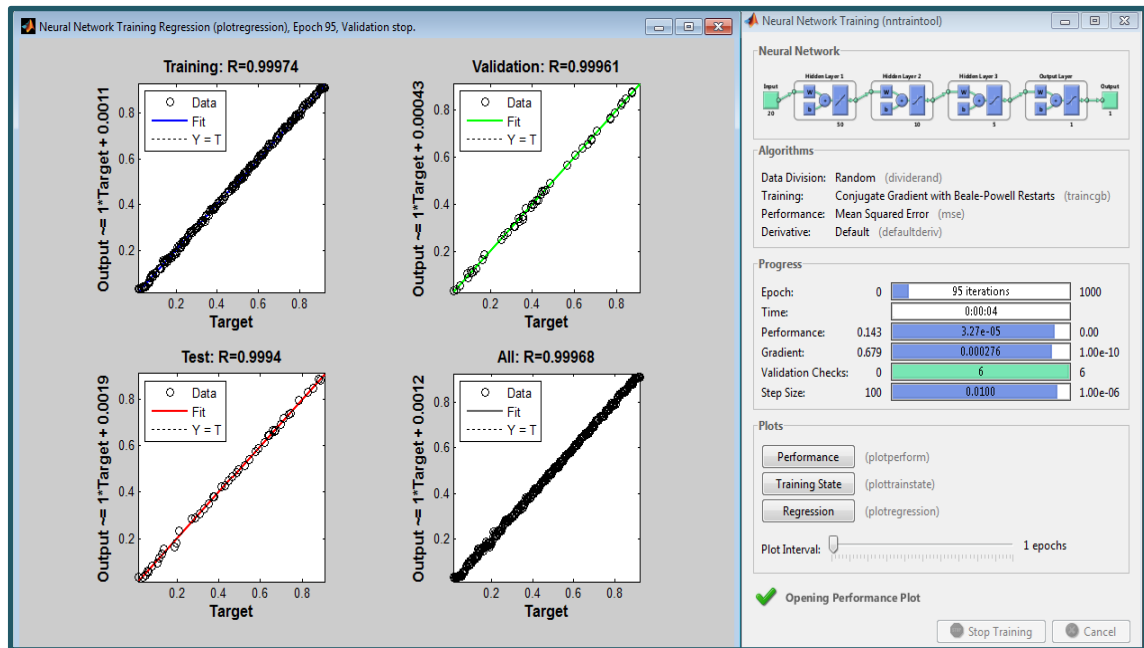
$$\text{NN Output} \approx \text{Target} + 1.2 \text{ km} \quad (5.4)$$


Figure (5.10): Regression plot of training negative to ground fault locator NN.

5.5.8 Testing of Negative to Ground Fault Locator Neural Network

To test the previous NN in Figure (5.10), the measurements of 71 different locations of HVDC TL for –ve/GND faults have been tested with the NN. The NN outputs of these data were compared with the targets to test the NN. Table (5.5) shows a sample of the tested locations and the NN outputs and errors between them. The error is varying between 0.3- to 17.5- km with an average of 6.2 km. Figure (5.11) shows the relation between target and output data of the used NN in testing level. The outputs can be represented by equation (5.5):

$$\text{Output} \approx \text{Target} + 2.9 \text{ km} \quad (5.5)$$

Table (5.5): Errors of testing -ve/GND fault locator NN

Target output	NN output	Error	Target output	NN output	Error	Target output	NN output	Error
28	35.3	7.3	314	307.2	6.8	665	661.6	3.4
41	38.1	2.9	340	329.4	10.6	704	714.4	10.4
67	62.3	4.7	379	380.8	1.8	743	737.6	5.4
80	88.5	8.5	418	419.8	1.8	782	792	10
106	110	4	457	461.2	4.2	821	827.2	6.2
119	121	2	470	464.6	5.4	847	843.4	3.6
145	142.8	2.2	509	517.4	8.4	860	850.2	9.8
184	189.3	5.3	535	539.2	4.2	899	905.3	6.3
223	205.5	17.5	587	579.7	7.3	912	906.3	5.7
262	266.3	4.3	626	626.3	0.3	925	909.1	15.9

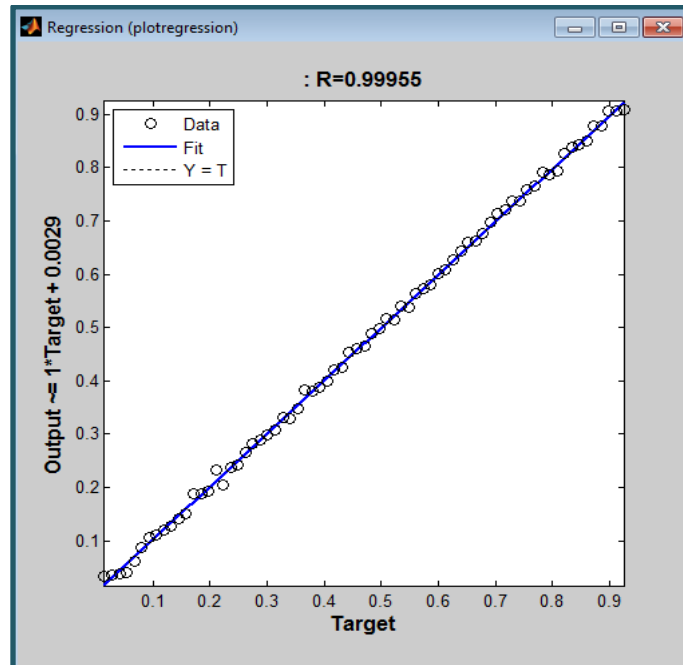


Figure (5.11): Regression plot of testing negative to ground fault locator NN

5.5.9 Training of Positive to Negative Line Fault Locator Neural Network

The third type of discussed faults is the positive to negative line fault. To create a NN that can understand the +ve/-ve fault behavior when the fault location changes, the HVDC TL model simulated with +ve/-ve fault hundred times to take the measurements at the rectifier and inverter sides and feed them as inputs of the NN. After many attempts, the NN of 20-40-5-3-1 topology and Levenberg-Marquardt training function was chosen to reach the +ve/-ve fault location. Figure (5.12) shows the chosen NN locator of +ve/-ve fault for HVDC TL model and performance regression plot. A MSE of 4.87×10^{-5} was reached in the NN training. Total outputs of the trained data can be represents by equation (5.6):

$$\text{Output} \approx \text{Target} + 0.8 \text{ km} \quad (5.6)$$

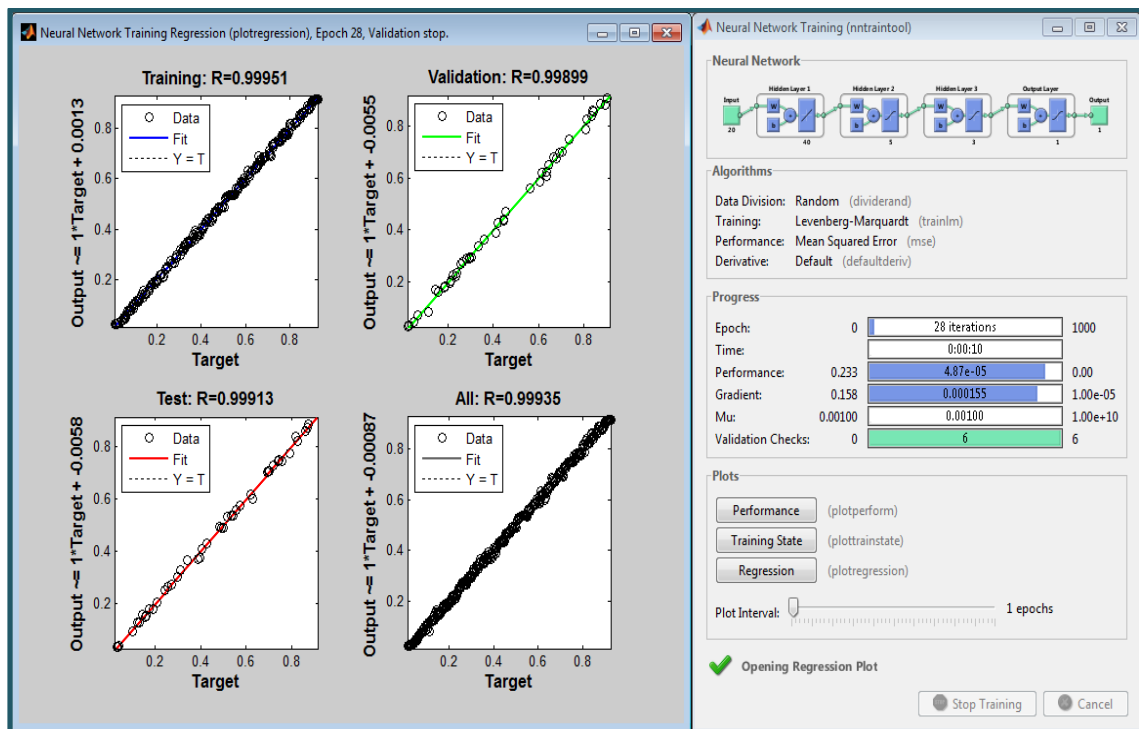


Figure (5.12): Regression plot of training positive to negative line fault locator NN

5.5.10 Testing of Positive to Negative Line Fault Locator Neural Network

After choosing the NN, it have to be tested to be sure that it can work precisely. The measurements at the rectifier and the inverter for 71 different locations of the +ve/-ve fault differs from that used in the training level were used to test the chosen NN. Table (5.6) shows a sample of NN outputs and their assumed targets and errors between them. The errors vary from 0.3 km to 22.8 km with an average of 7 km error. Figure (5.13) shows the plot of the relation between the NN outputs and the assumed targets in testing level. The NN tested outputs can be represented by the following equation (5.7):

$$\text{Output} \approx \text{Target} + 1.9 \text{ km} \quad (5.7)$$

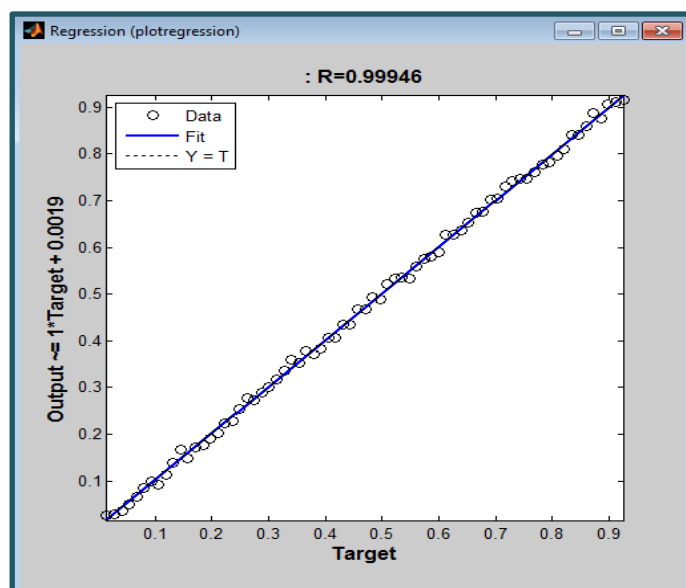


Figure (5.13): Regression plot of testing positive to negative line fault locator NN

Table (5.6): Errors of testing +ve/-ve fault locator NN

Target output	NN output	Error	Target output	NN output	Error	Target output	NN output	Error
28	28.6	0.6	314	317.7	3.7	665	675.2	10.2
41	35.6	5.4	340	359.2	19.2	704	704.9	0.9
67	66.7	0.3	379	371.4	7.6	743	747.8	4.8
80	84.3	4.3	418	407.2	10.8	782	777.8	2.2
106	91.9	14.1	457	468	11	821	809.2	11.8
119	112.6	6.4	470	467.7	2.3	847	841.1	5.9
145	167.8	22.8	509	521.5	12.5	860	859.5	0.5
184	176.8	7.2	535	535.9	0.9	899	905.1	6.1
223	224.3	1.3	587	579.2	7.8	912	910.7	1.3
262	277.5	15.5	626	628	2	925	914.6	10.4

5.5.11 Training of Positive Line Open Circuit Fault Locator NN

Two types of open circuit faults can happen in bipolar HVDC TL, positive line open circuit fault and negative line open circuit fault. To create a NN that can determine the location of the positive line open circuit fault, many topologies of NN have been simulated. The NN topology of 20-20-5-3-1 was chosen to determine fault location of this type. Figure (5.14) shows the chosen NN performance and the relation between NN outputs and their assumed targets in each level of the NN training. A MSE of 1.43×10^{-5} was achieved and the NN outputs have values near their assumed targets. The chosen NN outputs can be represented by equation (5.8):

$$\text{Output} \approx \text{Target} + 0.9 \text{ km} \quad (5.8)$$

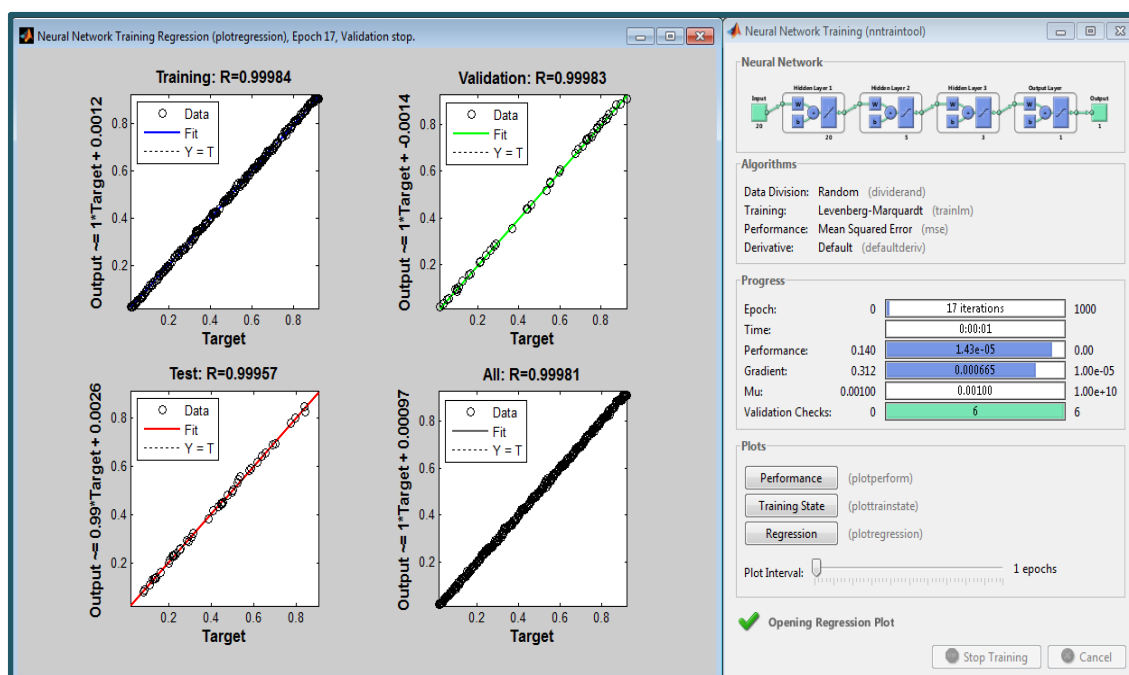


Figure (5.14): Regression plot of training positive line open circuit fault locator NN..

5.5.12 Testing of Positive Line Open Circuit Fault locator NN

The chosen NN in previous section was tested with measurements of 71 different locations differ from that in training level to test the NN performance. Table (5.7) shows a sample of the tested locations and the NN output for each location with the errors between them and their assumed targets. The errors vary from 0.2 km to 21.4 km with an average of 5 km error found at all tested cases.

Figure (5.15) shows the relation between the tested NN outputs and their assumed targets. The following equation (5.9) represents the NN outputs related to their targets:

$$\text{Output} \approx \text{Target} + 0.039 \text{ km} \quad (5.9)$$

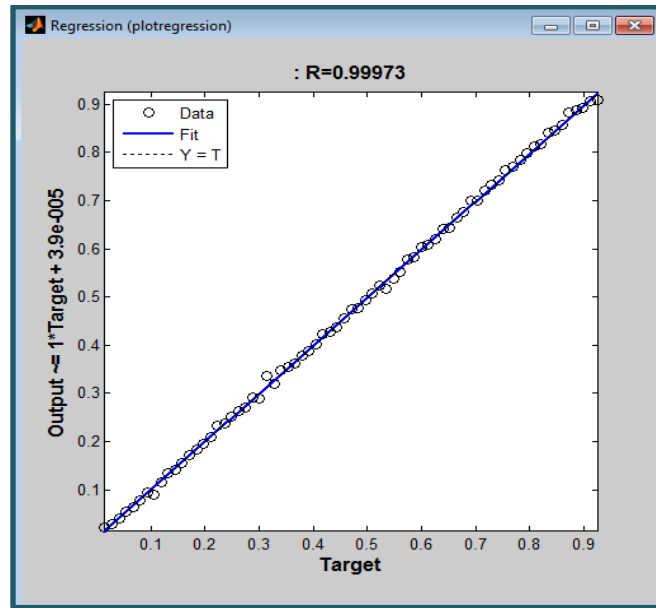


Figure (5.15): Regression plot of testing positive line open circuit fault locator NN

Table (5.7): Errors of Testing +Ve O.C fault locator NN.

Target output	NN output	Error	Target output	NN output	Error	Target output	NN output	Error
28	28.2	0.2	314	335.4	21.4	665	664.6	0.4
41	41.4	0.4	340	348	8	704	700.1	3.9
67	64.5	2.5	379	377.9	1.1	743	742.1	0.9
80	79	1	418	423	5	782	783.6	1.6
106	91.1	14.9	457	454.9	2.1	821	817.9	3.1
119	117	2	470	473.9	3.9	847	845.8	1.2
145	142.3	2.7	509	507.8	1.2	860	855.9	4.1
184	183.8	0.2	535	516.4	18.6	899	892.1	6.9
223	233	10	587	582.9	4.1	912	906.6	5.4
262	263.2	1.2	626	621	5	925	908.4	16.6

5.5.13 Training of Negative Line Open Circuit Fault Locator NN

The last type of faults is the negative line open circuit fault. As in the previous NN locators, the rectifier and inverter measurements of 304 different -ve/OC fault locations chosen as NN inputs to train a NN that can approximate the location of the -ve/OC fault from the rectifier side. A NN of 20-20-5-3-1 topology was chosen to achieve this task. Figure (5.16) shows the used NN and the relation between its outputs and their targets which is the best relation of all previous NNs. The NN outputs can be represented by equation (5.10) as follows:

$$\text{Output} \approx \text{Target} + 0.059 \text{ km} \quad (5.10)$$

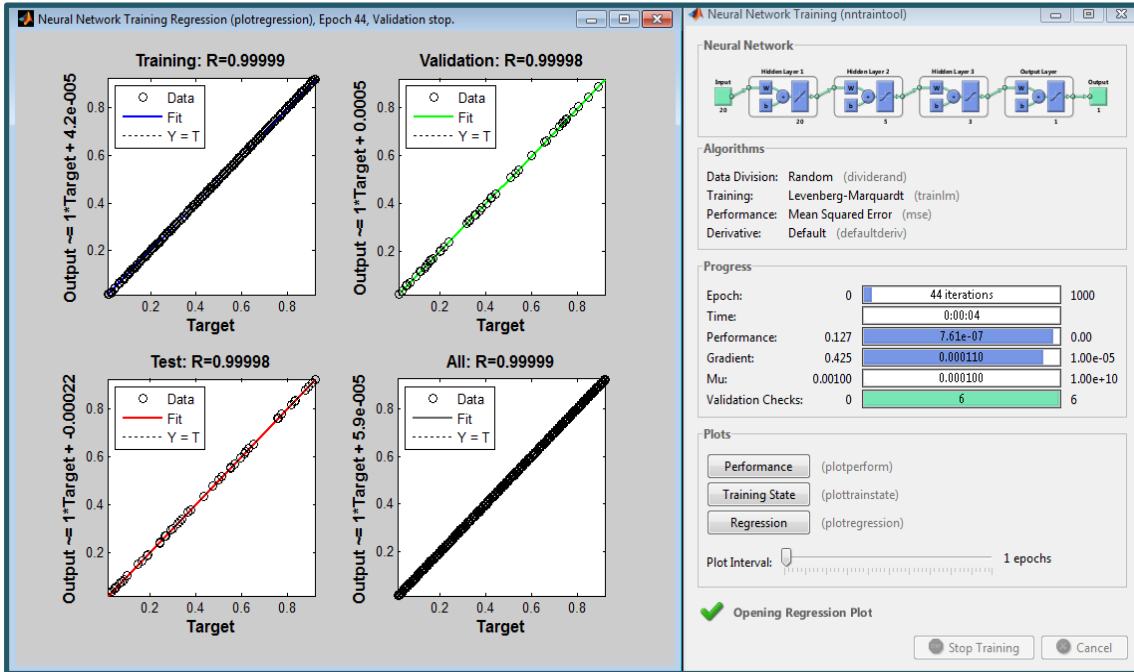


Figure (5.16): Regression plot of training negative line open circuit fault locator NN

5.5.14 Testing of Negative Line Open Circuit Fault Locator NN

Table (5.8) shows the chosen NN outputs for 30 different positions of negative line open circuit fault. From this table the errors vary from 0 to 16.6 km with an average of 1.8 km error. This result is the best of all locators. The NN outputs can be represented by the following equation (5.11):

$$\text{Output} \approx \text{Target} + 0.45 \text{ km} \quad (5.11)$$

Figure (5.17) shows the NN regression plot between the NN outputs and their targets where outputs adjacent to their targets except some errors in range of 500-600 km away from the rectifier station.

Table (5.8): Errors of Testing –Ve O.C fault locator NN

Target output	NN output	Error	Target output	NN output	Error	Target output	NN output	Error
28	25.5	2.5	314	315.2	1.2	665	663.2	1.8
41	42.5	1.5	340	339.4	0.6	704	703.6	0.4
67	67.8	0.8	379	377.3	1.7	743	743.5	0.5
80	78.1	1.9	418	419.5	1.5	782	782.5	0.5
106	102.6	3.4	457	456	1	821	822.3	1.3
119	120.1	1.1	470	469.3	0.7	847	846.9	0.1
145	145.8	0.8	509	525.6	16.6	860	862.3	2.3
184	182.9	1.1	535	534.8	0.2	899	899.4	0.4
223	222.1	0.9	587	587.5	0.5	912	913	1
262	262	0	626	623	3	925	920.4	4.6

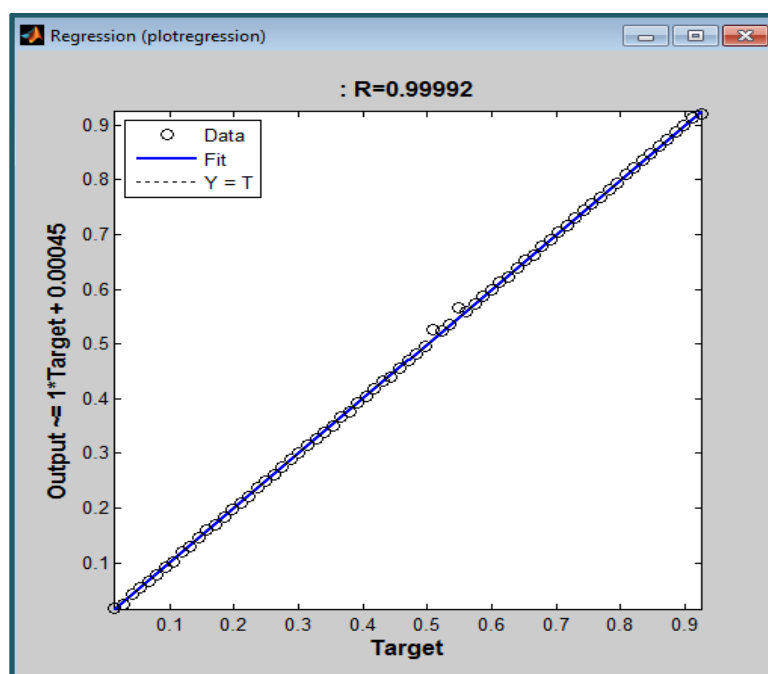


Figure (5.17): Regression plot of testing negative line open circuit fault locator NN

5.6 Simulation Summary

The next table (5.9) summarizes the used NN's and their performances and the maximum tested error for each NN related to overall HVDC TL length.

Table (5.9): Summary of the used NNs.

NN	Topology	Training function	Best training performance (MSE)	Maximum testing error %	Average testing error %
Detection fault	4-4-8-1	Conjugate Gradient with Beale Powell Restarts	1×10^{-11}	ZERO	ZERO
	10-10-10-1	Conjugate Gradient with Beale Powell Restarts	6.18×10^{-13}	ZERO	ZERO
Classifying faults	4-10-20-20-3	Conjugate Gradient with Beale Powell Restarts	8.8×10^{-12}	ZERO	ZERO
	10-10-20-3	Conjugate Gradient with Beale Powell Restarts	1.62×10^{-12}	ZERO	ZERO
Determining location of:					
+Ve/GND fault	20-50-10-5-1	Conjugate Gradient with Beale Powell Restarts	6.7×10^{-5}	3.9%	0.78%
-Ve/GND fault	20-50-10-5-1	Conjugate Gradient with Beale Powell Restarts	3.27×10^{-5}	1.86%	0.66%
+Ve/-Ve fault	20-40-5-3-1	Levenberg-Marquardt	4.87×10^{-5}	2.42%	0.74%
+Ve O.C fault	20-20-5-3-1	Levenberg-Marquardt	1.43×10^{-5}	2.27%	0.53%
-Ve O.C fault	20-20-5-3-1	Levenberg-Marquardt	7.61×10^{-7}	1.76%	0.19%

From table (5.9) many points can be concluded:

1. For the fault detection and classifying there is an ability to use only 4 inputs represent the DC measurements at the rectifier station with acceptable performance but by using ten inputs of AC and DC measurements at the rectifier station, the system becomes more accurate and faster to learn.
2. By using four-layer NN topology, both the detecting and classifying levels can be achieved where for the determining fault location NN, the use of five layer NN topology gives more accurate results.
3. In the fault detecting and classifying levels, only four or ten different inputs which represents measurements of DC alone or AC and DC voltages and currents

at the rectifier terminal were used to construct NNs. In determining fault location, twenty different inputs of AC and DC Voltages and currents at both inverter and rectifier ends are needed to get an accepted results.

4. Two training functions were used to train the selected NNs: Conjugate Gradient with Beale Powell Restarts (traincgb) and Levenberg-Marquardt (trainlm) function. These two functions got the best results after too many simulations.
5. The Mean Square Errors for all the used NNs are acceptable with values near to zero.
6. From simulation; a maximum percentage error related to overall HVDC TL length of 3.9% in the worst case was got when uses the NN to determine the fault location of +Ve/GND fault locator. While, zero errors in testing both fault detection and classifying NNs were obtained.
7. The maximum average testing error related to the TL overall length was 0.78% and this result is accepted.
8. In this thesis both detecting and classifying HVDC TL faults are done accurately where determining the short part of HVDC TL where the fault occurred accurately were succeed.

CHAPTER 6 CONCLUSIONS



A feed-forward back propagation neural networks have been constructed and trained for detecting and classifying most frequent types of faults and determine the location of that fault on HVDC transmission lines. The model employed in this research is a 940 km long, ± 500 kV overhead bipolar HVDC line. The post-fault measurements of AC and DC voltages and currents at the inverter and rectifier sides of HVDC system related to their pre-fault measurements were used as inputs for the chosen NNs. A period of one cycle before and one cycle after fault occurrence is all the needed time to get all the required measurements. These measurements are monitored normally in the sending and receiving stations and don't need special hardware to be measured. There is an ability to use only DC measurements of voltages and currents at the rectifier station as NN inputs to detect and classify faults by using four layer, 4-4-8-1 topology, NN for detection and five layer, 4-10-20-20-3, NN for classifying faults.

By using DC and AC measurements at rectifier station the NN becomes more accurate and faster in learning. A four layer NN of 10-10-10-1 topology was used to detect the existence of fault with approximately no error when tested. Five types of HVDC TL faults were classified by using four layer network of 10-10-20-3 topology with no error in all the research tested cases.

Before determining the fault location, fault type must be known. Different NNs were constructed to determine the fault location related to the rectifier station for each fault type. The best results were by using five layer NN topologies for all locator NNs. The maximum average testing error related to the HVDC TL length was 0.74% and this results is accepted.

The used technique is easy, reliable and gives results in accepted time. This method works on-line and don't need more than one cycle time after fault occurrence to take the needed data, where the practical switch-off relays need about 3-5 cycle times to switch off, which makes this method very fast to get the wanted results.

As a possible extension to this work, it would be quite useful to analyze all the possible neural network architectures and to provide a comparative analysis on each of the architectures and their performance characteristics.

The possible neural network architectures that can be analyzed apart from back propagation neural networks are radial basis neural network (RBF) and support vector machines (SVM) networks.

ABBREVIATIONS

3GC	Three Gorges with Changzhou
+ve/GND	Positive Line to Ground
+ve/-ve	Positive Line to Negative Line
+ve O.C	Positive Line Open Circuit
-ve/GND	Negative Line to Ground
-ve O.C	Negative Line Open Circuit
AC	Alternating Current
AI	Artificial Intelligence
ANFIS	Adaptive Neuro-Fuzzy Inference System
ANN	Artificial Alternate Current Neural Network
CSCs	Current Source Converters
CT	Current Transformer
CVT	Capacitive Voltage Transformer
DC	Direct Current
DWT	Discrete Wavelet Transform
FIS	Fuzzy Inference System
FNN	Fuzzy Neural Network
GA	Genetic Algorithm
GPS	Global Position System
HVDC	High Voltage Direct Current
IGBT	Insulated-Gate Bipolar Transistor
LCC	Line Commutated Current
MSE	Mean Square Error
PEs	Processing Elements
PWM	Pulse-Width Modulation
RBF	Radial Basis Neural Network
SVM	Support Vector Machines`
TL	Transmission Line
trainbfg	BFGS Quasi-Newton Training Function
trainbr	Bayesian Regularization Training Function
traincgb	Conjugate Gradient with Powell/Beale Restarts Training Function
traincgf	Fletcher-Powell Conjugate Gradient Training Function

traincgp	Polak-Ribière Conjugate Gradient Training Function
traingd	Gradient Descent Training Function
traingdm	Gradient Descent with Momentum Training Function
traingdx	Variable Learning Rate Gradient Descent Training Function
trainlm	Levenberg –Marquardt Training Function
trainoss	One Step Secant Training Function
trainrp	Resilient Backpropagation Training Function
trainscg	Scaled Conjugate Gradient Training Function
VHF	Very High Frequency
VLF	Very Low Frequency
VSC	Voltage Source Converter
XPSs	Expert System Techniques

REFERENCES

- [1] Power Transmission Line Fault Location Based on Current Travelling Waves , Abdelsalam Mohamed Elhaffar, Doctoral Dissertation, Helsinki University of Technology,2008.
- [2] Fault Location on Power Networks, Murari Mohan Saha, Jan Izykowski, Eugeniusz Rosolowski, Springer, 2010.
- [3] Hybrid Simulation of ± 500 kV HVDC Power Transmission Project Based on Advanced Digital Power System Simulator, Lei Chen, Kan-Jun Zhang, Yong-Jun Xia, and Gang Hu, Journal of Electronic Science and Technology, vol.11, no. 1, March 2013.
- [4] Zimmermann H-J, Zadeh LA, Gaines BR (1984) Fuzzy Sets and Decision Analysis. North-Holland, Amsterdam
- [5] On line fault section estimation in power systems with radial basis function neural network, Electrical Power and Energy Systems 24 (2002) 321-328, ELSEVIER.
- [6] Artificial Neural Network Based Fault Location for Transmission Lines, Suhaas Bhargava Ayyagari, 2011, University of Kentucky.
- [7] Cichoki A, Unbehauen R, "Neural networks for optimization and signal processing", John Wiley & Sons, Inc., 1993, New York.
- [8] Neural Networks, A comprehensive foundation, S Haykin, Macmillan Collage Publishing Company, 1994, New York.
- [9] Dalstein T, Kulicke B, "Neural network approach to fault classification for high speed protective relaying", IEEE Transactions on Power Delivery, vol. 4, 1995, pp.1002 – 1009.
- [10] A Novel Technique for The Location of Fault on a HVDC Transmission Line , A. Swetha, P. Krishna Murthy, N. Sujatha and Y. Kiran, ARPN Journal of Engineering and Applied Sciences, VOL. 6, NO. 11, NOVEMBER 2011.
- [11] Kezunovic M, Rikalo I, Sobajic DJ, "Real-time and Off-line Transmission Line Fault Classification Using Neural Networks", Engineering Intelligent Systems, vol. 10, 1996, pp. 57-63.
- [12] Artificial Neural Network Approach to Single-Ended Fault Locator for Transmission Lines, Zhihong Chen and Jean-Claud Maun, IEEE Transaction on Power Systems, VOL. 15. NO. I, February 2000.
- [13] Radial Basis Function Neural Networks for Fault Diagnosis in Controllable Series Compensated Transmission Lines, Y.H. Song(SM) A.T. Jolins(SM) Q.Y. Xuan, Electrotechnical Conference, 1996. MELECON '96., 8th Mediterranean.
- [14] Fault Identification in an AC-DC transmission system using neural networks, N. Kandil, V.K. Sood, Transactions on Power Systems, Vol. 7, No. 2, May 1992.
- [15] HVDC systems fault diagnosis with neural networks, L.L La1, F.Ndeh-Che, Tejedo Chari, The European Power Electronics Association, 1993.
- [16] Application of a Radial Basis Function (RBF) Neural Network for Fault Diagnosis in a HVDC System, K. G. Narendra, V. K. Sood , IEEE Transactions on Power Systems, Vol. 13, No. 1, February 1998.
- [17] Neural Network Based Fault Diagnosis in an HVDC System, H.Etemadi, V.K.Sood, K.Khorasni, R.V.Patel, International Conference on Electric Utility Deregulation and Restructuring and Power Technologies, April 2000.
- [18] Analysis and Identification of HVDC System Faults Using Wavelet Modulus Maxima ,L. Shang, G. Herold; J. Jaeger, R. Krebs, A. Kumar , AC-DC Power Transmission, 28-30 Conference Publication No. 485 @ IEE 2001, November 2001.

- [19] A Novel Fault-Location Method for HVDC Transmission Lines, Jiale Suonan, Shuping Gao, Guobing Song, Zaibin Jiao, and Xiaoning Kang, IEEE Transaction on Power Delivery, vol. 25, no. 2, April 2010.
- [20] Fault Location in Extra Long HVDC Transmission Lines using Continuous Wavelet Transform, Kasun Nanayakkara, A.D. Rajapakse, Randy Wachal, International Conference on Power Systems Transients, June 2011.
- [21] Identification of Faults in HVDC System using Wavelet Analysis, K.Satyanarayana , S. Hussain MD, B.Ramesh , International Journal of Electrical and Computer Engineering (IJECE),vol.2,no.2, pp.175-182, April 2012.
- [22] Classification of Fault Analysis of HVDC Systems using ANN, P. Sanjeevikumar, B. Paily, M.a Basu, M. Conlon, IEEE, 2014.
- [23] HVDC for Beginners and Beyonds, Carl Barker, ALSTOM Grid Worldwide magazine, 2010.
- [24] HVDC the Proven Technology for Power Exchange, Siemens Company - Energy Sector, 2011.
- [25] The ABCs of HVDC Transmission Technology, Michael Bahrman and Brian Johnson IEEE Power & Energy Magazine Vol. 5 No. 2, March/April 2007.
- [26] CIGRÉ session, PL Sorensen, B Franzén, JD Wheeler, RE Bonchang, CD Barker, RM Preedy, MH Baker, B4-207, 2004.
- [27] Design aspects of Korean mainland to Cheju island HVDC transmission, JL Haddock, FG Goodrich, Se Il Kim, Power Technology International, Sterling Publication Ltd p.125, 1993.
- [28] Technical and Economic Aspects of Tripole HVDC, L. O. Barthold , Fellow, IEEE, International Conference on Power System Technology, 2006.
- [29] Reactive Power Compensation and Harmonic Filters for HVDC Classic, Dipti Khare, ABB.
- [30] Fault Location Identification for a VSC-HVDC System with a Long Hybrid Transmission Medium, Hashim Abbas M. Al Hassan, Master Thesis, University of Pittsburgh, 2014.
- [31] IEEE Guide for Determining Fault Location on AC Transmission and Distribution Lines, IEEE Std C37.114-2004 , 2005.
- [32] Accurate fault location technique for distribution system using fault-generated high frequency transient voltage signals, Bo ZQ, Weller G, Redfern MA, IEE Proc – Gener Transm Distrib 1999.
- [33] A new non-unit protection scheme based on fault generated high frequency current travelling waves Bo ZQ, Johns AT, Aggarwal RK, Proc of Int. Conf. on Advance in Power System Control, Operation & Management, APSCOM-95, 1995.
- [34] Fault location using wavelets, Magnago FH, Abur A, IEEE Trans on Power Deliv. , 1998
- [35] Fault Identification in HVDC using Artificial Intelligence – Recent Trends and Perspective, M Ramesh, Research Scholar, A. Jaya Laxmi, Member, IEEE, 2012.
- [36] Neural Networks a Comprehensive Foundation, 2nd edition, Simon Haykin, Pearson Education, 1999.
- [37] Artificial Neural Networks, Principe, J.C., Ed. Richard, C. Dorf, CRC Press LLC, 2000
- [38] Neural Networks for Optimization and Signal Processing, Cichocki A, Unbehauen R John Wiley & Sons, Inc., New York, 1993.

- [39] Design and evaluation of an adaptive distance protection scheme suitable for series compensated transmission feeders, Erezzaghi MEL, Crossley PA, Elferes , Proc of 8th Int. Conf. on Developments in Power System Protection,2004.
- [40] Handbook of Measuring System Design, Peter H. Sydenham and Richard Thorn , John Wiley & Sons Ltd, 2005 .
- [41] Neural Network Toolbox™, User's Guide, Mark Hudson Beale, Martin T. Hagan, Howard B. Demuth, MATLAB, 2012.
- [42] Neural Network Design, Hagan, M.T., H.B. Demuth, and M.H. Beale, Boston, 1996.
- [43] Role Of Three Gorges-Ghangzhou HVDC in Enter Connecting Central and East China, Abhay Kumar, Yuan Qingyun , Shanghai Symposium, 2003.
- [44] Thyristor-Based HVDC Transmission System, Silvano Casoria, MATLAB MathWorks, 2007.